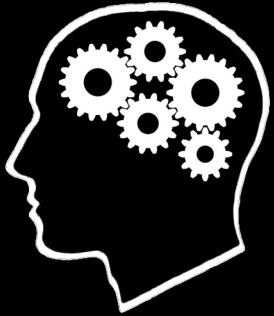
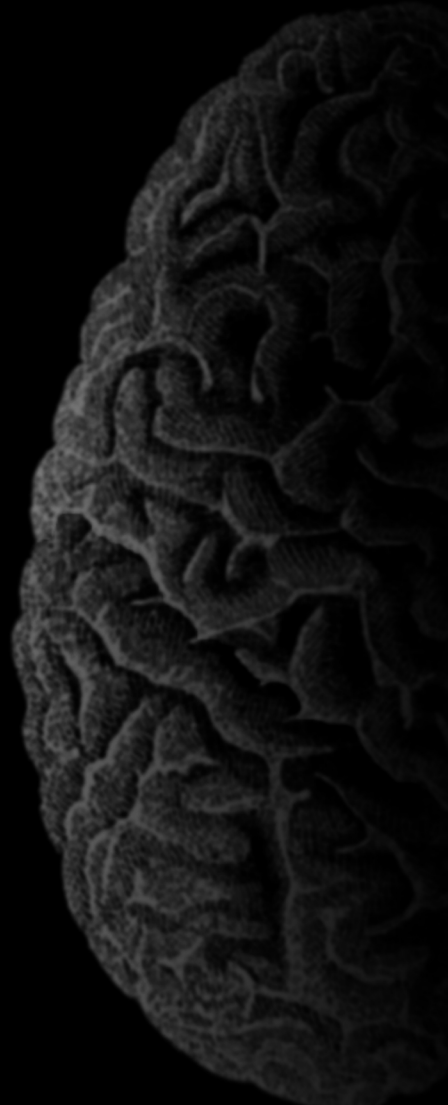
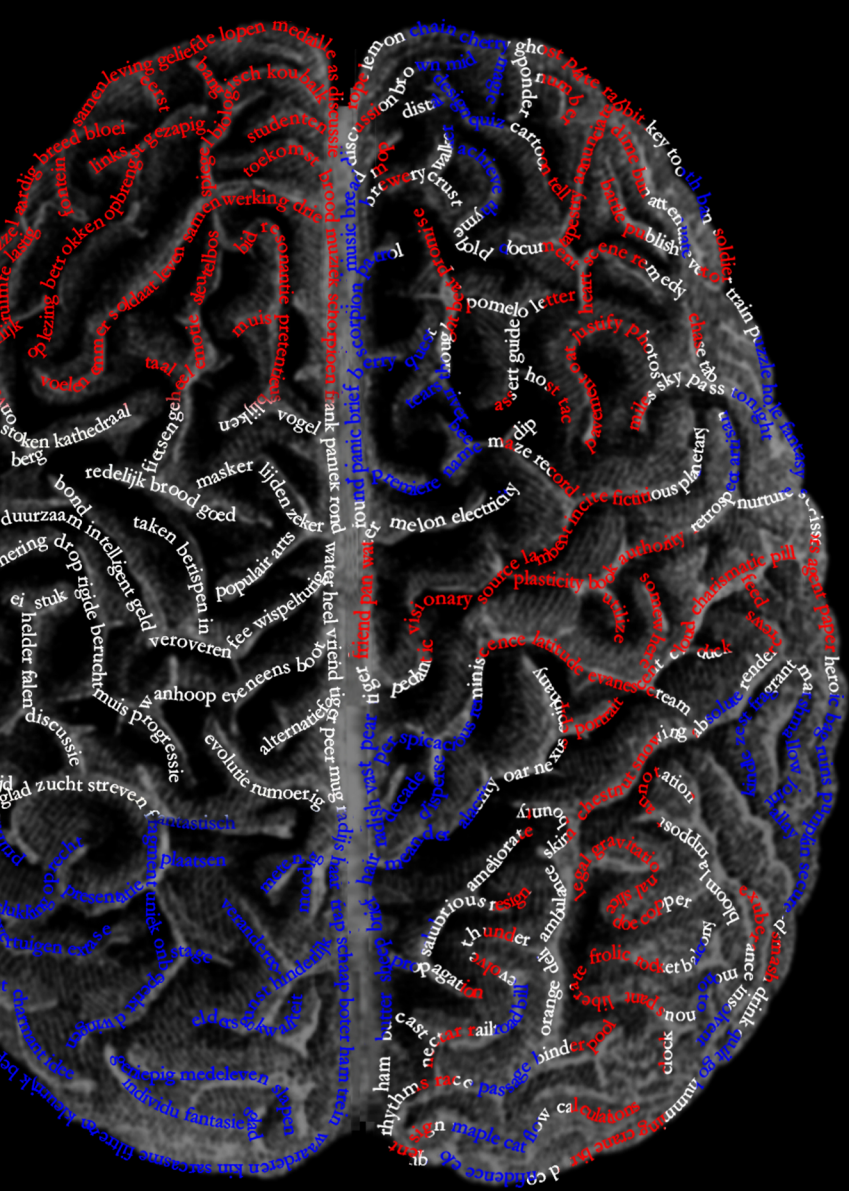


# COGNITIVE NEUROSCIENCE



*Volume 7, Issue 1, March 2012*



## Table of Contents

---

<b>Editorials</b>	<b>2</b>
<i>Markus van Ackeren</i>	
<b>Requesting Without Asking: Contributions of Motor and Theory-of-Mind Systems to Language Understanding</b>	<b>5</b>
<i>Lieneke Janssen</i>	
<b>Neuronal Responsiveness in Rat Primary and Secondary Somatosensory Cortex is Differentially Affected by Brain State</b>	<b>18</b>
<i>Malte Köster</i>	
<b>Quantifying the Contribution of Alpha and Beta Amplitude to Somatosensory Perception and its Improvement with Attentional Orienting</b>	<b>32</b>
<i>Adjmal Sarwary</i>	
<b>Adaptation and Retention of Motor Memories During Self-Motion: The Role of the Vestibular System</b>	<b>48</b>
<i>Flora Vanlangendonck</i>	
<b>Conflict in the Bilingual Brain: The Case of Cognates and False Friends</b>	<b>61</b>
<i>Marjolein van der Waal</i>	
<b>The Tactile Speller: An ERP-based Brain-Computer Interface for Communication</b>	<b>79</b>
<b>Abstracts</b>	<b>91</b>
<b>Institutes associated with the Master's Programme in Cognitive Neuroscience</b>	<b>93</b>

---

## From the Editors-in-Chief of the CNS Journal



Dear Reader,

We are thrilled to present the latest issue of the *Proceedings of the Master's Programme Cognitive Neuroscience*. Seven years ago a group of enthusiastic students founded this unique project to showcase their accomplishments in the Master's Programme. Since then, we have grown into a large team which consists of several departments, each contributing uniquely to the publication process. The continuous realization of a new issue of the journal involves the commitment and interaction of first and second year students of the master's programme. In each issue a selection of the best articles is published in a printed version of the student journal and all other submissions are available on our website. This year, we have adapted the structure of our team by introducing a subediting department to facilitate the publication process. In continuously improving our publication process we strive to produce a professional collection of scientific articles reflecting the excellent research done by our master's students.

Each year we welcome more and more students into our interdisciplinary programme. In parallel the Cognitive Neuroscience Master's has expanded from three to four research themes to continue to attract a diverse group of young researchers. The current volume features articles from three specializations: 'Psycholinguistics', 'Action, Perception and Consciousness', and 'Neurocognition'. The next volume will contain articles from four domains corresponding to the research themes of the Donders Institute for Brain, Cognition and Behavior: 'Language and Communication', 'Perception, Action and Control', 'Learning, Memory and Plasticity' and 'Brain Networks and Neuronal Communication'.

The current issue, which you are holding in your hands, would not be possible without the contribution of each member of the editorial board. We also appreciate the time and effort spent by the authors and reviewers without which this issue would not be possible. The guidance from our senior advisor Prof. Dr. Roshan Cools, programme director Prof. Dr. Ruud Meulenbreuk and programme coordinator Dr. Arno Koning has also been very valuable to us. Finally, we appreciate your interest in our student journal and we hope you enjoy reading it.

On behalf of the editorial board,

**Ricarda Braukmann & Nietzsche Lam**  
Editors-in-Chief

## From the Director of the Donders Centre for Cognition



Dear Reader,

It is a great pleasure to be writing an editorial note for this issue of the *Proceedings of the Master's Programme Cognitive Neuroscience*. It is an exciting time for everyone training or working in cognitive neuroscience. The field has come a long way since the time of the ancient Greek philosophers. Conflicting views of Plato and his 'trainee' Aristotle on the home of the mind – brain versus heart – ultimately led to Descartes' mind-body dualism, later refuted by the phrenologists, the forerunners of the localizationist doctrine. Through work by investigators such as Broca and Wernicke this doctrine promoted the field of neuropsychology, which we still know today. Development of new technologies further turned philosophical thinking into scientific understanding, charting out the brain's anatomy, its neurons, their connections and physiology. But even the neuron doctrine now appears to be too limited to understand complex brain function, and further refinements are still required. Mindful of this history, the future of cognitive neuroscience must now try to cross boundaries between the various disciplines that make up this field. Making this progress requires well-trained students, a new type of researcher who can apply state-of-the-art technologies, develop strong computational frameworks and theories, and design innovative behavioral research paradigms. The contents of this issue of the students' journal, as with previous issues, show that the students of the Nijmegen CNS program meet this standard. What will you find? There are two unique contributions dealing with language processing, from conflict in bilingualism to how the motor system aids in language understanding. Two further studies report on the role of attentional and other brain states in somatosensory processing. There is also a report included describing how arm movements are adapted in accelerating environments, when the role of the vestibular system becomes relevant. Finally, you will find an interesting report on how a brain-computer interface based on event-related potentials can be exploited in tactile spelling, a useful alternative for the visual speller for patients whose eye movements are impaired. I congratulate all authors with the appearance of their high-quality work in this edition.

I compliment the editorial board with this new issue, and wish you much pleasure with reading about this progress in Nijmegen cognitive neuroscience.

**Prof. Dr. Pieter Medendorp**  
Director Donders Centre for Cognition

# Proceedings of the Master's Programme Cognitive Neuroscience of the Radboud University Nijmegen

---

*Editors-in-Chief*

**Ricarda Braukmann  
Nietzsche Lam**

*Editor Action, Perception & Consciousness*

**Ricarda Braukmann**

*Assistant Editor Action, Perception & Consciousness*

**Jeffrey Martin**

*Editor Neurocognition*

**Sarah Beul**

*Assistant Editor Neurocognition*

**Charl Linssen  
Yvonne Melzer**

*Editor Psycholinguistics*

**Ashley Lewis**

*Assistant Editor Psycholinguistics*

**Angela de Bruin**

*Layout Chief*

**Claudia Lüttke**

*Layout Assistants*

**Katrin Bangel  
Suzanne Jongman  
Nietzsche Lam  
Alessandra Piatti**

*Public Relations Chief*

**Johanna van Schaik**

*Public Relations Assistant*

**Dalya Samur**

*Subeditor*

**Suzanne Jongman**

*Assistant Subeditors*

**Yağmur Güçlütürk  
Jana Kruppa**

*Webmaster*

**Martine Verhees**

*Assistant Webmaster*

**Lies Cuijpers**

---

*Programme Director:*

**Ruud Meulenbroek**

*Senior Advisor:*

**Roshan Cools**

*Cover Image:*

**T.L.A**

*Journal Logo:*

**Claudia Lüttke**

*Photo Editors-in-Chief:*

**Johanna van Schaik**

*Contact Information:*

**Journal CNS  
Radboud University  
Postbus 9104  
6500 HE Nijmegen  
The Netherlands**

[nijmegencns@gmail.com](mailto:nijmegencns@gmail.com)

# Requesting Without Asking: Contributions of Motor and Theory of Mind Systems to Language Understanding

Markus J. Van Ackeren<sup>1</sup>

Supervisors: Daniel Casasanto<sup>2</sup>, Harold Bekkering<sup>1</sup>, Peter Hagoort<sup>1</sup>, Shirley-Ann Rueschemeyer<sup>3</sup>

<sup>1</sup>Donders Institute for Brain, Cognition and Behaviour, Radboud University Nijmegen, The Netherlands

<sup>2</sup>New School for Social Research, New York, USA

<sup>3</sup>University of York, York, United Kingdom

In everyday language use it is necessary to decode meaning from arbitrary symbols. Research from the past decade has shown that language comprehension recruits a distributed network of areas, some of which are shared with domain-specific perceptual processes. For example, understanding words denoting actions and executing these actions engage an overlapping frontal-parietal network. What is not known, however, is whether the activation of this network during language comprehension is triggered by the word-form of an action concept, or rather by the concept itself. The latter would suggest a coupling between regions that support action understanding and more general communicative functions. The current study addresses this issue using functional magnetic resonance imaging (fMRI). Subjects listened to implied requests for action. Implied requests for action are speech acts in which access to an action-concept takes place although it is not explicitly encoded in the language. For example, the utterance “It is hot here!” in a room with a window is likely to be interpreted as a request to open the window. However, the same utterance in a desert will be interpreted as a statement. The results showed that regions in the medial superior frontal gyrus (SFG) and the inferior parietal lobule (IPL) were sensitive to both action execution and implied requests for action. These areas were accompanied by regions in the medial prefrontal cortex (mPFC) and left-lateralized temporo-parietal junction (TPJ), which constitute part of the classical theory of mind network. The current findings extend previous research by showing that language and action share a common neural substrate above and beyond the level of the lexical word-form. In addition, the data suggest that both simulation and theory of mind networks are critical for language understanding.

*Keywords:* embodied cognition, conceptual knowledge, semantic memory, implicature, communication, theory of mind

---

Corresponding author: Markus J. van Ackeren, email: m.vanackeren@psych.york.ac.uk

## 1. Introduction

The human language system is the most sophisticated communication system in the animal kingdom. Specifically, language allows us to encode complex semantic knowledge in a very concise, symbolic way. However, the relationship between symbolic representations and the knowledge they refer to is still debated. Embodied theories of language postulate that understanding the meaning of words and utterances involves the same systems we use to perceive and interact with the physical world (Barsalou, 1999, 2008; Fischer & Zwaan, 2008). In other words, understanding a word like cup will also involve the systems we have been using to perceive and manipulate cups throughout our life.

A plethora of previous studies using a variety of experimental techniques have reliably demonstrated that language referring explicitly to actions (e.g. object nouns, action verbs and action sentences) modulates the neural activity in the cerebral motor system (Glenberg & Kaschak, 2002; Hauk, Johnsrude, & Pulvermüller, 2004; Rüschemeyer et al., 2009; Tettamanti et al., 2005). For example, Glenberg and Kaschak (2002) have shown that subjects will respond faster to sentences denoting a movement away from the body (e.g., close the drawer), when they are prepared to respond in the same direction. Accordingly, when they prepared a movement towards the body, response times were faster for sentences denoting an action in the same direction (e.g., open the drawer). In a study using functional magnetic resonance imaging, Hauk and colleagues (2004) demonstrated that regions that respond to movement execution with the hand, foot or mouth will also respond to verbs denoting actions (e.g. pick, kick, lick). Specifically, the activation patterns revealed a somatotopic organization of action verbs in the primary and premotor cortices. These results have been interpreted as evidence that semantic knowledge is stored, at least in part, in neural areas that are primarily dedicated to perception and action.

However, there is still much debate regarding the functional contribution of the action system to the representation of semantic knowledge. In some theories action information is constitutive of lexical-semantic knowledge (Barsalou, 1999, 2008; Pulvermüller, 1999, 2005). Specifically, it has been postulated that the perception of a word-form like kick often coincides with the physical execution of a movement. As a result, systems that are involved in language and action become coupled at a neural level. Thus, accessing the meaning of a word-form like kick is implemented in the brain as spreading

activation from language into action systems (Pulvermüller, 1999, 2005). However, other accounts argue that action information is epiphenomenal to semantic knowledge (Mahon & Caramazza, 2008, 2009). According to this hypothesis, the activation of the action system in response to language is a result of semantic access rather than being part of it. Finally, in cascading theories the action system contributes to language understanding; but other sorts of information are also important (Meteyard et. al, *in press*; Rüschemeyer et. al, 2010). One problem in all of these accounts is that they make very similar predictions. Thus, a majority of the findings is consistent with all three theories. In conclusion, there is no consensus regarding the functional contribution of modality-specific information to the representation of semantic knowledge.

One way to dissociate between different theories in the embodied language framework is to study utterances in which the literal and the speaker meaning are dissimilar. For example, in idiomatic expressions like kick the bucket the literal meaning of the utterance denotes an action with the foot. However, the speaker meaning denotes that a person has passed away. Raposo and colleagues (2009) compared idiomatic expressions like these with literal sentences denoting actions and found that the former did not activate the neural motor system in the same way as literal sentences. Yet another way to test different predictions about the relation between language and action is the study of utterances in which no action verbs are used, but an action is nevertheless implied. During natural communication humans do not always express themselves in a literal way. This notion has been coined conversational implicature (Grice, Cole, & Morgan, 1975). For example, Tom might say that some guests had already left the party at 10pm - implying that not all guests had left before 10pm. Importantly, this inference relies heavily on shared knowledge between the interlocutors (Levinson, 1983). In other words, each person has to be aware of the mental state of the interlocutor. This very much relates to the concept of having a theory of mind (ToM) (Frith & Frith, 2005, 2010). Recent research has shown that parts of the brain network that is activated when we think about mental states of others, also respond when the pragmatic demands of the task increase (Sassa et al., 2007; Willems et al., 2010). Taken together, understanding implicatures is dependent on conversational and communicative principles and not on decoding the literal meaning of the utterance alone (Clark & Brennan, 1991). However, some implicatures are highly context-dependent.

These are called particularized implicatures (Grice et al., 1975; Levinson, 1983, 2000). For example, when two persons are in a room with a window and one produces the utterance “It is very hot here”, the interlocutor most likely will interpret this as a request to open the window. However, the same utterance will be interpreted as a plain statement in a naturally hot environment, like a desert. In this example, an action is conveyed in the absence of an action verb. In sum, utterances in which literal and speaker meaning are dissociated allow us to investigate at which level, during language comprehension, the neural motor system could become important.

The goal of the present study was to dissociate between theories that postulate a direct association between language and action at the word-form level only (Pulvermüller, 1999; 2005), and those that hypothesize that the action system becomes activated either during (Meteyard et al., in press; Rüschemeyer et al., 2010), or after semantic knowledge retrieval (Mahon & Caramazza, 2008; 2009). Hemodynamic changes in the brain were measured while subjects listened to implied requests for actions (e.g., It is very hot here). Humans derive action meaning from these kinds of particularized implicatures with a very high accuracy. Therefore, it was hypothesized that a) this should be accompanied by haemodynamic changes in the action system. Specifically, we expected activation in neural motor areas that are involved in movement planning (Brodmanns area 6) and areas that are associated with object manipulation and action goals (IPL (PF)) (Fogassi et al., 2005). Importantly, these areas have also been shown to be involved in the comprehension of action related language in a large number of studies (Postle, McMahon, & Ashton, 2009; Rüschemeyer et al., 2009). Sensitivity of these areas to implied requests would be evidence that language activates the neural motor system at a level beyond lexical-semantics. In addition, we expected that b) the interpretation of an implied request cannot rest solely on running a motor simulation. Therefore we predicted activation in classical theory of mind (ToM) areas such as the medial prefrontal cortex (mPFC) and the temporo-parietal junction (TPJ) (Gallagher & Frith, 2003).

## 2. Materials and methods

### 2.1 Participants

The subjects were sixteen students from the local university and college. However, three

subjects had to be excluded from the data due to excessive movement, responding on no-go trials, and health related problems that were not known to the experimenter prior to the experiment. The remaining thirteen subjects were all healthy, female adults between the ages of 18 and 24 with normal or corrected to normal vision and no hearing impairments ( $N = 13$ ; mean age = 21.39) All subjects were native speakers of Dutch and right handed. In addition, none of the subjects reported any known neurological impairment. Prior to the experiment, each participant gave written consent to participation. This was in accordance with the declaration of Helsinki. For participating in the experiment, subjects either received a financial compensation or course credits. The study fell under the general ethical approval of the Donders Institute for Brain and Behaviour.

### 2.2 Stimuli

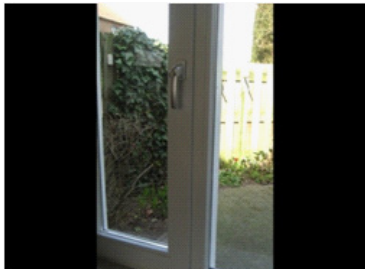
The stimuli consisted of 128 images visual scenes and 128 spoken sentences. The spoken sentences were recordings from a native speaker of Dutch. The visual scenes were assembled from multiple image-search-engines on the web, which are publicly available (e.g. flickr.com; images/google.com).

The stimuli were segregated into 64 unique item-sets. One item-set comprised four distinct sentence-scene combinations. The four conditions were implied request (IR), picture control (PC), utterance control (UC) and baseline control (BC) (Table 1). Within each item-set, only one of these combinations was associated with an implied request. The other three sentence-scene combinations could be interpreted as a plausible statement but not as requests. However, the three control conditions were included to control for the effect of the visual scene and the utterance alone. This assumption was tested in an online survey before MRI data acquisition. Participants in the questionnaire study ( $N=20$ ) viewed randomized combinations of one visual scene and one sentence from a single item set. Their task was to decide whether they thought that the interlocutor wanted something from them. The items in the IR-condition were interpreted as requests much more often than in the other three conditions (IR:  $M=71\%$ ; SE=4; PC:  $M=26\%$ ; SE=3; UC:  $M=18\%$ ; SE=2; BC:  $M=14\%$ ; SE=2). This difference was significant at an alpha level of .05 ( $F(1.92,36.33)=110.31, p<.001$ , partial  $\eta^2=.85$ )<sup>1</sup>.

In addition, a localizer task was used to identify a)

<sup>1</sup> Greenhouse-Geisser-correction was used to correct for violations of sphericity.

**Table 1.** Example of an item-set from the implicature-task illustrating the conditions a) implied request (IR), b) picture control (PC), c) utterance control (UC) and d) baseline control(BC).

Visual Scene	Spoken utterance	Meaning
	a) <i>It is very hot here</i>	Implied request
	b) <i>It is very nice here</i>	Statement
	c) <i>It is very hot here</i>	Statement
	d) <i>It is very nice here</i>	Statement

regions that were specifically activated when thinking about another person's beliefs and desires (ToM) and b) regions that were involved in simple hand actions. The theory of mind network was identified with the localizer during time windows at which the subjects read a story and subsequently judged statements about the story. The stories required either an inference on the physical state of an object (false photograph), or another person's belief (false belief). Each participant saw 24 physical state and 24 mental state stories. The stimuli were introduced by the Saxe lab<sup>2</sup> (Dodell-Feder, Koster-Hale, Bedny, & Saxe, 2010; Saxe & Kanwisher, 2003) and translated into Dutch for the present experiment. Regions that were involved in simple hand actions were localized during time windows in which subjects produced button presses with their right index and middle finger. Hand regions were targeted because the implicated requests required simple hand actions as well.

### 2.3 Stimulus presentation

For both the main task and the functional localizer, subjects lay supine in the scanner. All visual material was presented via a projector outside the scanner. Subjects viewed the screen via a nonmagnetic mirror. The auditory stimuli were presented via nonmagnetic headphones that also dampened the noise from the scanner. Before the start of the experiment the volume of the headphones was adjusted to the

subjects convenience. Participants' responses to the tasks were recorded via a nonmagnetic button box inside the scanner.

The implicature task was an epoch-related design in which each participant saw two independent sentence-scene combinations from each item set, resulting in a total number of 128 stimuli per participant (32 items per condition). The items were individually pseudo-randomized in such a way that the same condition was never presented more than two times in a row. Additionally, sixteen null events were included in the design. In order to maintain participants' vigilance and ensure that they processed the stimuli more deeply, fifteen percent of the experimental trials were accompanied by a catch-question (Do you think that the person made a request?), to which participants could respond with a button press indicating either a yes or no response. In order to make the trial onset unpredictable for the subject and to enhance the resolution of the time-window within a trial, the inter-trial interval was randomly jittered in a range of 4000ms-6000ms ( $M=5000\text{ms}$ ). The trial began with the presentation of a fixation cross for 500ms, followed by the visual scene. After 200ms the sentence stimulus was presented (mean duration: 1357ms). At the sentence offset, a variable interval filled the remaining time so that every picture presentation lasted 2300ms. Thus, every trial lasted exactly 3000ms. Subjects were instructed to listen to the sentences carefully and decide whether they think the person wanted

<sup>2</sup>The collection of stimuli was provided by Rebecca Saxe and Jessica Andrews-Hanna.

something from them or not while listening. Before the actual start of the experiment, there was a practice run outside the scanner.

After the implicature task, subjects proceeded with the localizer task. The procedure of this task is described in Dodell-Feder et al., 2010. Also for this task, there was a practice run outside the scanner, prior to the experiment.

## 2.4 fMRI data acquisition

MRI data acquisition was performed on a Siemens Magnetom Trio scanner (Siemens Medical System, Erlangen, Germany) with a magnetic field strength of three Tesla. The functional scans for the implicature task and the localizer were acquired using a multi-echo gradient pulse sequence (TR=2390ms; TE=9.4ms, 21.17ms, 32.94ms, 44.71ms, 56.48ms; flip angle=90°). Each volume consisted of 31 transversal slices with a thickness of 3 mm. The voxel resolution was 3.5mm x 3.5mm x 3.5mm.

After the collection of functional data, a structural scan was performed for each individual subject. The image was a T1-weighted 3D MPRAGE sequence comprising 192 sagittal slices (TR=2300ms; TE=3.03ms; slice thickness=1mm).

## 2.5 fMRI data analysis

The raw MR-images were pre-processed and analyzed using the Matlab toolbox SPM8 (Statistical Parametric Mapping, [www.fil.ion.ucl.ac.uk/spm](http://www.fil.ion.ucl.ac.uk/spm)). Prior to the analysis, the first six volumes were excluded to control for T1 equilibration effects. Six movement parameters (three translations and three rotations) were extracted from the first echo of each volume and subsequently used to correct for small head movements in all five echoes of each volume. Subsequently, all five echoes were combined into a single volume using a weighted average. To correct for delays in slice timing during image acquisition, the time courses of each voxel were realigned towards slice 16. After segmentation into grey and white matter, images were normalized to a standard EPI template within MNI space and resampled at an isotropic voxel size of 3mm. Lastly, the images were convolved with a Gaussian smoothing kernel with 8mm full width at half maximum (FWHM). To correct for slow drifts in the signal, a high pass filter was applied at 128 seconds.

The combined and pre-processed time-series of the implicature-task were analyzed as an epoch-related design (epoch = 1.5 sec) on a subject-by-subject basis. Within a general linear model (GLM)

framework each condition was convolved with a canonical hemodynamic response function (HRF) and used as a regressor. In addition, the movement parameters from the realignment algorithm, time, and dispersion derivatives were included as effects of no interest.

A single contrast comparing IR versus three control (PC, UC & BC) conditions was generated for each subject individually. Since the images from each subject had been aligned to standard MNI space, a second level random effects analysis could be performed at the group level. The critical contrasts from all subjects were included in the model and a group analysis was performed using a one-sample t-test. To control for multiple comparisons, a cluster extend threshold was determined using a Monte Carlo simulation with 1000 iterations (Slotnick, Moo, Segal, & Hart, 2003). The simulation results indicated that a cluster with  $p<0.0001$  (uncorrected) and a cluster size  $k>12$  (3243) was significant at  $p<.01$  (corrected).

The localizer task was used to identify areas that were selectively active during inferences about mental states and hand movements. In order to extract the signal, which was related to the ToM-network, the images were analyzed as a block design. Each block was defined as the period of time from the onset of the story to the offset of the statement. Subsequently, this time window was convolved with a canonical HRF. Only movement parameters were included as effects of no interest. A contrast comparing the false belief stories versus the false photograph stories was created for each subject individually. Subsequently, a random effects group analysis was conducted on the individual-subject contrast images using a one-sample t-test.

Additionally, button presses with the right hand were analyzed to identify regions that are involved in action execution. Manual button presses were analyzed as an event-related design. The moment a subject pressed a button was modelled with a canonical HRF and used as a regressor. In addition, the movement parameters from the realignment algorithm, time and dispersion derivatives were used as effects of no interest.

## 2.6 ROI analysis

Regions of interest (ROI) analyses were conducted in order to investigate whether the condition in which the utterance and the visual context formed an implicature exerted a stronger effect on a) the neural motor network that is involved in hand actions and b) the ToM-network. Four ROI's

**Table 2.** Brain regions from whole brain analysis of the localizer task showing significantly more activation during false belief versus false photograph stories ( $p < .0001$ ,  $k > 12$ ). Only the largest peak voxel per cluster is depicted.

Region	Cluster level (voxels)	Peak voxel level		MNI coordinates		
		T	equivZ	x	y	z
Precuneus	491	14.56	5.83	-3	-58	22
Left medial prefrontal cortex	23	8.33	4.71	-6	50	40
Right temporo-parietal junction	115	7.88	4.59	57	-55	22
Left temporo-parietal junction	156	8.93	4.86	-51	-49	31

**Table 3.** Brain regions whole brain analysis of the localizer task that were significantly active during button presses with the right hand ( $p < .0001$ ,  $k > 12$ ). The results were restricted to anatomically defined neural motor regions (BA 6, bilateral IPC (PF)).

Region	Cluster level (voxels)	Peak voxel level		MNI coordinates		
		T	equivZ	x	y	z
Brodmann area 6	458					
Left superior frontal gyrus		12.66	5.56	-24	-1	67
Left precentral gyrus		11.84	5.43	-24	-10	64
Left medial SFG		10.90	5.27	-6	23	58
Right inferior parietal cortex (PF)	113					
Left inferior parietal lobule		13.21	5.64	-48	-46	37
Right inferior parietal cortex (PF)	40					
Right supramarginal gyrus		7.00	4.34	66	-40	28

for the ToM-network were defined as the clusters in the whole-brain analysis that were sensitive to the contrast false belief vs. false photograph (Table 2).

With respect to the action network, there were very strong anatomical hypotheses. Therefore, the contrast image for hand actions (Action>0) from the second level whole-brain analysis was masked with cytoarchitectonically defined probability maps of Brodmann area 6 (Geyer, 2004) and left and right inferior parietal cortex (PF) (Caspers et al., 2006, 2008) (Table 3).

Subsequently, MNI-coordinates for peak values within the largest active cluster were used to create spheres of 6mm radius using the ROI toolbox Marsbar (Brett, Anton, Valabregue, & Poline, 2002).

The ROI's from the localizer task were interrogated with respect to the four conditions (IR, PC, UC, BC) from the implicature task. Percent signal change was extracted and averaged within each participant. Thus, for each of the 13 participants in our study, there were four values. With these four conditions analyses of variance (ANOVAs) with repeated measures were conducted for each ROI.

### 3. Results

#### 3.1 Behavioural results

Behavioural responses to catch trials were analyzed to test whether subjects responded as

predicted by the questionnaire study. First, a one-sample t-test was conducted on the percentage of correct responses, to assess whether subjects were able to do the implicature task. This assumption was confirmed ( $t(12) = 9.64, p < .001$ ,  $M = 80\%$ ,  $SE = 3$ ). Subsequently an ANOVA with repeated measures was conducted to test for differences in task difficulty between the conditions (IR, PC, UC, BC). This test was significant ( $F(2.14,24.43)=3.56, p < .05$ , partial  $\eta^2=.23$ ). Planned comparisons revealed subjects responded to the IR condition faster than to the PC ( $F(1,12)=13.13, p < .005$ , partial  $\eta^2=.52$ ; IR:  $M= 045\text{ms}$ ,  $SE=86\text{ms}$ ; PC:  $M=1299\text{ms}$ ,  $SE=116\text{ms}$ ), the UC ( $F(1,12)=6.1, p < .05$ , partial  $\eta^2=.34$ ; UC:  $M=1193\text{ms}$ ,  $SD=91\text{ms}$ ), and BC ( $F(1,12)=5.05, p < .05$ , partial  $\eta^2=.3$ ; BC:  $M=1314\text{ms}$ ,  $SE=131\text{ms}$ ) condition. The fact that subjects responded faster giving positive responses is not surprising; however, it shows that recognizing IR was not more difficult than recognizing statements. Lastly, an ANOVA with repeated measures tested whether subjects recognized requests more often in the IR condition. The results replicated the findings from the questionnaires ( $F(2.74,32.93)=49.76, p < .001$ , partial  $\eta^2=.81$ ). Specifically, requests were more often identified in the IR condition than in the PC ( $F(1,12)=113.81, p < .001$ , partial  $\eta^2=.91$ ; IR:  $M=83\%$ ,  $SE=4$ ; PC:  $M=19\%$ ,  $SE=4$ ), UC ( $F(1,12)=71.44, p < .001$ , partial  $\eta^2=.86$ ; UC:

M=34%, SE=6) and BC ( $F(1,12)=101.57$ ,  $p<.001$ , partial  $\eta^2=.9$ ; BC: M=12%, SE=7) condition.

### 3.2 fMRI results

#### 3.2.1 Theory of mind localizer

A whole-brain analysis on the ToM-localizer was conducted in which the story and the statement were modelled as one block. The pattern of results replicated previous findings in English (Dodell-Feder et al., 2010). That is, regions that are part of the ToM-network showed a higher BOLD response

during false belief stories versus false photograph stories (Table 1). These were clusters in the left and right temporo-parietal junction (TPJ), the left Precuneus, and the medial prefrontal cortex (mPFC). These clusters were interrogated in the subsequent ROI-analysis of the ToM-network.

#### 3.2.2 Action localizer

In order to identify regions that were sensitive to action execution, a whole-brain analysis was conducted on the localizer. Specifically, the moment of a button press, convolved with a canonical HRF,

**Table 4.** Brain regions from whole brain analysis of the implicature task showing significantly more activation during implied requests (IR) versus controls (PC, UC and BC) ( $p<.0001$ ,  $k>12$ ).

Region	Cluster level extent (voxels)	Peak voxel level		MNI coordinates		
		T	equivZ	x	y	z
Medial frontal cortex	323					
Right anterior cingulate cortex		9.08	4.89	15	32	25
Left anterior cingulate cortex		8.40	4.73	-3	44	19
Right anterior cingulate cortex		8.02	4.63	6	41	19
Right middle frontal gyrus	52	8.76	4.82	21	56	28
Right pars opercularis	21	6.92	4.32	45	17	13
Left precentral gyrus	13	6.76	4.26	-51	2	46
Right insular cortex	69					
Right insula lobe		7.77	4.56	39	26	-5
Pars triangularis		6.70	4.24	42	35	-2
Right putamen		6.02	4.01	24	23	-8
Left insular cortex	139					
Left insula lobe		8.08	4.65	-36	20	-5
Pars orbitalis		7.59	4.51	-39	23	-14
Thalamus	37					
Right thalamus		7.04	4.35	9	-7	7
Left thalamus		6.54	4.19	-6	-19	13
Right middle temporal gyrus	12	6.53	4.19	51	-49	13
Right posterior middle temporal gyrus	15	7.46	4.48	45	-31	-5
Posterior cingulate cortex	232					
Posterior cingulate cortex		9.03	4.88	-6	-37	22
Left middle cingulate cortex		8.17	4.67	-12	-40	37
Cingulate gyrus		8.09	4.65	6	-34	25
Left temporo-parietal junction	179					
Left supramarginal gyrus		9.07	4.89	-60	-46	28
Left angular gyrus		9.07	4.89	-48	-49	31
Right temporo-parietal junction	19					
Right supramarginal gyrus		6.46	4.16	63	-43	25
Right superior temporal gyrus		5.81	3.94	63	-52	22
Right supramarginal gyrus		5.49	3.81	51	-40	28
Right precuneus	53					
Right precuneus		11.16	5.31	6	-67	37
Right precuneus		6.42	4.15	18	-52	37
Left precuneus	21					
		9.90	5.07	-9	-64	37

was used as regressor. Since there were very specific anatomical predictions, the image was masked with an anatomical map of Brodmann area 6 and bilateral inferior parietal cortex (PF). Table 3 shows the peak activations within these regions. Specifically, activation peaks were found in left superior frontal gyrus (SFG), left precentral gyrus and left medial superior frontal gyrus. In functional terms these peaks are located within the left premotor cortex (PMd) and the left pre-supplementary motor area (pre-SMA). In addition, there were peak activations in the left and right inferior parietal lobule (IPL), overlapping with the supramarginal gyrus. The peak activations in the frontal motor regions (left SFG, left PCG and left pre-SMA) as well as the strongest activation peak in left and right IPL were used to create 6-mm spheres for the subsequent ROI-analysis.

### 3.3 Whole brain analysis

An overview of significant peak activations in the whole-brain analysis of the implicature task is depicted in Table 4. On the medial surface of the

brain, a widespread cluster of activation was found in the mPFC and the insular cortex, extending into the orbitofrontal gyrus. Additionally, regions in the posterior and middle cingulate cortex were sensitive to the manipulation. On the lateral surface, there were clusters of activation around the left and right temporo-parietal junctions. However, the latter was much more dominant in the left hemisphere. Lastly, both thalamci showed selective activation to IR.

### 3.4 ROI analysis

In the ROI analysis, ROI's from the ToM and Action localizer were interrogated with respect to the average percent signal change in the implicature task. All inferential statistics in this section were evaluated at an alpha level of  $p < .05$ . ANOVA's with repeated measures were corrected for violations of sphericity using Greenhouse-Geisser correction.

#### 3.4.1 Theory of mind ROI's

ANOVA's with repeated measures were conducted for each ROI from the ToM localizer

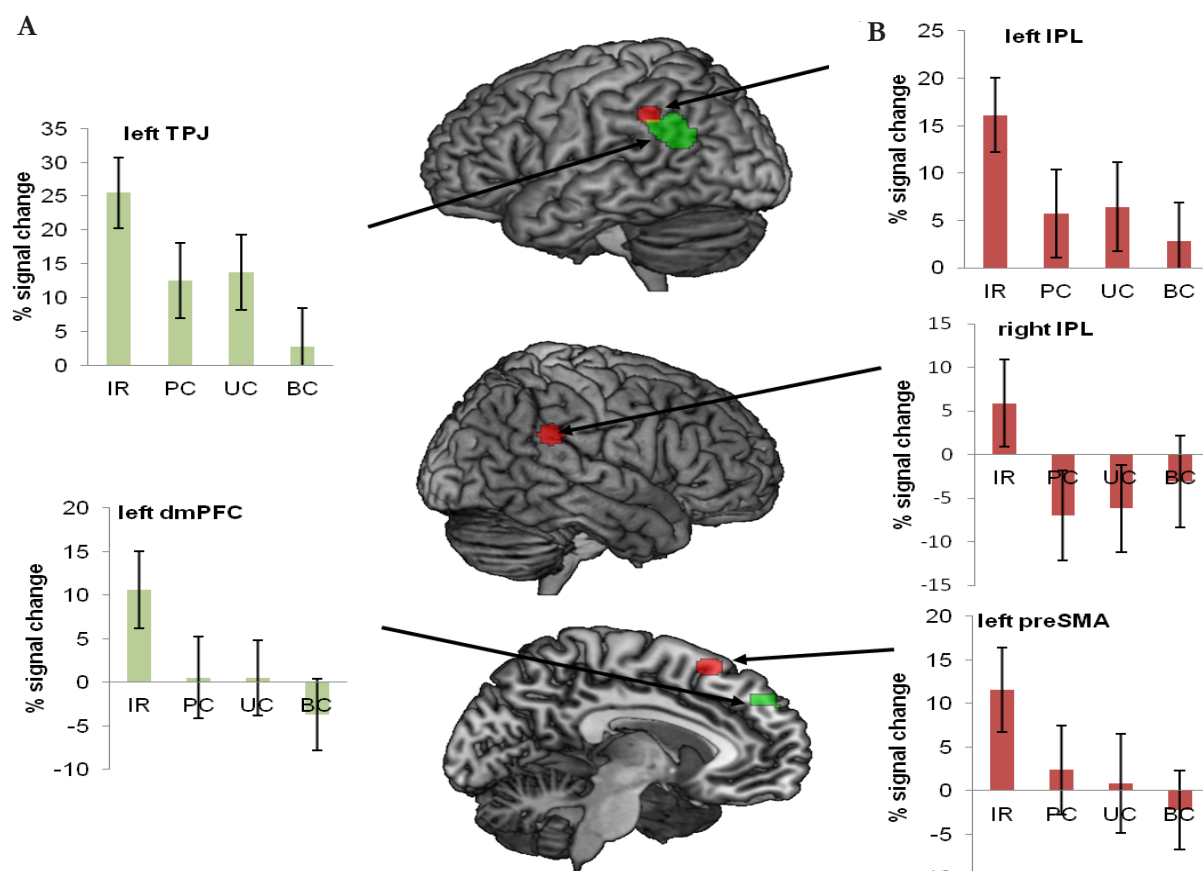


**Fig. 1** Regions of interest were interrogated with respect to the conditions IR, PC, UC, and BC. The image shows all ROI's, superimposed on a brain template. The bar diagrams illustrate mean percent signal change for each condition. The error bars depict the standard error. **A.** Green ROIs show regions from the ToM localizer (mPFC and TPJ). **B.** Red ROIs refer to regions that were activated during action execution (pre-SMA and bilateral IPL).

(mPFC, Precuneus, left TPJ and right TPJ) to test whether these regions were sensitive to implied requests. Interrogation of the mPFC revealed a significant main effect of condition ( $F(2.39,28.72)=4.68, p<.05$ , partial  $\eta^2=.28$ ). Planned comparisons indicated that the average percent signal change was higher in the IR condition than in the PC ( $F(1,12)=5.39, p<.05$ , partial  $\eta^2=.31$ ; IR:  $M=.11, SE=.04$ ; PC:  $M=.01, SE=.05$ ), UC ( $F(1,12)=14.14, p<.005$ , partial  $\eta^2=.54$ ; UC:  $M=.01, SE=.04$ ), and BC ( $F(1,12)=16.29, p<.005$ , partial  $\eta^2=.58$ ; BC:  $M=-.04, SE=.04$ ) condition (Figure 1A). ANOVA's on the left TPJ also revealed a significant main effect of the condition ( $F(2.35,28.21)=10.47, p<.001$ , partial  $\eta^2=.47$ ). Specifically, planned comparisons showed that average percent signal change was higher in the IR condition than in the PC ( $F(1,12)=15.19, p<.005$ , partial  $\eta^2=.56$ ; IR:  $M=.26, SE=.05$ ; PC:  $M=.13, SE=.06$ ), UC ( $F(1,12)=12.91, p<.005$ , partial  $\eta^2=.52$ ; UC:  $M=.14, SE=.06$ ) and BC condition ( $F(1,12)=27.02, p<.001$ , partial  $\eta^2=.69$ ; PC:  $M=.03, SE=.06$ ) (Figure 1A). In addition, the there was a significant main effect in the right TPJ ( $F(1.92,22.98)=5.04, p<.05$ , partial  $\eta^2=.3$ ). However, planned comparisons revealed that percent signal change in the IR condition were higher than in the PC ( $F(1,12)=11.91, p<.01$ , partial  $\eta^2=.5$ ; IR:  $M=.17, SE=.05$ ; PC:  $M=.06, SE=.1$ ) and BC condition ( $F(1,12)=8.6, p<.05$ , partial  $\eta^2=.42$ ; BC:  $M=-.03, SE=.05$ ), but not the UC condition ( $F(1,12)=3.33, p=.09$ ; UC:  $M=.10, SE=.06$ ). This suggests that the effect in the right TPJ is driven by the utterance alone, but not by the implicature. Lastly, the analysis of the Precuneus did not reach significance ( $F(1.78,21.33)=2.06, p>.1$ )

### 3.4.2 Action ROI's

ANOVA's with repeated measures were conducted for each of the five cytoarchitectonically, and functionally defined ROI's from the action localizer (left SFG, left PCG, left pre-SMA, left IPL and right IPL) to estimate the sensitivity of these areas to implied requests. Interrogation of the left pre-SMA revealed a significant effect of condition ( $F(2.21,26.5)=5.92, p<.01$ , partial  $\eta^2=.33$ ). Planned comparisons indicated that the level of activation in the IR condition was higher than in the PC ( $F(1,12)=9.86, p<.01$ , partial  $\eta^2=.45$ ; IR:  $M=.12, SE=.05$ ; PC:  $M=.02, SE=.05$ ), UC ( $F(1,12)=5.49, p<.05$ , partial  $\eta^2=.31$ ; UC:  $M=.01, SE=.06$ ) and BC condition ( $F(1,12)=16.94, p<.005$ , partial  $\eta^2=.59$ ; BC:  $M=-.02, SE=.05$ ) (Figure 1B). The analysis of the left IPL yielded a significant

effect of the condition ( $F(2.69,32.29)=9.63, p<.001$ , partial  $\eta^2=.45$ ). Planned comparisons indicated that the average percent signal change was higher in the IR condition than in the PC ( $F(1,12)=14.65, p<.005$ , partial  $\eta^2=.55$ ; IR:  $M=.16, SE=.04$ ; PC:  $M=.06, SE=.05$ ), the UC ( $F(1,12)=15.18, p<.005$ , partial  $\eta^2=.56$ ; UC:  $M=.06, SE=.05$ ), and the BC condition ( $F(1,12)=30.09, p<.001$ , partial  $\eta^2=.72$ ; BC:  $M=.03, SE=.04$ ) (Figure 1B). Also, there was a main effect of condition in the right IPL ( $F(2.68,32.17)=5.02, p < .01$ , partial  $\eta^2=.3$ ). Planned comparisons showed that average percent signal change was higher in the IR condition than in the PC ( $F(1,12)=13.77, p<.005$ , partial  $\eta^2=.53$ ; IR:  $M=.06, SE=.05$ ; PC:  $M=-.07, SE=.05$ ), UC ( $F(1,12)=10.58, p<.01$ , partial  $\eta^2=.47$ ; UC:  $M=-.06, SE=.05$ ), and BC condition ( $F(1,12)=6.2, p<.05$ , partial  $\eta^2=.34$ , BC:  $M=-.03, SE=.05$ ) (Figure 1B). However, ANOVA's with repeated measures, investigating the effect of condition in the left SFG and the left PCG did not reach significance ( $F(2.9,34.81)=1.34, p>.1$  and  $F(1.77,21.2)=.94, p>.1$ , respectively).

## 4. Discussion

Previous research has demonstrated that language referring explicitly to actions (e.g., action verbs, nouns referring to tools, action sentences) reliably activates motor areas in the brain (Glenberg & Kaschak, 2002; Hauk, Johnsrude, & Pulvermüller, 2004; Rüschemeyer et al., 2009; Tettamanti et al., 2005). In the current study we asked whether language used to refer implicitly to actions (i.e., without any explicit lexical reference to action) shows a similar pattern of activation. In other words, do implicit references to action activate neural motor areas in a manner similar to that seen for action verbs and nouns? To this end participants were presented with spoken utterances, some of which could be understood as implied requests (IR) for actions (e.g., "it is very hot here," as a request that one open the window), and some of which were simply descriptions of visual scenes (e.g., "it is very hot here," in the context of a dessert scene). The results indicate (1) that comprehension of IR sentences activates neural motor areas reliably more than comprehension of sentences devoid of any implicit motor information. This is true despite the fact that IR utterances contain no lexical reference to action. (2) Comprehension of IR sentences also reliably activates substantial portions of the theory of mind (ToM) network, known to be involved in making inferences about others' mental states (Frith & Frith, 2005, 2010; Gallagher & Frith, 2003; Saxe & Kanwisher, 2003). The implications of

these findings for embodied theories of language are discussed below.

#### **4.1 Implied requests and the neural motor system**

IR sentences activated areas within the larger neural motor system significantly more than sentences in any of the three control conditions (Figure 1B). This activation pattern was assessed in two ways: (1) In a ROI-analysis and (2) in a whole-brain analysis.

In the ROI analysis, voxels in BA 6 and bilateral IPL (PF) that were also sensitive to finger movements during the localizer task (button presses) were identified as ROI's. These regions comprised voxels in the left PMC, bilateral IPL and pre-SMA. Interrogation of these ROI's with regard to the four language conditions showed that the bilateral IPL and pre-SMA were sensitive to the implicit motor content in IR sentences. In other words, bilateral IPL and pre-SMA showed significantly greater activation for IR sentences than for sentences in any of the three control conditions. In the following paragraphs we discuss the potential role of the areas targeted by the ROI analysis to processing IR sentences.

The inferior parietal lobe is a sensorimotor area that is often associated with the representation of action goals (Fogassi et al., 2005). Fogassi and colleagues (2005) addressed this hypothesis using single cell recordings in non-human primates. The authors found that a different set of neurons fired when a monkey grasped food to put it in a container than when it was going to eat the food. In addition, some neurons showed the same dissociation during action observation. These results provide strong evidence that the IPL codes for the goal of an action. Recently, Aziz-Zadeh and Damasio (2008) have argued that the IPL encodes the set of sensorimotor events that coincide with action execution. For example, a movement such as grasping a cup will elicit somatosensory, proprioceptive, and visual feedback. The signals from these three different sources are aligned in time and therefore more likely to be associated in the brain (Aziz-Zadeh & Damasio, 2008). The integration of sensory information and action is particularly important for the functional manipulation of tools. Numerous neuropsychological studies have associated lesions in the IPL with a disability in manipulating objects and tools in a meaningful way (apraxia) (for a review see Wheaton & Hallett, 2007). The IPL is also consistently activated in studies investigating the comprehension of action-language (Rüschemeyer

et al., 2009). In a study using functional imaging, Rüschemeyer and colleagues (2009) found that the IPL was more sensitive to words denoting functionally manipulable objects (e.g., cup) as compared to volumetrically manipulable words (e.g., bookend). In sum, the type of action information stored in the IPL (i.e., information about complex action plan and how to manipulate objects) appears to be relevant both for executing actions and for processing conceptual information about tools and actions.

The pre-SMA is usually associated with executive aspects of motor control (Picard & Strick, 2001; Rushworth, Walton, Kennerley, & Bannerman, 2004). Specifically, Rushworth and colleagues (2004) have suggested that the pre-SMA is involved in selecting and changing between task-relevant action sets. That is, the selection of a specific response from a set of possible responses to a sensory stimulus. This idea is supported by the finding that changing an action set is perturbed if rTMS is applied to the medial SFG (REF). Although the pre-SMA is not consistently activated in studies investigating the comprehension of action-language, this is certainly not the first time that this area has been observed (e.g., Rüschemeyer et al., 2010; Postle, 2008). For example, Postle and colleagues investigated the sensitivity of neural motor system (BA6 and BA4) to action verbs and found that the pre-SMA but not M1 is sensitive to action verbs. In the current study, we argue that once a participant has understood that a request for action is being made, he/she must evaluate what action is being requested. The pre-SMA could potentially reflect the attempt of the listener to select the best action alternative from the set of possible actions one could perform in any given situation.

In the whole brain analysis activation elicited by IR stimuli compared to the three control conditions was assessed. The results demonstrate that IR sentences activated a fronto-parietal network comprising the posterior middle frontal gyrus, left precentral gyrus and several regions in the bilateral inferior parietal lobe, most notably the supramarginal gyrus. These results are largely consistent with the pattern observed in the ROI analysis, and thus provide converging evidence for the involvement of neural motor areas in the processing of IR sentences compared to sentences devoid of any motor content.

Our results indicate that language material devoid of explicit motor content activates neural motor areas in the brain if presented in a situation in which reference to an action is communicatively implied. This result stands in contrast to theories postulating a direct, invariable coupling between surface-level

language (e.g., the word-form) and the neural motor system (Pulvermüller, 1999, 2005).

Importantly, these results indicate that action information is retrieved during language comprehension at a higher level than lexical-semantics. Specifically, the current study suggests that action information becomes important at the level of speaker meaning, rather than lexical-semantics. In experimental paradigms, speaker meaning and lexical-semantics commonly overlap. For example, the word “kick”, presented in isolation, is unlikely to be understood to refer to anything other than a movement with the foot. However, in cases where speaker meaning diverges from lexical-semantics (e.g., implied requests and idiomatic phrases); embodied effects appear to reflect the global message that is conveyed by the utterance in context.

This hypothesis has direct implications for the questions how the language system and the neural motor system are related. It clearly stands in contrast to the idea that only word-forms activate action information directly and automatically (Pulvermüller, 1999, 2005). However, it is consistent with the idea that action information is only epiphenomenal (Mahon & Caramazza, 2008, 2009). Also, it supports a cascading perspective in which meaning is derived by concurrently evaluating both words and context, such as the visual scene in the current study (Meteyard et al., *in press*; Rüschemeyer et al., 2010).

## 4.2 Implied requests and theory of mind

In order to understand the message of an utterance, the listener needs to infer the communicative intent of the speaker (Grice et al., 1975). Making inferences about mental states of others is referred to as having a theory of mind (ToM). Recent neuroimaging studies have addressed the relationship between language and communication. Converging evidence suggests that the brain regions that correlate with communicative behaviour overlap with classical ToM regions, but not language regions (Sassa et al., 2007; Willems et al., 2010). For example, Willems and colleagues (2010) asked subjects to describe a word to another person. The authors manipulated the communicative intent of the speaker by claiming that the other person either knows, or does not know, the target word. In addition, Willems et al. manipulated the linguistic difficulty, by restricting the words a subject was allowed to use in the description. Specifically, the words had either a high or low semantic relation with the target word. The

results indicated that a region in the mPFC was sensitive to the communicative demands of the task while the linguistic demands were represented in the left IFG. Importantly, a region in the pSTS was sensitive to the interaction between linguistic and communicative demands of the task. A similar study by Sassa and colleagues (2007) found that the mPFC, the temporal poles and the left TPJ were sensitive to the communicative intention of the speaker. In sum, higher communicative task demands seem to correlate with higher activation of areas in the classical ToM network.

In the present study, IR sentences showed greater activation than control sentences in a network of areas known to be involved in solving ToM tasks. This was assessed using an ROI approach: during an independent scan participants performed a classic ToM task (Dodell-Feder et al., 2010), and areas were identified which were sensitive to the ToM manipulation. Specifically, voxels were identified that showed greater activation for processing false beliefs in contrast to inaccurate physical descriptions (for a more detailed description see Saxe and Kanwisher, 2003). As in previous studies, this contrast elicited activation in a network of areas including the mPFC, the Precuneus and the bilateral TPJ. Areas identified by the ToM localizer task also showed selective sensitivity for the comprehension of IR sentences. In other words, IR sentences showed more activation in ToM areas than sentences from any of the three control conditions. This suggests that understanding implied request for action requires a similar inference on the mental state of the speaker as classical theory of mind tasks. We speculate that the activation of action information in implied requests may be dependent on being able to reflect on the speaker’s mental state and potential communicative intent, however future research is needed to better characterize the connection between ToM abilities and language comprehension.

## 4.3 Summary and conclusion

The current study investigated whether utterances with no explicit reference to an action activate the neural motor system if the action is communicatively implied. Specifically, brain responses to sentence-picture combinations, with implied requests (IR), were compared to control statements (PC, UC & BC). The results showed that parts of the neural motor system were sensitive to IR sentences (pre-SMA and bilateral IPL). These findings are at odds with theories postulating a rigid coupling between the word-form and the action system (Pulvermüller,

1999, 2005). In addition, areas that were involved in thinking about mental states of others were also sensitive to IR sentences (mPFC, left TPJ); suggesting a joint contribution of the neural motor system and areas that are sensitive to communicative task demands.

Future research is needed to establish (1) functional connectivity between ToM and action areas during language processing, (2) the direction of information flow between these and other neural systems, and (3) the dependency of interpreting communicative intent on ToM abilities.

## References

- Aziz-Zadeh, L., & Damasio, A. (2008). Embodied semantics for actions: findings from functional brain imaging. *Journal Of Physiology Paris*, 102, 35-39.
- Barsalou, L. W. (1999). Perceptual symbol systems. *Behavioral Brain Science*, 22, 560-577.
- Barsalou, L. W. (2008). Grounded cognition. *Annual Review of Psychology*, 59, 617-645.
- Brett, M., Anton, J., Valabregue, R., & Poline, J. (2002). Region of interest analysis using an SPM toolbox [abstract]. 8th International Conference on Functional Mapping of the Human Brain June 26 2002 Sendai Japan.
- Caspers, S., Eickhoff, S.B., Geyer, S., Schepersjans, F., Mohlberg, H., Zilles, K., & Amunts, K. (2008). The human inferior parietal lobule in stereotaxic space. *Brain Structure and Function*, 212, 481-95.
- Caspers, S., Geyer, S., Schleicher, A., Mohlberg, H., Amunts, K., & Zilles, K. (2006). The human inferior parietal lobule: cytoarchitectonic parcellation and interindividual variability. *Neuroimage*, 33, 430-448.
- Clark, H. H., & Brennan, S. (1991). Grounding in communication. In L.B. Resnick, J.M. Levine & S.D. Teasley (Eds.) *Perspectives on Socially Shared Cognition*. (pp. 127-149). American Psychological Association .
- Creem, S. H., & Proffitt, D. R. (2001). Grasping objects by their handles: A necessary interaction between cognition and action. *Journal of Experimental Psychology Human Perception and Performance*, 27, 218-228.
- Dodell-Feder, D., Koster-Hale, J., Bedny, M., & Saxe, R.. (2010). fMRI item analysis in a theory of mind task. *NeuroImage*, 55, 705-712.
- Fischer, M. H., & Zwaan, R. A. (2008). Embodied language: a review of the role of the motor system in language comprehension. *The Quarterly Journal of Experimental Psychology*, 61, 825-850.
- Fogassi, L., Ferrari, P.F., Gesierich, B., Rozzi, S., Chersi, F., & Rizzolatti, G. (2005). Parietal lobe: from action organization to intention understanding. *Science*, 308, 662-667.
- Frith, C.D. & Frith, U. (2005). Theory of mind. *Current Biology*, 15, 644-645.
- Frith, U. & Frith, C.D. (2010). The social brain: allowing humans to boldly go where no other species has been. *Philosophical Transactions of the Royal Society*, 365, 165-176.
- Gallagher, H. L. & Frith, C. D. (2003). Functional imaging of "theory of mind." *Trends in Cognitive Sciences*, 7, 77-83.
- Geyer, S. (2004). The microstructural border between the motor and the cognitive domain in the human cerebral cortex. *Advances in Anatomy, Embryology and Cell Biology*, 174, 1-89.
- Glenberg, A.M. & Kaschak, M.P. (2002). Grounding language in action. *Psychonomic Bulletin & Review*, 9, 558-565.
- Grice, H. P., Cole, P., & Morgan, J. (1975). Logic and conversation. In P. Cole & Jerry L. Morgen (Eds.), *Syntax and Semantics, Vol.3, Speech Acts* (pp. 45-47) New York: Academic Press
- Hauk, O., Johnsrude, I., & Pulvermüller, F. (2004). Somatotopic representation of action words in human motor and premotor cortex. *Neuron*, 41, 301-307.
- Levinson, S. (1983). *Pragmatics* (Cambridge Textbooks in Linguistics). Cambridge University Press.
- Levinson, S. (2000). *Presumptive Meanings*. MIT Press.
- Mahon, B. Z. & Caramazza, A. (2008). A critical look at the embodied cognition hypothesis and a new proposal for grounding conceptual content. *Journal of Physiology Paris*, 102, 59-70.
- Mahon, B. Z. & Caramazza, A. (2009). Concepts and categories: a cognitive neuropsychological perspective. *Annual Review of Psychology*, 60, 27-51.
- Meteyard, L., Rodriguez Cuadrado, S., Bahrami, B.,& Vigliocco, G. (in press). Coming of age: a review of embodiment and the neuroscience of semantics. *Cortex* (Special Issue: Language and the Motor System).
- Picard, N. & Strick, P. L. (2001). Imaging the premotor areas. *Current Opinion in Neurobiology*, 11, 663-672. Elsevier.
- Postle, N., McMahon, K., Ashton, R.,& de Zubiray, G.I. (2008). Action word meaning representations in cytoarchitectonically defined primary and premotor cortices. *NeuroImage*, 43, 634-44.
- Pulvermüller, F. (1999). Words in the brains language. *Behavioral and Brain Sciences*, 22, 253-336.
- Pulvermüller, F. (2005). Brain mechanisms linking language and action. *Nature Reviews Neuroscience*, 6, 576-582.
- Raposo, A., Moss, H. E., Stamatakis, E. A., & Tyler, L. K. (2009). Modulation of motor and premotor cortices by actions, action words and action sentences. *Neuropsychologia*, 47, 388-396.
- Rüschemeyer, S. A., Rooij, D. van, Lindemann, O., Willems, R M, & Bekkering, H. (2009). The function of words: distinct neural correlates for words denoting differently manipulable objects. *Journal of Cognitive Neuroscience*, 22, 1844-1851.
- Rüschemeyer, S.-A., Glenberg, A. M., Kaschak, M. P., Mueller, K., & Friederici, A. D. (2010). Top-Down and Bottom-Up Contributions to Understanding

- Sentences Describing Objects in Motion. *Frontiers in Psychology*, 1, 1-11.
- Rushworth, M. F. S., Walton, M. E., Kennerley, S. W., & Bannerman, D. M. (2004). Action sets and decisions in the medial frontal cortex. *Trends in Cognitive Sciences*, 8, 410-417.
- Sassa, Y., Sugiura, M., Jeong, H., Horie, K., Sato, S., & Kawashima, R. (2007). Cortical mechanisms of communicative speech production. *NeuroImage*, 37, 985-992.
- Saxe, R., & Kanwisher, N. (2003). People thinking about thinking people - The role of the temporo-parietal junction in "theory of mind." *NeuroImage*, 19, 1835-1842.
- Slotnick, S. D., Moo, L. R., Segal, J. B., & Hart, J. (2003). Distinct prefrontal cortex activity associated with item memory and source memory for visual shapes. *Brain Research*, 17, 75-82.
- Tettamanti, M., Buccino, G., Saccuman, M.C., Gallese, V., Danna, M., Scifo, P., Fazio, F., Rizzolatti, G., Cappa, S.F., & Perani, D. (2005). Listening to action-related sentences activates fronto-parietal motor circuits. *Journal of Cognitive Neuroscience*, 17, 273-281.
- Wheaton, L.A. & Hallett, M. (2007). Ideomotor apraxia: a review. *Journal of the Neurological Sciences*, 260, 1-10.
- Willem, R. M., De Boer, M., De Ruiter, J. P., Noordzij, M. L., Hagoort, P., & Toni, I. (2010). A dissociation between linguistic and communicative abilities in the human brain. *Psychological Science*, 21, 8-14.

# **Neuronal Responsiveness in Rat Primary and Secondary Somatosensory Cortex is Differentially Affected by Brain State**

Lieneke Janssen<sup>1</sup>

Supervisors: Anne Fransen<sup>1</sup>, George Dimitriadis<sup>1</sup>, Eric Maris<sup>1</sup>

*<sup>1</sup>Donders Institute for Brain, Cognition and Behaviour, Radboud University Nijmegen, The Netherlands*

Perception and its underlying neurophysiological activity are affected by the current state of the brain. Processing of sensory input has been shown to differ with sleep, depth of anesthesia, and different levels of wakefulness (e.g. locomotion, quiet wakefulness). Along these lines, UP and DOWN states can be distinguished as two discrete, alternating states that occur during slow wave sleep and anesthesia. Recordings from single neurons and populations of neurons within cortical areas suggest that neuronal properties and network dynamics differ between these states, while they are highly similar for the UP state and wakefulness. Here we addressed the question how brain state affects tactile processing on the interregional network level. By comparing ketamine anesthesia to wakefulness and recording intracranial EEG from an epidural 32-microelectrode array overlying barrel cortex (SI) and secondary somatosensory cortex (SII) in rats ( $n=2$ ), we showed that neuronal responsiveness (i.e. N1 amplitude) in SI was much larger under anesthesia as compared to wakefulness. Additionally, N1 amplitude varied highly under anesthesia and was negatively associated with prestimulus gamma power (60-100Hz). In contrast, SII was only found to be involved in tactile processing during wakefulness. This was likely due to inhibited recurrent processing between SI and SII under anesthesia, which may disrupt interaction between cortical areas while leaving thalamic input to primary sensory cortex intact. Together these preliminary findings suggest that neuronal responsiveness in SI and SII is differentially affected by the current state of the brain, reflecting the complexity of the brain's ability to control neuronal communication effectively.

*Keywords:* ongoing activity, tactile processing, barrel cortex, secondary somatosensory cortex (SII), gamma, oscillations, intracranial EEG

---

Corresponding author: Lieneke Janssen, e-mail: lieneke.janssen@gmail.com

## 1. Introduction

Ongoing network activity defines the state of the brain and determines information processing capacities of the neuronal network. Dynamic modulation of processing capacities, as indexed by responsiveness to sensory stimuli, reflects the ability of the network to control the flow of communication (Haider & McCormick, 2009). Sensory processing may thus critically depend on the instantaneous state of the network.

The state of the network requires a careful balance between excitation and inhibition (Shu et al., 2003; Haider et al., 2006; Haider & McCormick, 2009), and is strongly affected by cholinergic and noradrenergic neuromodulation (Goad & Dan, 2009; Hirata & Castro-Alamancos, 2010; Constantinople & Bruno, 2011). These neurotransmitters are generally associated with arousal, which is correlated with the level of activity during wakefulness. Accordingly, a range of behavioral states (e.g. quiet and active waking) has been shown to affect sensory processing differentially (Fanselow & Nicolelis, 1999; Ferezou et al., 2006, 2007; Niell & Stryker, 2010). In line with findings from Fanselow and Nicolelis (1999), Ferezou et al. (2006, 2007) showed reduced responsiveness of neurons in barrel cortex to whisker deflection when mice were behaving actively (e.g. whisking or moving freely) as compared to when they were being inactive during wakefulness. Reduced responsiveness was likely due to higher levels of arousal during action (Constantinople & Bruno, 2011). But also in the absence of overt behavior, different states of the brain, as reflected in deeper levels of sleep or anesthesia, can reduce responsiveness to sensory stimuli (Erchova et al., 2002; Devonshire et al., 2010).

Further insights in ongoing activity and its effect on sensory processing mainly come from studies focusing on slow oscillations in the range of 0.5–4Hz. Slow oscillations occur during non-REM sleep and under anesthesia (Steriade et al., 1993; Contreras & Steriade, 1995; Steriade & Amzica, 1998; Destexhe et al., 1999; Crunelli & Hughes, 2010), and are sometimes observed during quiet wakefulness (Petersen et al., 2003; Crochet & Petersen, 2006; Poulet & Petersen, 2008). Slow oscillations arise from two discrete alternating states, namely a state of neuronal activity and one of neuronal quiescence, commonly referred to as UP and DOWN state, respectively (Contreras & Steriade, 1995; Shu et al., 2003; Alkire et al., 2008). UP states are characterized by membrane potentials close to firing threshold

and high-conductance, resulting in spontaneous firing rates similar to wakefulness. Instead, DOWN states are characterized by low membrane potential and low-conductance, resulting in the absence of spontaneous firing (Destexhe et al., 2003). These characteristics differentially affect the integrative properties of neurons. When injecting current into neurons that are either in the UP or the DOWN state, neurons respond vigorously in an UP, but not in a DOWN state (Hasenstaub et al., 2007). Paradoxically, in barrel cortex it has been consistently shown that neuronal responsiveness to somatosensory stimulation is reduced in the UP state as compared to the DOWN state (Petersen et al., 2003; Sachdev et al., 2004; Haslinger et al., 2006; Hasenstaub et al., 2007). According to Petersen et al. (2003), the depolarized membrane potential in the UP state likely results in a reduced excitatory and increased inhibitory driving force. This is in line with findings of Destexhe et al. (2003), suggesting that the high-conductance nature of the UP state is dominated by high inhibitory conductance.

The neuronal properties of the UP state have been shown to be remarkably similar to the neuronal properties during wakefulness (Destexhe et al., 1999, 2003, , 2007). The similarity between the UP state and wakefulness also becomes apparent in the desynchronized fast (low amplitude) EEG activity observed in both states. Destexhe et al. (2007) thus argue that UP states are ‘fragments of wakefulness’. However, most findings contributing to this notion come from studies on single neurons or a population of neurons within a cortical area, often in rat or mouse barrel cortex (Steriade et al., 1993; Destexhe et al., 1999, , 2003; Bartos et al., 2007; Haider & McCormick, 2009). Little is known about the resemblance of neuronal responsiveness between the UP state and wakefulness on network level, beyond primary somatosensory cortex (SI).

In this study, we investigate how ongoing activity in different brain states affects tactile processing on the network level. In particular, our aim was to shed light on the degree of resemblance between the UP state and wakefulness. To achieve that we addressed two questions, namely: 1) how does tactile processing in SI and SII compare between wakefulness and anesthesia in rats? and 2) how do the rapid alterations in ongoing activity under anesthesia affect tactile processing in SI and SII?

In contrast to classical whisker deflection, we presented tactile stimulation to the rat’s upper lip. For this purpose we have developed a stimulation device based on a Braille cell that enabled us to stimulate the microvibrissal area in a controlled

way, while allowing the rat to move freely. Brain state was manipulated by using ketamine anesthesia which is known to result in stable UP and DOWN states (Destexhe et al., 1999, , 2007; Crunelli & Hughes, 2010), and which preserves amplitude of somatosensory evoked potentials (Goss-Sampson & Kriss, 1991). Ketamine anesthesia was contrasted to wakefulness. Intracranial EEG data was recorded from barrel cortex (SI) and SII using a relatively novel method, namely a flexible 32-microelectrode array implanted epidurally (Hosp et al., 2008). This enabled us to study interregional network activity in the rat somatosensory cortex during both anesthesia and wakefulness.

## 2. Materials and methods

### 2.1 Animals

Five outbred, male Long-Evans rats (12-15 months old, 600-700g) participated in the experiment. Due to bad signal quality in three of these, we only report the results of the remaining two animals here. Rats were housed in pairs in type IV macrolon cages. Cage tops were heightened by 8 cm to increase the rats' exploring behavior on hind paws and to reduce the risk of the recording chamber getting stuck in the mesh cage tops. In addition to sawdust bedding and brown nesting materials, cages were enriched with a red tinted tunnel, small amounts of foraging materials, and Nestlets to promote natural rat behavior. Rats were kept in a 12/12h reverse day/night cycle. In both the housing and the experimental

room, temperature and humidity were kept constant around 21-22°C and 50-70%, respectively. Food and water were available ad libitum. All experiments were in accordance with the Dutch law concerning animal welfare and approved by the Committee for Animal Experiments of the Radboud University Nijmegen, The Netherlands. All efforts were made to minimize animal suffering.

### 2.2 Surgery

Rats underwent surgery in which a flexible 32-channel microelectrode array was implanted between the skull and dura, overlying barrel cortex and part of SII (Figure 1A). The side of the implant (left or right hemisphere) was alternated across surgeries. Prior to surgery, rats received 5 mg/kg Rimadyl s.c. and 20 µg/kg Temgesic s.c. (analgesics), 0,5 mg Atropine i.m. (muscle relaxant), and 1 mg/kg Dexamethason i.p. (anti-inflammatory, to reduce brain swelling). Surgery was performed while the animal was placed in a stereotactic frame and anesthetized with isoflurane (2-3%). Body temperature was monitored rectally and supported by a heating pad if necessary. A craniotomy of 2.5 x 5.5 mm (coordinates relative to Bregma: 1.5 mm anterior, 4 mm posterior, 1.5-4 mm lateral) was performed using a dentist drill (Piezosurgery, Mectron). While the brain tissue was exposed, PBS (0.1M) was repeatedly applied to wet the brain. After separating the dura from the skull at the lateral side of the cranial window, the electrode array was carefully inserted through the cranial window to a depth of

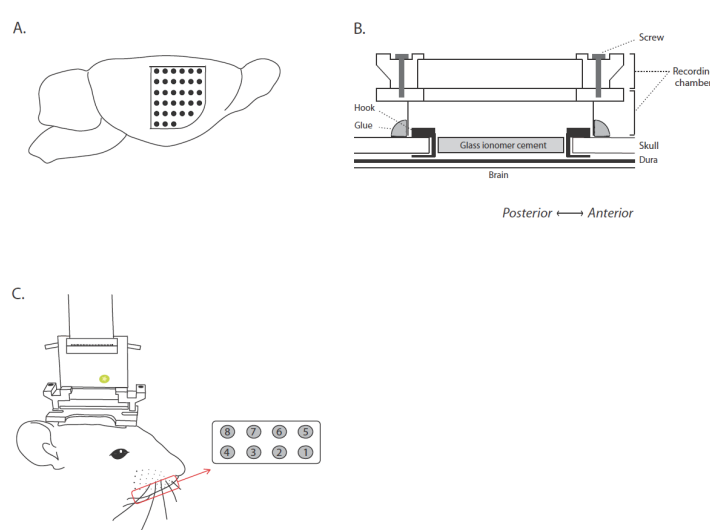


**Fig. 1** Surgery procedure and experimental setup. **A.** The position of the 32-channel microelectrode array overlying barrel cortex and part of SII. **B.** A schematic drawing of the recording chamber as it is anchored to the skull using hooks and UV-curable glue. **C.** During experiments, data was acquired by connecting a head stage to the recording chamber and stimuli were presented to the target area (marked by the red box) of the rat's snout by a Braille cell consisting of 8 independently movable pins.

5.5-6 mm, after which the cranial window was sealed with glass ionomer cement (GC Fuji). Additionally, a skull reference was placed. The microelectrode array was connected to a PCB board and fixed onto a metal scaffold (i.e. the recording chamber). Hooks were placed at the anterior and posterior end of the cranial window, parallel to the midline, such that they clamped around the skull. The hooks and UV curable glue (Venus Flow, Heraeus) anchored the recording chamber to the skull (Figure 1B). Generally, recording chambers remained in place for 2-3 months ( $N = 5$ ,  $M = 11.2$  weeks,  $SD = 3.6$ ).

### 2.3 Experimental setup

We have developed a novel way to present the rat with controlled tactile stimulation while allowing the animal to move freely (Figure 1C). By mounting a device onto the recording chamber that holds a piezoelectric Braille cell (Metec, Stuttgart, Germany), containing 2 rows of 4 independently operable pins each, rats were enabled to move freely during stimulation, in contrast to classical whisker deflection. The device consists of a cap that can be screwed onto the recording chamber before every experimental session. Attached to the cap is an arm that holds the Braille cell touching the rat's upper lip. To ensure controlled stimulation across sessions, we made a customized device for each rat.

Brain state was manipulated by applying anesthetic drug. Rats were injected with a mixture of ketamine/dexmedetomidine, (0.75 mg/kg; 0.1 mg/kg, i.p.). Recordings under anesthesia were compared with recordings in wakefulness. Recording sessions under anesthesia generally lasted for 35-45 min. (due to the duration of the anesthetics), whereas awake sessions lasted up to 1h. Although rats were unrestrained and able to move freely in the awake condition, they were mostly in a state of quiet wakefulness.

During the experiment, rats were stimulated contralaterally to the side of the implanted electrode array. On each trial one pin was raised, and lowered again after 20 ms. Intertrial intervals varied randomly between 1.5 and 4.5s (awake) and between 1.5 and 2.5s (anesthesia). We ran 2 awake and 3 anesthesia sessions per rat. The order in which pins were raised was randomized and every pin was stimulated  $\pm 100$  times (with the exception of 1 awake session: only  $\pm 35$  trials per stimulation site). Sessions were consistently run around noon and rats participated in no more than one session per day. Tactile stimulation was randomly paused 3 times every session for at least 20s. These periods were used to investigate

differences in ongoing activity between anesthesia and wakefulness.

Local field potentials (LFPs) from the 32-channel microelectrode array were acquired using Neuralynx hardware (DigitalLynx10S, Neuralynx, Inc.) and software (Cheetah 5, Neuralynx, Inc.). Channels were skull referenced. The recorded signal was pre-amplified (gain = 1), high-pass filtered at 0.5 Hz, and digitized at 5 kHz. All recordings were done in a dark and sound-shielded Faraday cage. Infrared led light enabled us to monitor the animal's overt behavior on video.

### 2.4 Histological assessment

After the last recording session, four animals were euthanized with an overdose of ketamine/xylazine. The remaining animal was still taking part in experiments at the time of staining. To verify the exact location of the multi-electrode array and to exclude potential brain damage due to surgery, we performed post-mortem examination of the cortical area underlying the array. The cortices were flattened and fixated overnight in formaldehyde (4%). Tangential slices of 150  $\mu$ m were made using a vibratome and stained with cytochrome oxidase to visualize the barrels. Slices were mounted on slides using Aqua-Poly/Mount and then cover-slipped.

### 2.5 Data analysis

All data-analyses were performed using custom-written functions and the open-source FieldTrip Toolbox (Oostenveld et al., 2011) in Matlab (Mathworks, <http://www.mathworks.com>).

#### 2.5.1 Anesthesia vs. wakefulness

Averaged event related potentials (ERPs) were calculated for each stimulation site and for each state (awake, anesthesia), with a 300ms prestimulus baseline interval. Topographic plots at several time points were constructed to examine the spatial dynamics of the ERPs. No differences were observed in the evoked responses between stimulation sites for both states. Therefore, trials were pooled over stimulation sites in subsequent analyses. Trials and channels that were excessively noisy (e.g. exhibiting clipping or jumps) were removed from the analyses.

We investigated differences in power and coherence between anesthesia and wakefulness. Both measures were calculated based on 6-second data segments in which no stimuli were presented.

This duration was chosen such that spectral power could be estimated for slow oscillations (0.5-4Hz), and such that the number of segments acquired from the stimulus free-periods was optimized. Spectral power was estimated between 0.5-120Hz using the multitapering method (Percival & Walden, 1993) with 5Hz smoothing. The power difference was quantified as a power ratio, obtained by dividing power during anesthesia by power during wakefulness for all frequencies. Coherence is a frequency-indexed measure of the phase consistency between two channels. Coherence was calculated as the normalized cross-spectrum, with normalization by the square-root of the power estimates in the two channels. Coherence was calculated for all possible channel pairs and for all frequencies.

### 2.5.2 Selection large vs. small N1 amplitude trials

To study the effect of ongoing network activity under anesthesia on differential neuronal responsiveness, trials were split into two groups. The initial aim was to separate trials based on prestimulus network activity by identifying the state of the brain (i.e. UP or DOWN) at the time of stimulus onset. However, identifying UP and DOWN states from EEG data alone has proven to be very difficult and unreliable, and is still a matter of debate (Steriade & Amzica, 1998; Cash et al., 2009; Amzica, 2010). In the absence of information on firing rate or membrane potential, UP and DOWN states cannot be identified unequivocally. Therefore, trials were split up into groups based on neuronal responsiveness, namely the amplitude of the early N1 component, which is known to arise in SI (Jellema et al., 2004). The rationale for this was that neuronal responsiveness in SI was previously found to vary highly under anesthesia on a trial-to-trial basis, which likely reflects differences in neuronal responsiveness between UP and DOWN states (Erchova et al., 2002; Petersen et al., 2003; Jellema et al., 2004; Sachdev et al., 2004). Trials were selected on a single-trial basis in the channel with the strongest N1 response (referred to as selection channel). As a measure for N1 amplitude, the average N1 amplitude in a 15-35ms poststimulus interval (N1\_Int) was subtracted from a -20-0ms prestimulus baseline interval (B\_Int), and thresholded separately for large and small N1 trials.

$$\text{N1 measure} = \text{B\_Int} - \text{N1\_Int}$$

To prevent false positives (e.g. trials with a high baseline value, due to high amplitude fluctuations

under anesthesia, and small N1 amplitude), the additional criterion of a minimum N1 amplitude for large and a maximum N1 amplitude for small N1 trials was applied. Thresholds of the N1 measure and minimum/maximum criterion were chosen such that the distribution of trials within each group (large and small) in the anesthesia condition was similar. The same criteria were applied to the awake condition, which resulted predominantly in small N1 amplitude trials (large N1 trials: 0.4%).

### 2.5.3 Prestimulus power

After selection, we estimated time-resolved spectral power (0.5-120Hz) for both groups in a time-window of -1 to 0 s prestimulus using a Hanning window. For the anesthesia condition, the power ratio was calculated by dividing the prestimulus power of large N1 trials by the prestimulus power of small N1 trials per frequency. Because of the absence of large N1 amplitude trials in the awake condition, no power ratio could be calculated. The logarithm of the power ratio was taken as a measure of the difference between both selected groups.

### 2.5.4 Statistics

In all cases where single-channel differences were tested statistically, the independent t-test was applied. Instead, when statistics involved all channels, analyses were done using cluster-based permutation (with the independent t-test as test statistic), based on 500 permutations. The type-1 error rate was controlled at 0.05, correcting for multiple comparisons.

The normalized effect size for the difference in prestimulus gamma was calculated as follows:

$$\text{Normalized effect size} = \frac{\bar{X}_{\text{large}} - \bar{X}_{\text{small}}}{(\text{SD}_{\text{large}} + \text{SD}_{\text{small}})/2}$$

Where  $\bar{X}_{\text{large}}$  and  $\bar{X}_{\text{small}}$  are the mean broadband gamma power in the range of 60-100Hz (-120-0ms prestimulus) for large and small N1 trials, respectively;  $\text{SD}_{\text{large}}$  and  $\text{SD}_{\text{small}}$  denote the accompanying standard deviations. This normalized effect size expresses the mean difference in standard deviation units (i.e. the average standard deviation of the two groups). This measure can be interpreted in terms of the overlap between the two distributions of broadband gamma power (i.e. large and small N1 trials): assuming a normal distribution, a value of 0 corresponds to a 100% overlap between the two distributions, a value 0.5 to a 80% overlap, a value of 1 to a 62% overlap, etc.

### 3. Results

We recorded intracranial EEG from 2 rats (B2R7 and B2R10; right and left hemisphere respectively), during wakefulness and ketamine anesthesia. Signals were obtained using an epidural 32-microelectrode array overlying barrel cortex (SI) and part of secondary somatosensory cortex (SII). Post-mortem assessment of the brain ( $N = 2$ ) showed that there was no damage underneath the implanted electrode array (Figure 2A). Cytochrome oxidase staining ( $N=1$ ) revealed the exact location of the electrode array relative to the barrel cortex and verified that we recorded from barrel cortex and SII (Figure 2B). Tactile stimuli were presented to the rat's upper lip using a Braille cell, targeting 8 separate sites within the area. Since no differences were observed in the evoked responses between stimulation sites, trials were pooled across them in subsequent analyses. After cleaning the data, 0.5-0.8% of the trials in the anesthesia condition and 2.5-3.3% of the trials in the awake condition were removed. The total number of trials remaining for each rat in each condition can be found in Table 1. Additionally, due to bad signal quality, 4 channels from rat B2R7 and 11 channels from rat B2R10 were removed. Removed channels could be reconstructed by linear interpolation, but only reliably for rat B2R7. Therefore, topographies were calculated for rat B2R7 only.

#### 3.1 ERPs under anesthesia and during wakefulness exhibit quantitative and qualitative differences

To investigate how tactile processing compares between wakefulness and anesthesia in general, we first calculated averaged ERPs for both conditions and compared them statistically. The averaged ERPs differed significantly in amplitude in the channel cluster covering SI, most prominent in the early N1 peak ( $t = 25\text{ms}$ ), which was stronger (more negative;  $p < 0.01$ ) under anesthesia than during wakefulness (Figure 2C, E). Quantitatively, the ERPs differed in their spatiotemporal pattern. The first negative peak mainly covered the barrel cortex, although the exact location differed slightly between the awake and anesthesia condition (Figure 2D1, F1). In the awake condition there was a second negative peak ( $t = 55\text{ms}$ ), which was larger than the initial negative peak in wakefulness and which was highly specific to the recording sites covering SII (Figure 2F). Under anesthesia, no SII activity was observed (Figure 2D).

We then characterized the ongoing activity under

anesthesia and in wakefulness in terms of power and coherence. Respectively 23 and 30 segments were acquired from the stimulus-free periods for rat B2R7 and B2R10. Although slow oscillations similar to those observed during anesthesia and sleep were previously found to occur in quiet wakefulness as well (Petersen et al., 2003; Crochet & Petersen, 2006; Petersen, 2007), we only observed these oscillations in the anesthesia condition, not in (quiet) wakefulness.

Figure 3A shows the power ratio of stimulus-free periods, i.e. power during anesthesia divided by the power during wakefulness, for each animal. For both animals, power in the lower frequencies ( $<20\text{Hz}$ ) was notably higher for the anesthesia condition as compared to the awake condition. Between 0.5-4Hz and between 5-10Hz there were clear peaks in the power ratio. The former reflected the relatively high-amplitude slow oscillations that are mainly present during anesthesia (Steriade et al., 1993; Contreras & Steriade, 1995; Alkire et al., 2008; Haider & McCormick, 2009; Crunelli & Hughes, 2010), whereas the latter was likely to reflect the high-amplitude bursts, or K-complexes present during anesthesia (Steriade & Amzica, 1998; Alkire et al., 2008). In addition, for both animals there was a decrease in power in intermediate frequencies, and a slight increase in power in high frequencies for anesthesia as compared to wakefulness, although the exact frequencies differed between animals (i.e. 25-65Hz (intermediate) & 80-120Hz (high) versus 20-50Hz (intermediate) & 50-85Hz (high)).

There were also differences between anesthesia and wakefulness in the averaged coherence across recording sites. In fact, we observed a difference in the averaged coherence of slow oscillations (0.5-4Hz) for rat B2R7, but not for rat B2R10, and a difference in the averaged coherence of low gamma oscillations (45-65Hz) for rat B2R10, but not for rat B2R7 (Figure 3B). We cannot explain the difference between animals. However, the observed differences in coherence between conditions may be explained in terms of the extent of coherence in these frequency bands. If coherence is high over longer distances, the averaged coherence will also be high, whereas coherence limited to nearby channel pairs (i.e. local coherence) will lead to low averaged coherence. One might expect the extent of gamma coherence to be reduced for the anesthesia as compared to the awake condition (Alkire et al., 2008), whereas the extent of coherence of slow oscillations is expected to be larger for the anesthesia condition (Steriade et al., 1993; Destexhe et al., 1999). We investigated this hypothesis by calculating the distance between

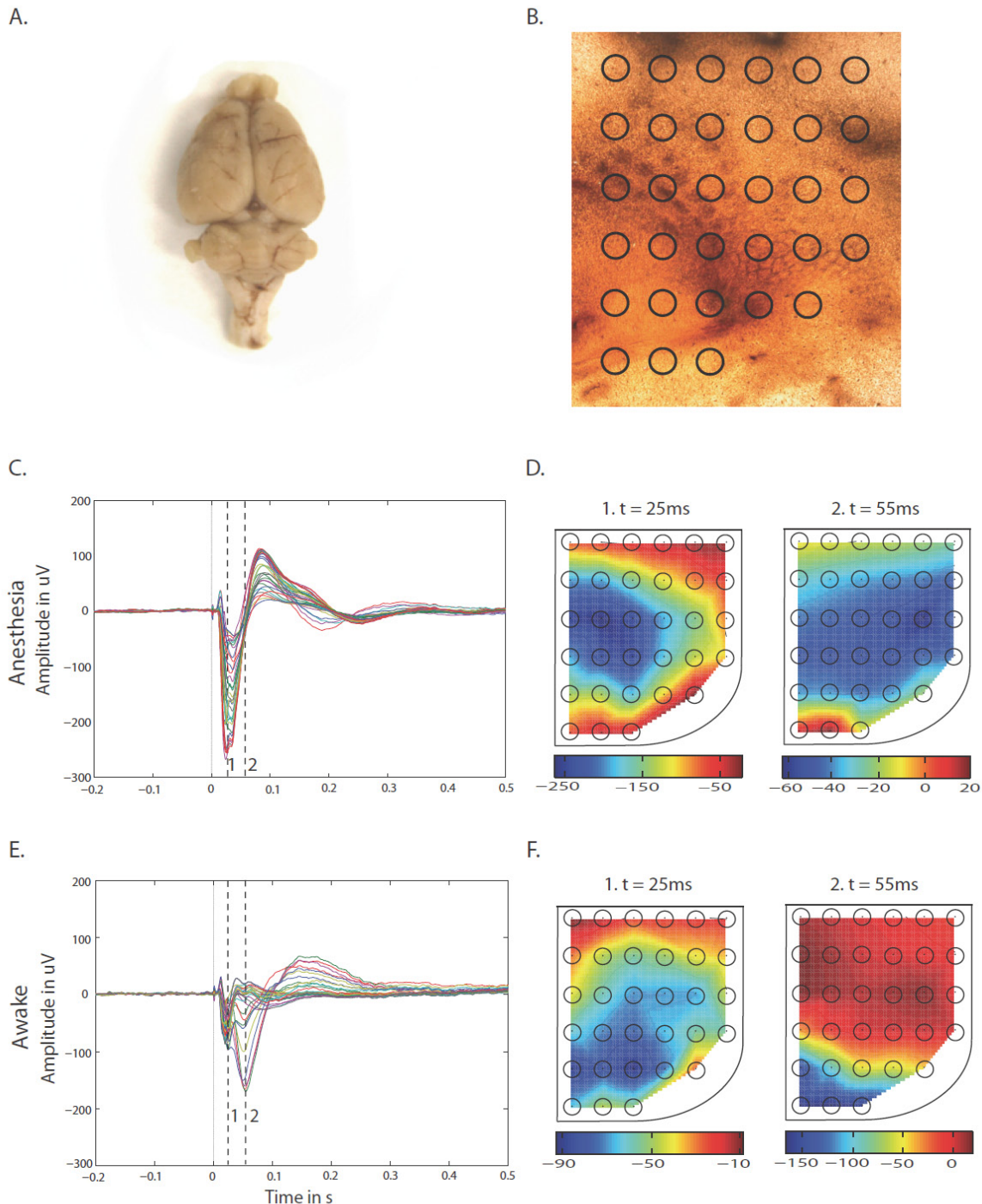


**Fig. 2** Evoked responses of tactile stimulation over barrel cortex and part of SII under anesthesia and during wakefulness. **A.** Picture of the undamaged brain of rat B2R10 (left hemisphere implant). **B.** Overlay of the electrode array and the cytochrome oxidase staining of rat B2R7 brain sections (right hemisphere implant), showing electrodes covering the barrel cortex and part of SII (lower left corner). **C.** The averaged ERP under anesthesia and **E.** during wakefulness (separate lines represent the different channels) differed significantly ( $p < 0.01$ ). Time = 0 denotes stimulus onset. In **D.** the topographies of the ERP at times  $t = 25$  and  $55$  ms are shown for the anesthesia condition. In **F.**, likewise for the awake condition. The topographies show the difference in spatiotemporal pattern between the conditions, i.e. despite the presence of an early negative peak over barrel cortex in both conditions, a second negative peak over secondary somatosensory cortex is only observed in the awake condition. Note: color bars are scaled differently.

electrode pairs and averaging coherence for both frequency bands per distance. The extent of coherence was compared between anesthesia and wakefulness. With increasing distance between electrode pairs, coherence generally decreased for both frequency bands. No differences were observed in the degree of this decrease over distance (i.e. the extent) between anesthesia and wakefulness (results not shown).

### 3.2 Dissociating differential neuronal responsiveness under anesthesia based on N1 amplitude

To study the effect of ongoing network activity under anesthesia on neuronal responsiveness, ERPs were split up into two groups. Identifying UP and DOWN states in the ongoing activity in EEG data alone proved to be unreliable and highly subjective. However, in accordance with previous literature, neuronal responsiveness in SI was observed to vary highly across trials (Erchova et al., 2002; Petersen et al., 2003; Jellema et al., 2004; Sachdev et al., 2004). Therefore, the ERPs were split up based on neuronal responsiveness, namely the amplitude of the N1 component arising in SI (around  $t = 25\text{ms}$ ), and prestimulus activity was analyzed in terms of spectral power.

N1 amplitude was quantified as described in the methods section. In Table 1, a summary of the selection procedure and outcome is given. For rat B2R7, the selection resulted in 871 large N1 trials and 821 small N1 trials under anesthesia. For rat B2R10, the selection resulted in 914 large N1 trials and 881 small N1 trials under anesthesia. In the awake condition only 0.4% of the trials were classified as large. Here, we focused only on large and small N1 amplitude trials under anesthesia. Selection under anesthesia was verified by testing the difference between the averaged small and large N1 amplitudes statistically. As shown in Figure 4A, N1 amplitude

in the selection channel was significantly different between both groups ( $t < -20.0$ ,  $p < 0.0001$ ). This difference was not limited to the selection channel, but extended to the neighboring channels that also showed an N1. Instead, the average N1 amplitude of small N1 trials was more similar to the average N1 amplitude observed in the awake condition. However, neither group under anesthesia displayed an SII peak as observed in the awake condition. Note that the averaged ERPs for large and small N1 trials also differed in the baseline period, reflected by the 100ms prestimulus bump for large N1 trials in the selection channel (Figure 4A). This difference could not be readily explained. To rule out a selection bias towards a specific stimulation site or time in the experiment (i.e. the duration of anesthesia), the distribution of selected trials was taken into account. The percentage of trials per stimulation site did not show differences between groups, except for site 5 (Figure 4B). However, this one exception does not represent a clear bias in terms of stimulation site. In addition, there was no sign of selection bias in terms of time (Figure 4C).

### 3.3 High prestimulus gamma power is associated with small sensory evoked responses

We then investigated whether the ongoing network activity could dissociate between the large and small N1 amplitude groups under anesthesia. Therefore we estimated time-resolved power in the 1s prestimulus interval for all selected trials. On average, we found that for the selection channel, large N1 trials were preceded (-120-0ms) by significantly less power in broadband gamma (60-100Hz) as compared to small N1 trials in both animals ( $t < -10$ ,  $p < 0.0001$ ). In Figure 4D, this effect is shown in terms of the logarithm of the power ratio (power large N1 trials/power small N1 trials), where a value below 0 denotes a decrease in power for large as

**Table 1.** Summary of N1 selection procedure.

Animal	Selection	Selection criteria		Number of trials	
		[Baseline - N1]	Min N1	Anesthesia	Awake
	All trials			2962	1288
B2R7	Large	> 250	< -325	871	1234
	Small	< 250	> -250	821	5
	All trials			3013	1681
B2R10	Large	> 325	< -500	914	1607
	Small	< 325	> -400	881	7

compared to small N1 trials. For rat B2R10 a more general decrease in power (20-100Hz) was observed for large as compared to small N1 trials. Despite a difference between animals in the precise frequency band and time-interval for which the decrease is shown, the effect was present for both animals in broadband gamma for at least 120ms prestimulus. Moreover, the decrease in power in broadband gamma for large N1 trials was shown to be reduced in all other channels, comprising 1 large cluster, as can be seen in Figure 4E (N = 1; p < 0.0001). The difference in prestimulus gamma power between large and small N1 trials cannot be ascribed to the

poststimulus difference in ERPs, because our power estimates were calculated on the prestimulus signal only.

To address the question of whether this prestimulus effect in broadband gamma exists on a single-trial basis, we averaged prestimulus power in the 60-100Hz frequency bin over the -120-0ms prestimulus interval and plotted it against the minimum N1 amplitude in the N1 amplitude interval (15-35ms poststimulus) for each selected trial (Figure 4F). Although the effect clearly exists on average, it was not the case that high prestimulus gamma power consistently preceded small sensory

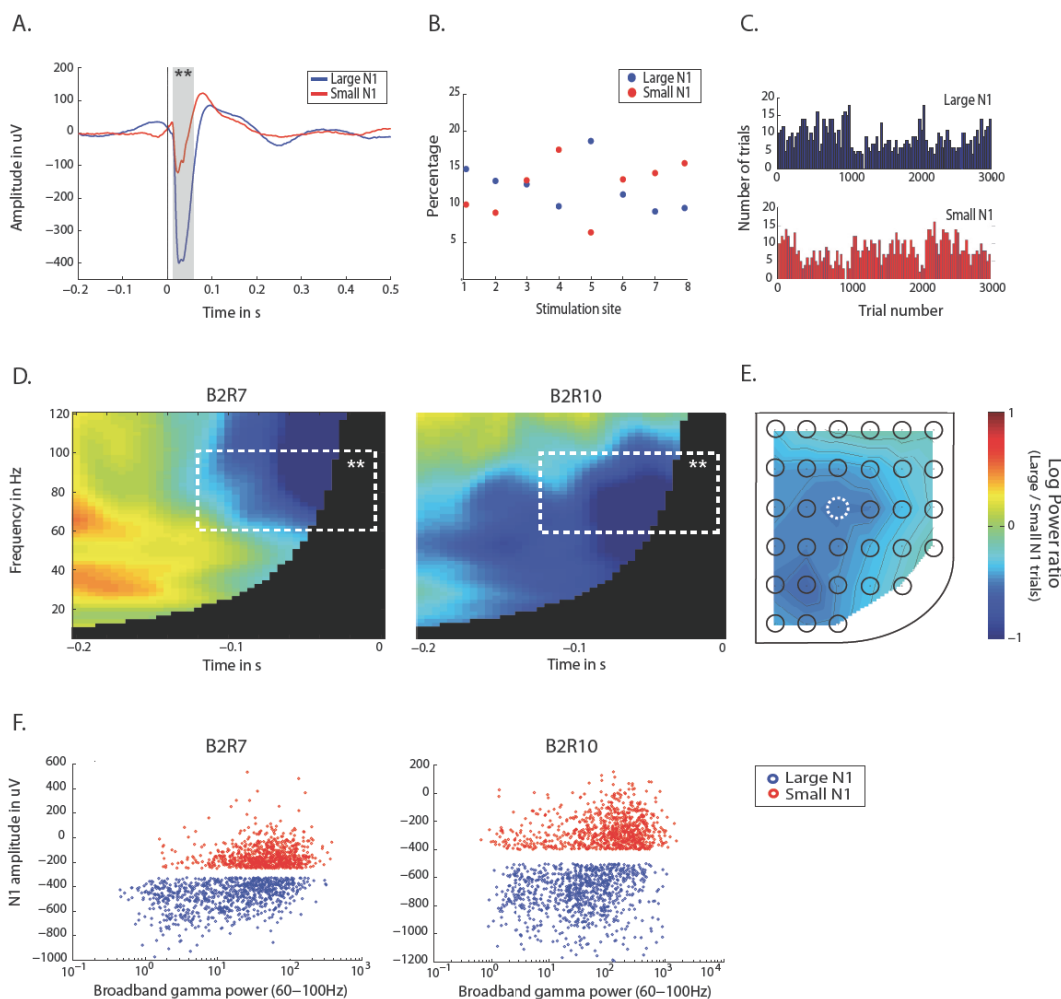


**Fig. 4** Prestimulus power of small and large N1 amplitude trials. **A-C.** Verification of ERP selection. In the selection channel, the averaged ERPs for the small and large N1 amplitude groups differed ( $t < -20.0$ ,  $p < 0.0001$ ) **A.** Selection was not biased to stimulation site **B.**, nor to time in the experiment, as quantified by the number of selected trials within a bin of 100 consecutive trials (of all trials within the anesthesia condition) **C.** **D.** The log power ratio ( $\log(\text{power large N1 trials} / \text{power small N1 trials})$ ) of the selection channel is shown for rat B2R7 and B2R10 separately. The averaged power within the white dashed box was significantly reduced for large as compared to small N1 trials ( $t < -20.0$ ,  $p < 0.0001$ ). Marked in black are the frequencies that could not be estimated. **E.** Topography of the log power ratio in a 60-100Hz frequency band and in a -120 – 0 prestimulus time-window (marked by the white box) for rat B2R7. Reduced power for large N1 trials was observed for all channels ( $p < 0.0001$ ). The selection channel is marked in white. **F.** The relationship between prestimulus broadband gamma power (x-axis) and minimum N1 amplitude (y-axis) on a single trial basis for both rat B2R7 and B2R10 (normalized effect sizes: -0.43 & -0.41 respectively).

evoked responses: the normalized effect sizes were only -0.43 (B2R7) and -0.41 (B2R10), which correspond to distributional overlap percentages of, respectively, 83% and 84%.

## 4. Discussion

We studied the effect of ongoing activity on tactile processing in the rat's vibrissal system by stimulating the upper lip using Braille cells, and recording intracranial EEG data from an epidural 32-microelectrode array overlying barrel cortex (SI) and secondary somatosensory cortex (SII). In summary, we found that ERPs under ketamine anesthesia and during wakefulness exhibit both quantitative as well as qualitative differences. The quantitative difference was prominent in the N1 amplitude arriving in SI, which was significantly larger under anesthesia than during wakefulness. Qualitatively, the spatiotemporal pattern of the ERPs during wakefulness differed from the anesthesia condition in that only during wakefulness was a second negative peak observed, which was highly specific to recording sites covering SII. Furthermore, when splitting up the anesthesia condition into two groups based on neuronal responsiveness, we found that trials with large N1 amplitude were generally preceded by low prestimulus power in broadband gamma oscillations (60-100Hz), whereas small N1 amplitude trials showed significantly higher power in this frequency band. In neither of the groups under anesthesia was an evoked response in SII observed.

### 4.1 Neuronal responsiveness in SI

Cortical hyperexcitability under anesthesia and during sleep has been reported previously (Massimini et al., 2005; Alkire et al., 2008; Ferrarelli et al., 2010). In our study, hyperexcitability of SI was reflected in the relatively large N1 amplitude of the averaged evoked response under anesthesia as compared to wakefulness. High trial-to-trial variability in neuronal responsiveness of SI under anesthesia, as also evidenced by our results, suggests that this effect is driven by only part of the trials (Jellema et al., 2004; Haslinger et al., 2006; Petersen, 2007). Accordingly, we found that neuronal responsiveness in SI under anesthesia was negatively associated with power in ongoing gamma oscillations at the time of tactile stimulation. Since gamma synchronization (30-80Hz) is known to reflect an activated state of the cortical network (Hasenstaub et al., 2005; Bartos et al., 2007; Haider & McCormick, 2009), our findings are in

line with previous studies that reported increased neuronal responsiveness to tactile stimulation in deactivated states as compared to activated states (Petersen et al., 2003; Sachdev et al., 2004; Bruno & Sakmann, 2006; Haslinger et al., 2006; Hasenstaub et al., 2007). In addition, we found that N1 amplitude in wakefulness was more similar to N1 amplitude preceded by high gamma power than by low gamma power under anesthesia. The observed increase in beta and low gamma (20-65Hz) power in ongoing activity for wakefulness, as compared to anesthesia in ongoing activity, likely reflects the persistent cortical activation that characterizes wakefulness (Steriade et al., 1993).

However, the state of activation of the cortical network may not be an optimal predictor for neuronal responsiveness in SI, as is evident from the small effect size of the difference in prestimulus gamma power for large and small N1 trials. According to Haslinger et al. (2006), a better predictor for neuronal responsiveness to sensory stimuli (e.g. whisker deflection) is the phase of the slow oscillation at the time of stimulus onset. The exact timing of sensory stimulation to the ongoing oscillation has repeatedly been shown to affect neuronal responsiveness (Erchova et al., 2002; Hasenstaub et al., 2007; Mazzoni et al., 2010). Therefore, taking both gamma power and the phase of the slow oscillation at the time of stimulation into account may result in a better prediction. In fact, Mazzoni et al. (2010) reported that cross frequency-coupling of delta (1-4Hz) phase and gamma (30-100Hz) amplitude during visual stimulation and stimulus-free periods in anesthetized monkeys can accurately predict spike rate in primary visual cortex.

### 4.2 Neuronal responsiveness in SII

Contrary to SI, neuronal responsiveness in SII seems to be differentially affected by the state of the brain, since no evoked response in SII was observed under anesthesia in general. Instead, while tactile stimulation evoked a response in SII during wakefulness, no such response was observed under anesthesia. Even when controlling for neuronal responsiveness in SI by only considering small N1 amplitude trials, ERPs under anesthesia and wakefulness still differed in terms of SII responsiveness. From this, we conclude that SII is not involved in tactile processing under anesthesia.

The absence of SII involvement in tactile processing under anesthesia may be explained by inhibited recurrent processing, which would disturb

SI-SII interaction and is likely affected by anesthetics in general (Alkire et al., 2008). The effective interaction between distant cortical areas, i.e. long-range connectivity, has consistently been shown to decrease under anesthesia and during slow wave sleep for humans (Massimini et al., 2005; Alkire et al., 2008; Ferrarelli et al., 2010) as well as animals (Imas et al., 2006), and is hypothesized to be involved in the loss of consciousness observed in these states. Although SI and SII are neighboring cortical areas, similar long-range connections exist between them (Chakrabarti & Alloway, 2006; Petersen, 2007; Liao & Yen 2008). These long-range connections are often excitatory (Haider & McCormick, 2009) and therefore likely affected by ketamine anesthesia, which is known to block excitatory neurotransmission by antagonizing NMDA receptors (Steriade & Amzica, 1998; Alkire et al., 2008). Still, it is not clear how exactly anesthetics inhibit recurrent processing. Several possibilities exist, which include a shift in the balance between synaptic inhibition and excitation towards inhibition, and bistability between the alternating active and inactive states during slow wave sleep and anesthesia (Destexhe et al., 2003; Petersen et al., 2003; Massimini et al., 2005; Petersen, 2007; Ferrarelli et al., 2010). This bistability is reflected in the burst-suppression pattern of cortical activity under anesthesia and in slow wave sleep (Alkire et al., 2008), where high-amplitude bursts of 5-10Hz oscillations, also called K-complexes (Steriade & Amzica, 1998) are alternated by periods of suppression. In our data, the presence of these high amplitude bursts in the anesthesia condition was evident from the notable increase in low frequency oscillations (<20Hz) relative to wakefulness. The alternating periods of suppression interrupt persistent depolarization and thereby the propagation of cortical activation, which may lead to the inability to sustain activity (Massimini et al., 2005; Alkire et al., 2008; Ferrarelli et al., 2010).

#### **4.3 Resemblance between UP state and wakefulness**

When addressing the question of whether UP states are similar to wakefulness in terms of neuronal responsiveness on the network level, we have to interpret our results with care.

It has been consistently shown that neuronal responsiveness in single neurons or of a population of neurons in rat and mouse SI is smaller when tactile stimuli are presented in the activated as compared to the deactivated state, the UP and DOWN state respectively (Petersen et al., 2003; Sachdev et al., 2004; Bruno & Sakmann, 2006; Haslinger et al.,

2006; Petersen, 2007). In addition, responsiveness of these neurons is highly similar between the UP state and wakefulness, due to their similarity in neuronal properties (Destexhe et al., 2003; 2007).

Interestingly, we found that large N1 amplitude trials were generally preceded by low power in ongoing gamma oscillations, whereas small N1 amplitude trials were generally preceded by high power in ongoing gamma oscillations. Since gamma oscillations (30-80 Hz) are associated with an activated state of the cortical network (Destexhe et al., 1999; Hasenstaub et al., 2005; Cash et al., 2009; Haider & McCormick, 2009; Mazzoni et al., 2010), these findings suggest that large N1 amplitude trials may reflect trials in the DOWN state, while small N1 amplitude trials may reflect trials in the UP state. In addition, we found that the averaged N1 amplitude of trials in the putative UP state was more similar to the N1 amplitude of trials in the awake condition than to the N1 amplitude of trials in the putative DOWN state. Based on our finding that SII was not involved in tactile processing during the putative UP state while it was during wakefulness, we might argue that UP states only resemble wakefulness in terms of network activity to some extent, but not regarding the interaction between SI and SII. As a consequence, the claim that UP states are ‘fragments of wakefulness’ in terms of neuronal properties and network dynamics (Destexhe et al., 2003; 2007) would not hold.

However, due to methodological limitations we were not able to unequivocally identify UP and DOWN states in our data. In fact, the small effect size of the difference in prestimulus gamma power for the putative UP and DOWN state suggests that our selection based on N1 amplitude did not lead to a strict separation of UP and DOWN state trials. Therefore, we cannot infer from our results that the UP state does not resemble wakefulness in terms of interregional network activity. Future research combining intracranial EEG and firing rate or membrane potential recordings may answer this question reliably.

#### **4.4 Methodological issues**

In addition, some methodological issues have to be taken into account because they may confound our finding that neuronal responsiveness in SI and SII is differentially affected by the state of the brain. First, we could not show the robustness of our results based on data from two animals only. Replication of these results in a larger group of animals could substantially strengthen our finding.

Second, the stimulation device might have been less well controlled than previously thought, as is reflected in the inconsistent location of the early N1 peak between the anesthesia and awake condition. When considering the overlay of the electrode array and cytochrome oxidase staining, the N1 peak under anesthesia was nicely localized to the barrel cortex. Notably, the early N1 peak during wakefulness was localized differently, i.e. slightly lower but still in barrel cortex. Despite the discrepancy, the activity observed in SII during wakefulness was highly specific. Furthermore, the latency of both negative peaks suggests that the first arose in SI and the second in SII (Jellema et al., 2004; Hooks et al., 2011). Since our aim was to focus on the interaction between SI and SII, the exact location of the N1 peak within SI was not relevant for the interpretation of our results. Third, since motor activity could only have been evoked during the awake condition, this may have confounded the observed ERP differences. A tendency of animals to move or to whisk consistently after stimulation could have resulted in both quantitative as well as qualitative differences in the ERP. Despite monitoring the animals' overt behavior on video during the experiment, it proved difficult to control for. The images could not easily be synchronized with the acquired neuronal data. Moreover, our equipment was not appropriate for specifically monitoring detailed whisker movements. However, since the animals were in a state of quiet wakefulness most of the time during the awake sessions, since gross whisker movements were absent, and since the number of trials we averaged across was very large (+1200 trials), it is unlikely that movements have affected the ERPs heavily. We are therefore confident that the differences in ERPs reflect a genuine effect due to state-dependent ongoing activity. Last, a potential confound for our interpretation of the difference in prestimulus gamma power under anesthesia is the observed difference in baseline amplitude between the averaged ERPs for small and large N1 trials (see Figure 4A). The large N1 ERP exhibited a bump in the 100ms prestimulus interval, the interval in which gamma power was found to be negatively associated with N1 amplitude. Although the bump might have been a consistent phenomenon that could dissociate between small and large N1 trials, it is impossible that power in the gamma band depended on this much slower frequency bump. Gamma oscillations are simply too fast to result in a smooth 100ms bump. Therefore, we believe that this baseline difference did not affect the finding that small and large N1 trials were generally preceded by high and

low broadband gamma power, respectively.

## 5. Conclusion

Although our results do not allow us to answer the question of whether UP state and wakefulness are similar in terms of interregional network activity, we did find evidence that neuronal responsiveness in SI and SII was differentially affected by the state of the brain. Whereas neuronal responsiveness in SI was negatively associated with power in the gamma band, and thus to the state of cortical activation, neuronal responsiveness in SII was independent of gamma oscillations. Instead, even when controlling for SI responsiveness, evoked responses to tactile stimulation were absent in SII when the animal was under anesthesia. It is likely that the burst-suppression pattern of cortical activity, as observed in slow wave sleep and under anesthesia, blocks long-range corticocortical interactions while leaving thalamic input to SI intact. The fact that a certain brain state can differentially affect neuronal responsiveness in distinct cortical areas highlights the complexity of the brain's ability to control neuronal communication effectively. Understanding perception, and the presence or absence of conscious experience accompanied with it, therefore undoubtedly requires thorough knowledge of the effect of ongoing activity across behavioral states on the processing capacities of neurons throughout the brain.

## Acknowledgements

The authors wish to thank Saskia Menting-Hermeling and Hans Krijnen, the animal caretakers, who have been of great help throughout the project. We are also grateful to Dirk Schubert and Moritz Negwer for their kind help with the cytochrome oxidase staining.

## References

- Alkire, M., Hudetz, A., & Tononi, G. (2008). Consciousness and Anesthesia. *Science*, 322, 876-880.
- Amzica, F. (2010). Comment on "The Human K-Complex Represents an Isolated Cortical Down-State". *Science*, 330, 35-a.
- Bartos, M., Vida, I., & Jonas, P. (2007). Synaptic mechanisms of synchronized gamma oscillations in inhibitory interneuron networks. *Nature Review Neuroscience*, 8(1), 45-56.
- Bruno, R. M. & Sakmann, B. (2006). Cortex is driven

- by weak but synchronously active thalamocortical synapses. *Science*, 312(5780), 1622-1627.
- Cash, S., Halgren, E., Dehghani, N., Rossetti, A., Thesen, T., Wang, C., et al. (2009). The Human K-Complex Represents an Isolated Cortical Down-State. *Science*, 324, 1084-1086.
- Chakrabarti, S. & Alloway, K. D. (2006). Differential origin of projections from SI barrel cortex to the whisker representations in SII and MI. *The Journal of Comparative Neurology*, 498(5), 624-636.
- Constantinople, C. M. & Bruno, R. M. (2011). Effects and Mechanisms of Wakefulness on Local Cortical Networks. *Neuron*, 69(6), 1061-1068.
- Contreras, D., & Steriade, M. (1995). Cellular Basis of EEG Slow Rhythms: A Study of Dynamic Corticothalamic Relationships. *Journal of Neuroscience*, 15(1), 604-622.
- Crochet, S., & Petersen, C. C. H. (2006). Correlating whisker behavior with membrane potential in barrel cortex of awake mice. *Nature Neuroscience*, 9(5), 608-610.
- Crunelli, V. & Hughes, S. W. (2010). The slow (<1 Hz) rhythm of non-REM sleep: A dialogue between three cardinal oscillators. *Nature Neuroscience*, 13(1), 9-17.
- Destexhe, A., Contreras, D., & Steriade, M. (1999). Spatiotemporal Analysis of Local Field Potentials and Unit Discharges in Cat Cerebral Cortex during Natural Wake and Sleep States. *Journal of Neuroscience*, 19(11), 4595-4608.
- Destexhe, A., Hughes, S., Rudolph, M., & Crunelli, V. (2007). Are corticothalamic 'up' states fragments of wakefulness? *Trends in Neurosciences*, 30(7), 334-342.
- Destexhe, A., Rudolph, M., & Paré, D. (2003). The high-conductance state of neocortical neurons in vivo. *Nature Reviews*, 4, 739-751.
- Devonshire, I. M., Grandy, T. H., Dommett, E. J., & Greenfield, S. A. (2010). Effects of urethane anaesthesia on sensory processing in the rat barrel cortex revealed by combined optical imaging and electrophysiology. *European Journal of Neuroscience*, 32(5), 786-797.
- Erchova, I. A., Lebedev, M. A., & Diamond, M. (2002). Somatosensory cortical neuronal population activity across states of anaesthesia. *European Journal of Neuroscience*, 15, 744-752.
- Fanselow, E.E. & Nicollelis, M.A.L. (1999). Behavioral Modulation of Tactile Responses in the Rat Somatosensory System. *Journal of Neuroscience*, 19(17), 7603-7616.
- Ferezou, I., Bolea, S., & Petersen, C.C.H. (2006). Visualizing the cortical representation of whisker touch: Voltage-sensitive dye imaging in freely moving mice. *Neuron*, 50(4), 617-629.
- Ferezou, I., Haiss, F., Gentet, L.J., Aronoff, R., Weber, B., & Petersen, C. C. H. (2007). Spatiotemporal dynamics of cortical sensorimotor integration in behaving mice. *Neuron*, 56, 907-923.
- Ferrarelli, F., Massimini, M., Sarasso, S., Casali, A., Riedner, B. A., Angelini, G., et al. (2010). Breakdown in cortical effective connectivity during midazolam-induced loss of consciousness. *Proceedings of the National Academy of Sciences, USA*, 107(6), 2681-2686.
- Goard, M. & Dan, Y. (2009). Basal forebrain activation enhances cortical coding of natural scenes. *Nature Neuroscience*, 12(11), 1444-1449.
- Goss-Sampson, M. A. & Kriss, A. (1991). Effects of pentobarbital and ketamine-xylazine anaesthesia on somatosensory, brainstem auditory and peripheral sensory-motor responses in the rat. *Laboratory Animals*, 25, 360-366.
- Haider, B., Duque, A., Hasenstaub, A. R., & McCormick, D.A. (2006). Neocortical network activity in vivo is generated through a dynamic balance of excitation and inhibition. *Journal of Neuroscience*, 26(17), 4535-4545.
- Haider, B. & McCormick, D. A. (2009). Rapid Neocortical Dynamics: Cellular and Network Mechanisms. *Neuron*, 62(2), 171-189.
- Hasenstaub, A., Sachdev, R. N. S., & McCormick, D.A. (2007). State Changes Rapidly Modulate Cortical Neuronal Responsiveness. *Journal of Neuroscience*, 27(36), 9607-9622.
- Hasenstaub, A., Shu, Y., Haider, B., Kraushaar, U., Duque, A., & McCormick, D. A. (2005). Inhibitory Postsynaptic Potentials Carry Synchronized Frequency Information in Active Cortical Networks. *Neuron*, 47(3), 423-435.
- Haslinger, R., Ulbert, I., Moore, C. I., Brown, E. N., & Devor, A. (2006). Analysis of LFP Phase Predicts Sensory Response of Barrel Cortex. *Journal of Neurophysiology*, 96, 1658-1663.
- Hirata, A., & Castro-Alamancos, M. A. (2010). Neocortex Network Activation and Deactivation States Controlled by the Thalamus. *Journal of Neurophysiology*, 103, 1147-1157.
- Hooks, B. M., Hires, S.A., Zhang, Y.-X., Huber, D., Petreanu, L., Svoboda, K., & Shepherd, G. M. G. (2011). Laminar Analysis of Excitatory Local Circuits in Vibrissal Motor and Sensory Cortical Areas. *Public Library of Science Biology*, 9(1), e1000572.
- Hosp, J. A., Molina-Luna, K., Hertler, B., Atiemo, C. O., Stett, A., & Luft, A. R. (2008). Thin-film epidural microelectrode arrays for somatosensory and motor cortex mapping in rat. *Journal of Neuroscience Methods*, 172(2), 255-262.
- Imas, O. A., Ropella, K. M., Wood, J. D., & Hudetz, A. G. (2006). Isoflurane disrupts antero-posterior phase synchronization of flash-induced field potentials in the rat. *Neuroscience*, 402, 216-221.
- Jellema, T., Brumia, C. H. M., & Wadman, W. J. (2004). Sequential activation of microcircuits underlying somatosensory-evoked potentials in rat neocortex. *Neuroscience*, 129, 283-295.
- Liao, C.-C. & Yen, C.-T. (2008). Functional Connectivity of the Secondary Somatosensory Cortex of the Rat. *The Anatomical Record: Advances in Integrative Anatomy and Evolutionary Biology*, 291(8), 960-973.
- Massimini, M., Ferrarelli, F., Huber, R., Esser, S. K.,

- Singh, H., & Tononi, G. (2005). Breakdown of Cortical Effective Connectivity during Sleep. *Science*, 309, 2228-2231.
- Mazzoni, A., Whittingstall, K., Brunel, N., Logothetis, N.K., & Panzeri, S. (2010). Understanding the relationships between spike rate and delta/gamma frequency bands of LFPs and EEGs using a local cortical network model. *NeuroImage*, 52(3), 956-972.
- Niell, C. M. & Stryker, M. P. (2010). Modulation of Visual Responses by Behavioral State in Mouse Visual Cortex. *Neuron*, 65, 472-479.
- Oostenveld, R., Fries, P., Maris, E., & Schoffelen, J. (2011). FieldTrip: Open Source Software for Advanced Analysis of MEG, EEG, and Invasive Electrophysiological Data. *Computational Intelligence and Neuroscience*, Volume 2011.
- Percival, D. B. & Walden, A. T. (1993). Spectral Analysis for Physical Applications: Multitaper and Conventional Univariate Techniques. Cambridge, Cambridge University Press.
- Petersen, C. C. H. (2007). The functional organization of the barrel cortex. *Neuron*, 56(2), 339-355.
- Petersen, C. C. H., Hahn, T. T. G., Mehta, M., Grinvald, A., & Sakmann, B. (2003). Interaction of sensory responses with spontaneous depolarization in layer 2/3 barrel cortex. *Proceedings of the National Academy of Sciences, USA*, 100(23), 13638-13643.
- Poulet, J. F. A. & Petersen, C. C. H. (2008). Internal brain state regulates membrane potential synchrony in barrel cortex of behaving mice. *Nature*, 454(7206), 881-U836.
- Sachdev, R. N. S., Ebner, F. F., & Wilson, C. J. (2004). Effect of Subthreshold Up and Down States on the Whisker-Evoked Response in Somatosensory Cortex. *Journal of Neurophysiology*, 92(6), 3511-3521.
- Shu, Y. S., Hasenstaub, A., & McCormick, D. A. (2003). Turning on and off recurrent balanced cortical activity. *Nature*, 423(6937), 288-293.
- Steriade, M. & Amzica, F. (1998). Slow sleep oscillation, rhythmic K-complexes, and their paroxysmal developments. *Journal of Sleep Research*, 7(Suppl 1), 30-35.
- Steriade, M., McCormick, D., & Sejnowski, T. (1993). Thalamocortical oscillations in the sleeping and aroused brain. *Science*, 262(5134), 679-685.

# Quantifying the Contribution of Alpha and Beta Amplitude to Somatosensory Perception and its Improvement with Attentional Orienting

Malte Köster<sup>1</sup>

Supervisors: Eric Maris<sup>1</sup>, Ole Jensen<sup>1</sup>, Freek van Ede<sup>1</sup>

<sup>1</sup>Donders Institute for Brain, Cognition and Behaviour, Radboud University Nijmegen, The Netherlands

Knowing when and where an upcoming sensory event will occur allows for the orienting of attention and improves perception. There is abundant evidence that this orienting of attention involves an anticipatory modulation of oscillatory amplitude within sensory cortex. At the same time, spontaneous fluctuations in oscillatory amplitude are predictive of subsequent perceptual performance. Together, these findings suggest that anticipatory amplitude modulation is an important neurophysiological mechanism underlying attentional orienting. However, at present it is unclear how much of the attentional improvement in perception can be accounted for by anticipatory amplitude modulation. To address this, we recorded magnetoencephalography (MEG) while human subjects performed a somatosensory detection task. In some trials a cue predicted the time and location of the stimulus, allowing for attentional orienting. First, we modeled the relation between prestimulus amplitude and perceptual performance utilizing spontaneous fluctuations in the absence of cueing. Then, we used this relation to predict the improvement in perception that would follow from the anticipatory amplitude modulation that occurred with cueing. Finally, by comparing the predicted with the actual attentional improvement we showed that up to 13% of the attentional improvement in perception can be accounted for by the anticipatory modulation of alpha- and beta-band amplitude. While both alpha- and beta-band modulations were involved in attentional orienting, their contributions to the perceptual improvement were to a large extend shared. To our knowledge, we have for the first time quantified the contribution of MEG recorded oscillatory amplitude to attentional improvement.

*Keywords:* alpha, beta oscillations, spontaneous fluctuations, attentional orienting, somatosensory perception

---

Corresponding author: Malte Köster, email: malte.koester@gmail.com

## 1. Introduction

Perception is an active process that integrates stimulus driven input and prior information. Prior knowledge about when and where a sensory stimulus will occur allows us to focus on a subset of available information and enhances processing (Ward, 2008). This phenomenon has been conceptualized as orienting of attention (Posner & Petersen, 1990). Recent studies have shown that orienting attention to an upcoming stimulus involves a modulation of oscillatory amplitude in human sensory cortex. In the visual domain, anticipating a lateralized stimulus involves a lateralized modulation of posterior alpha-band (8-14 Hz) amplitude (e.g. Bahramisharif, van Gerven, Heskes, & Jensen, 2010; Foxe, Simpson, & Ahlfors, 1998; Kelly, Lalor, Reilly, & Foxe, 2006; Sauseng et al., 2005; Siegel, Donner, Oostenveld, Fries, & Engel, 2008; Thut, Nietzel, Brandt, & Pascual-Leone, 2006; Worden, Foxe, Wang, & Simpson, 2000; Wyart & Tallon-Baudry, 2008; Yamagishi, Goda, Callan, Anderson, & Kawato, 2005). Similarly, in the somatosensory domain, anticipating a tactile event involves a lateralized modulation of alpha- and beta-band (15-30 Hz) amplitude in somatosensory cortex (e.g. Anderson & Ding, 2011; van Ede, de Lange, Jensen, & Maris, 2011; van Ede, Jensen, & Maris, 2010; Haegens, Handel, & Jensen, 2011; Jones et al., 2010), which we have recently shown to be constituted by a contralateral suppression (van Ede et al., 2011). These modulations are specific to the timing (*ibid.*) and features (color and motion; Snyder & Foxe, 2011) of an expected stimulus, and they are deployed in a graded manner depending on the probability of an upcoming stimulus (Gould, Rushworth, & Nobre, 2011; Haegens et al., 2011).

These properties (generality across modalities and dimensions and flexible deployment) suggest that anticipatory amplitude modulation is an important mechanism underlying the orienting of attention. This notion is further supported by the following three observations. First, during spontaneously occurring amplitude fluctuations, states of low amplitude are associated with increased cortical excitability (Becker, Reinacher, Freyer, Villringer, & Ritter, 2011; Romei et al., 2008; Sauseng, Klimesch, Gerloff, & Hummel, 2009; Tamura et al., 2005) and increased blood-oxygenation-level dependent (BOLD) response (Ritter, Moosmann, & Villringer, 2009; Scheeringa et al., 2011). Second, these states are also associated with improved psychophysical performance such as stimulus detectability, discriminability and reaction time. This has been shown for posterior alpha amplitude in visual tasks

(Dijk, Schoffelen, & Oostenveld, 2008; Ergenoglu et al., 2004; Hanslmayr et al., 2007; Händel, Haarmeier, & Jensen, 2011; Kelly et al., 2006; Romei, Gross, & Thut, 2010; Thut et al., 2006; Yamagishi, Callan, Anderson, & Kawato, 2008) and somatosensory alpha and beta amplitude in tactile tasks (van Ede et al., 2011; Haegens et al., 2011; Jones et al., 2010; Linkenkaer-Hansen, Nikulin, & Palva, 2004; Schubert, Haufe, Blankenburg, Villringer, & Curio, 2009; Zhang & Ding, 2010). Third, suppression of oscillatory amplitude might lead to a decorrelation of neuronal activity (Naruse, Matani, Miyawaki, & Okada, 2010; Pfurtscheller & Lopes da Silva, 1999), which is a key property of attentive brain states within sensory cortex (Cohen & Maunsell, 2009; Mitchell, Sundberg, & Reynolds, 2009).

Taken together, there is abundant evidence that orienting attention to upcoming sensory events involves a modulation of oscillatory amplitude in sensory cortex and that this modulation is associated with improved perception. However, while this link has previously been made, it is at present unclear how much of the improvement in perception that occurs with attentional orienting can be accounted for by anticipatory amplitude modulation. To address this question, we recorded oscillatory brain activity, using MEG, during a somatosensory detection task. First, we used spontaneous fluctuations to model the relation between oscillatory amplitude and perceptual performance in the absence of attentional orienting. Then, we used this relation and the anticipatory amplitude modulation to predict performance with attentional orienting. By comparing the predicted with the actual attentional improvement we quantified the contribution of the oscillatory amplitude modulation to the attentional improvement in perception. Our results confirm that prestimulus amplitude is related to psychophysical performance and that orienting attention involves a modulation of oscillatory amplitude alongside an improvement in perceptual performance. Quantifying these results, we find that MEG recorded anticipatory amplitude modulations explain up to 13% of the perceptual improvement that occurs with attentional orienting. Moreover, we show that although both prestimulus alpha- and beta-band amplitude are predictive of subsequent performance, their contributions are largely non-unique.

## 2. Methods

### 2.1 Participants

Fourteen healthy subjects voluntarily participated in the experiment. Two subjects were excluded from analysis because for one subject no stable behavioral performance could be obtained and another fell asleep during the experiment. This left data from twelve subjects (four male; mean age 29 years; range 22–49 years). All participants provided written consent and were paid in accordance with guidelines of the local ethics committee (Committee on Research Involving Human Subjects, Region Arnhem-Nijmegen, The Netherlands).

### 2.2 Experimental design and stimuli

Subjects performed a somatosensory detection task in which the spatial and temporal location of target stimuli was either cued or not. In every trial a brief tone (50 ms, white noise) occurred, that was paired with a tactile stimulus on half of the trials. This tactile stimulus was delivered to the left or the right thumb with equal probability (Figure 1). The tactile stimulus consisted of a short (0.5 ms) electrical pulse at approximately threshold intensity (see below). In each trial, the subjects' task was to indicate whether a tactile stimulus was presented or not at the time of the tone. In the uncued condition, time and location of an upcoming stimulus were subjectively difficult to predict. In fact, the time interval between a response and the next stimulus was drawn from a truncated negative exponential distribution (mean 3.5 s; limited to the range 2.5 to 12 s), which has the property that the hazard rate of a stimulus (its probability of occurrence given that it has not occurred yet) is constant over the response-

stimulus interval.

Also, the stimulus was equally likely to occur on either hand. In the cued condition, the time and location of the upcoming stimulus were fully predictable.

The response-stimulus interval was drawn from the same distribution as in the uncued trials, but 1.5 s before the stimulus an auditory cue (150 ms, pure tone) was presented that was informative with 100% validity about the time (after 1.5 s) and location (left/right thumb) of the upcoming stimulus (which was presented on 50 percent of the trials). Left or right thumb was indicated by the pitch of the tone being 500 or 1000 Hz (counterbalanced over subjects). Cued and uncued trials were randomly interleaved. In total, one third of the trials were cued.

After each trial, participants had to indicate whether a stimulus was present or not by pressing a button with the left or right index finger. For the response it did not matter which hand was stimulated. To prevent lateralized response preparation, the mapping of the perceptual decision (stimulus present or not) onto the response buttons was varied from trial to trial. One second after the potential stimulus had occurred, a response mapping tone was presented either to the left or the right ear (150 ms, 1000 Hz pure tone). To indicate the presence of a tactile stimulus, subjects had to press the button on the side where the tone was presented. Likewise, to indicate the absence of a tactile stimulus they had to press the button on the side opposite of the response-mapping tone. To keep subjects engaged in the task, auditory feedback was presented after hit and miss trials (50 ms frequency sweep going up for hits or down for misses).

The stimuli were brief (0.5 ms) current pulses generated by two constant current high voltage stimulators (type DS7A, Digitimer, Hertfordshire,

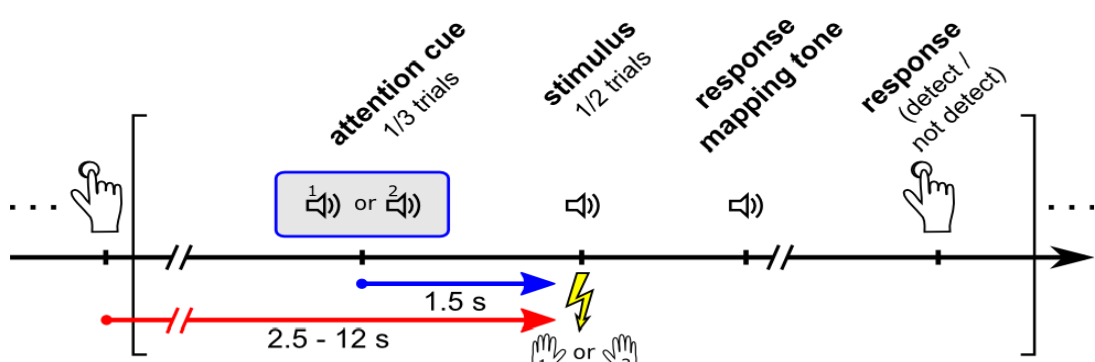


**Fig. 1** Experimental paradigm. Subjects performed a somatosensory detection task in which the time (after 1.5 s) and location (left/right thumb) of the upcoming relevant event was either cued or not. This event consisted of the occurrence of a brief tone that was, in half the trials, paired with an electric stimulus on the left or right thumb. In each trial subjects had to indicate whether they perceived a stimulus or not. Responses were delayed and mapped according to a response mapping tone (see Materials and Method). Uncued and cued trials were randomly interleaved.

UK). Stimuli were delivered to the thumbs via two pairs of custom build electrodes attached on the inside of the distal phalanx with an inter-electrode distance of 1 cm. Prior to the experiment, stimulus intensity was adjusted such that the hit rate in the cued condition was 80%. For this, we used QUEST (Watson and Pelli, 1983), an adaptive method for sensory threshold estimation implemented in the Matlab (<http://mathworks.com>) Psychophysics Toolbox (Brainard, 1997). Stimulus intensity ranged between 1.13 and 1.89 mA.

Participants completed around 1000 trials in two consecutive MEG sessions lasting approximately 70 minutes each. Each session was divided into blocks of 72 trials. Within each block, cue presence, cue side, stimulus presence, and stimulus side were counterbalanced. Subjects were instructed to keep their eyes closed during the experiment and lights were turned off or dimmed. At the end of each session we performed a localizer, in which 200 suprathreshold stimuli (130% of the experimental intensity) were delivered to the left and the right hand in a random order with an inter-stimulus-interval of 500 to 600 ms. All subjects practiced the task for approximately one hour on a day before the experiment.

### 2.3 Data acquisition

The MEG system (CTF MEG systems) contained 275 axial gradiometers and was housed in a magnetically shielded room. Synchronized with the MEG, we also recorded bipolar surface electromyogram (EMG) from the flexors of the forearm (cf. van Ede et al., 2011). Three localization coils, fixed to anatomical landmarks (nasion, left ear, right ear), were used to determine the position of the head relative to the gradiometers. All data were low-pass filtered by an anti-aliasing filter (300 Hz cut-off), digitized at 1200 Hz and stored for offline analysis. No electrooculography data were recorded because subjects were instructed to close their eyes during the experiment. Anatomical magnetic resonance (MR) images of the subjects' brains were acquired using a 1.5 T Siemens Magnetom Sonata system. Three vitamin E fiducial markers were fixed to the same anatomical landmarks as the MEG localization coils to allow co-registration of the MR images and MEG data.

### 2.4 Data analysis

Data were analyzed using FieldTrip (Oostenveld, Fries, Maris, & Schoffelen, 2011), an open-source Matlab toolbox developed at the Donders Institute for Brain, Cognition and Behaviour (Nijmegen, The Netherlands). For all epochs of interest, data was down-sampled to a sampling frequency of 600 Hz. Line noise was removed by subtracting the 50, 100 and 150 Hz components of the signal using a discrete Fourier transform filter and the signal's offset was removed by subtracting the mean of every epoch. All data epochs of interest were visually inspected and those contaminated by artifacts were removed.

### 2.5 Frequency analysis

We calculated oscillatory amplitude by means of the Fourier transform in combination with two tapering methods: a single Hanning taper and multiple discrete prolate spheroidal tapers (multitaper method; Percival & Walden, 1993). We calculated oscillatory amplitude estimates both with and without time resolution. All calculations with time resolution involved a 500 ms sliding time window that was moved in steps of 50 ms. Amplitude estimates were calculated for frequencies between 5 and 50 Hz, applying a single Hanning taper. Non-time-resolved amplitude estimates were calculated for the alpha- and beta-frequency bands using the multitaper method. The alpha-band was defined as 8 to 14 Hz for all subjects and the beta-band was individually determined for each subject. This was done on the basis of the stimulus-induced responses obtained from the localizer stimuli (see also van Ede et al., 2011; van Ede et al., 2010; Haegens et al., 2011). On average, beta-bands ranged from 16 to 28 Hz.

For our main analysis, we estimated the amplitude in these bands in a 1 s prestimulus window. Alpha-band amplitude was estimated using 5 orthogonal tapers. Beta-band amplitude was estimated using between 19 and 29 tapers, depending on the individual subject's bandwidth. To calculate topographies of the anticipatory modulation (Figure 2D), we estimated amplitude in a 1 s prestimulus window in a frequency band ranging from 8 to 30 Hz. For the spectral specificity analysis (Figure 4A) we estimated amplitude for frequencies ranging from 5 to 150 Hz with a frequency smoothing of 4 Hz.

## 2.6 Source reconstruction

For our main analyses we reconstructed oscillatory brain activity originating from the sensorimotor cortex. This involved three steps. First we used the localizer data to find the left and right somatosensory cortex for each participant. This was done in source space using a beamformer approach (dynamic imaging of coherent sources; Gross et al., 2001). To estimate source power, we calculated the cross-spectral density matrix for each subject's beta-band and combined it with the lead fields from a single shell volume conductor model (Nolte, 2003) based on the individual MR image. This way, we obtained optimal spatial filters for every voxel in the brain (0.5 cm resolution), which were multiplied with the sensor level data to reconstruct source activity. To localize somatosensory cortex, we contrasted post-stimulus beta-band power after a stimulation of the left and right thumb. This contrast was made for every voxel in the reconstructed brain. The maximum and minimum voxels in this contrasted volume were then used as loci for left and right sensorimotor cortex (in line with Cheyne et al., 2003; van Ede et al., 2011; van Ede et al., 2010; Gaetz & Cheyne, 2006; Haegens et al., 2011). Second, we estimated optimal spatial filters for reconstructing activity from the left and right somatosensory cortex. Again we used beamforming, but this time we calculated the cross-spectral density matrix using the prestimulus data and a 5 to 50 Hz frequency band. Third, we applied the obtained filters to our time-domain 275 channel data to reduce it to one left and one right virtual somatosensory cortex channel. All source-level analyses reported here were performed on these reconstructed time-courses.

## 2.7 Relating electrophysiological and behavioral data

Our main analyses were performed on two virtual channels representing activity from the left and right somatosensory cortex. We analyzed the relation between prestimulus oscillatory amplitude and behavioral performance as indexed by hit rates and reaction times. For every trial, we calculated four amplitude estimates, namely for the alpha- and beta-band in the left and right somatosensory cortex. To allow pooling of each subject's data over the two recording sessions and the two hemispheres, we normalized all amplitude estimates by linearly transforming them into the percentage change from the mean amplitude in the uncued condition of the

respective session and hemisphere. (A histogram of the normalized amplitude distributions for uncued and cued trials in the alpha- and beta-band is shown in Figure 3A, B lower panels. Note that the uncued distribution has zero mean as a result of the normalization.) Amplitudes from the left and right hemisphere were reassigned as contralateral or ipsilateral to the stimulus.

To qualitatively investigate the relationship between prestimulus oscillatory amplitude and perceptual performance, we binned trials according to this amplitude. This was done separately for each of the four amplitude variables. For every subject, we first sorted trials from low to high amplitude and grouped them into eight equally sized, non-overlapping bins resulting in approximately 30 trials per bin. For every bin, we calculated hit rate (number of hits / total number of stimulus trials), median reaction time and the mean amplitude. To account for individual differences in perceptual performance, we normalized hit rate and reaction time of each bin to the percentage change from the mean of the uncued condition. We then averaged the hit rate, reaction time, and amplitude of each bin over subjects. Binning was done separately for uncued and cued trials.

Next, we asked how much of the perceptual improvement occurring with attentional orienting (i.e. in the cued trials) could be explained by the anticipatory amplitude modulation. This involved four steps: (i) quantifying the anticipatory amplitude modulation in the cued trials, (ii) describing the amplitude-perception relation in the uncued trials with a regression model, (iii) using the amplitude modulation and the regression model to predict perceptual performance in the cued trials, (iv) comparing predicted and actual performance in cued trials. These steps are schematically illustrated in Figure 3 and we now describe them in detail for the analysis of hit rates. Reaction times analysis was identical except for the choice of the regression model. All steps were performed on individual subject data and separately for each of the four amplitude variables (i.e. alpha- and beta-band in the contralateral and ipsilateral hemisphere) as well as for pairs of those variables (e.g. contralateral alpha and beta as joint predictors).

- Step 1. The anticipatory amplitude modulation was quantified as the mean normalized prestimulus amplitude in the cued condition. (This was done after all amplitudes were normalized as percentage change from the mean amplitude in the uncued condition. Therefore, the mean normalized amplitude in the cued condition equals the mean difference between

cued and uncued conditions; cf. Figure 3 lower panels.)

- Step 2. The relation between normalized amplitude and hit rate in the uncued trials was modeled using logistic regression. The two important advantages of logistic regression over the binning procedure described earlier is that it does not require an arbitrary decision on the number of bins and allows using multiple predictor variables (see below). We used logistic regression to models the probability of a hit as a function of normalized prestimulus amplitude:

$$p(\text{hit}) = \frac{\exp(B_0 + B_1 \cdot \text{amplitude})}{1 + \exp(B_0 + B_1 \cdot \text{amplitude})}$$

The coefficients were estimated using the maximum likelihood criterion implemented in the Matlab functions `mnrfit`. The logistic regression coefficient  $B_1$  determines how strongly  $p(\text{hit})$  depends on the normalized amplitude. A negative  $B_1$  indicates a decrease in  $p(\text{hit})$  with increasing amplitude. For the reaction time analysis we used a linear rather than a logistic regression model because reaction times, in contrast to probabilities, are not bounded by 1.

- Step 3. Predicted hit rate in the cued condition was calculated from the mean cued amplitude (i.e. anticipatory modulation; step 1) and the regression equation (step 2).

- Step 4. Predicted hit rate and observed hit rate (i.e. subjects' actual performance) in the cued condition were expressed as improvement relative to the uncued condition by subtracting the mean hit rate in the uncued condition. The ratio between predicted and observed improvement then reflects how much of the improvement with attentional orienting is explained by amplitude modulation. In other words, percentage explained improvement = (predicted improvement) / (observed improvement) \* 100.

Furthermore, we investigated the extend to which alpha- and beta-band amplitude in the contra- and ipsilateral hemisphere contributed independently to the explained improvement. To this end, we computed regression models with two predictors (e.g. alpha and beta amplitude) and tested whether they could explain more of the attentional improvement than single predictor models (e.g. alpha amplitude). If two predictors are independent (i.e. uncorrelated across trials), then the percentage explained by the combined model equals the sum of the percentages explained by the two individual models.

All reported statistical tests were performed across subjects by means of one-sample or paired-samples t-tests.

### 3. Results

#### 3.1 Attentional orienting improves perception and involves anticipatory modulation of oscillatory amplitude

Twelve human subjects performed a somatosensory detection task in which, on half of the trials, a weak electrical stimulus was presented to either the left or the right thumb. Subjects' task was to indicate whether in a given trial a stimulus was present or absent. In one third of the trials an auditory cue indicated when (after 1.5 s) and where (left or right hand) this stimulus could occur (denoted: cued condition). This allowed subjects to orient their attention to the upcoming event. In the remainder of the trials no auditory cue was presented and the stimulus could occur at either hand at an unpredictable time (denoted: uncued condition).

As expected, orienting attention improved perception by increasing hit rates from  $52 \pm 3\%$  (mean over subjects  $\pm$  SEM) in the uncued to  $81 \pm 2\%$  in the cued condition ( $t(11) = 8.491, p < 0.001$ ), and reducing reaction times from  $685 \pm 83$  ms in the uncued to  $513 \pm 40$  ms in the cued condition ( $t(11) = -3.291, p < 0.01$ ). Data are shown in Figure 2, panels A and B. False alarm rates did not differ between conditions (uncued  $27 \pm 3\%$ , cued  $24 \pm 3\%$ ,  $t(11) = 1.023, p = 0.328$ ).

It is well-established that attentional orienting to upcoming sensory events involves a prestimulus modulation of oscillatory activity within sensory cortex (see Introduction). To verify this phenomenon in our data we computed time-frequency representations of oscillatory amplitude for the reconstructed left and right somatosensory sources (see Materials and Methods) in each subject. Figure 2C shows a grand average time-frequency resolved plot of the difference in contralateral oscillatory amplitude between cued and uncued trials.

We observed that anticipation of the upcoming tactile event involves an attenuation of oscillatory amplitude in both the alpha- and the beta-band (contralateral alpha:  $t(11) = -5.523, p < 0.001$ ; contralateral beta:  $t(11) = -7.215 p < 0.001$ ). Figure 2D shows source reconstructions of this anticipatory modulation, separately for anticipation of a left and right hand stimulus. The topography shows that the anticipatory modulation is constituted primarily by

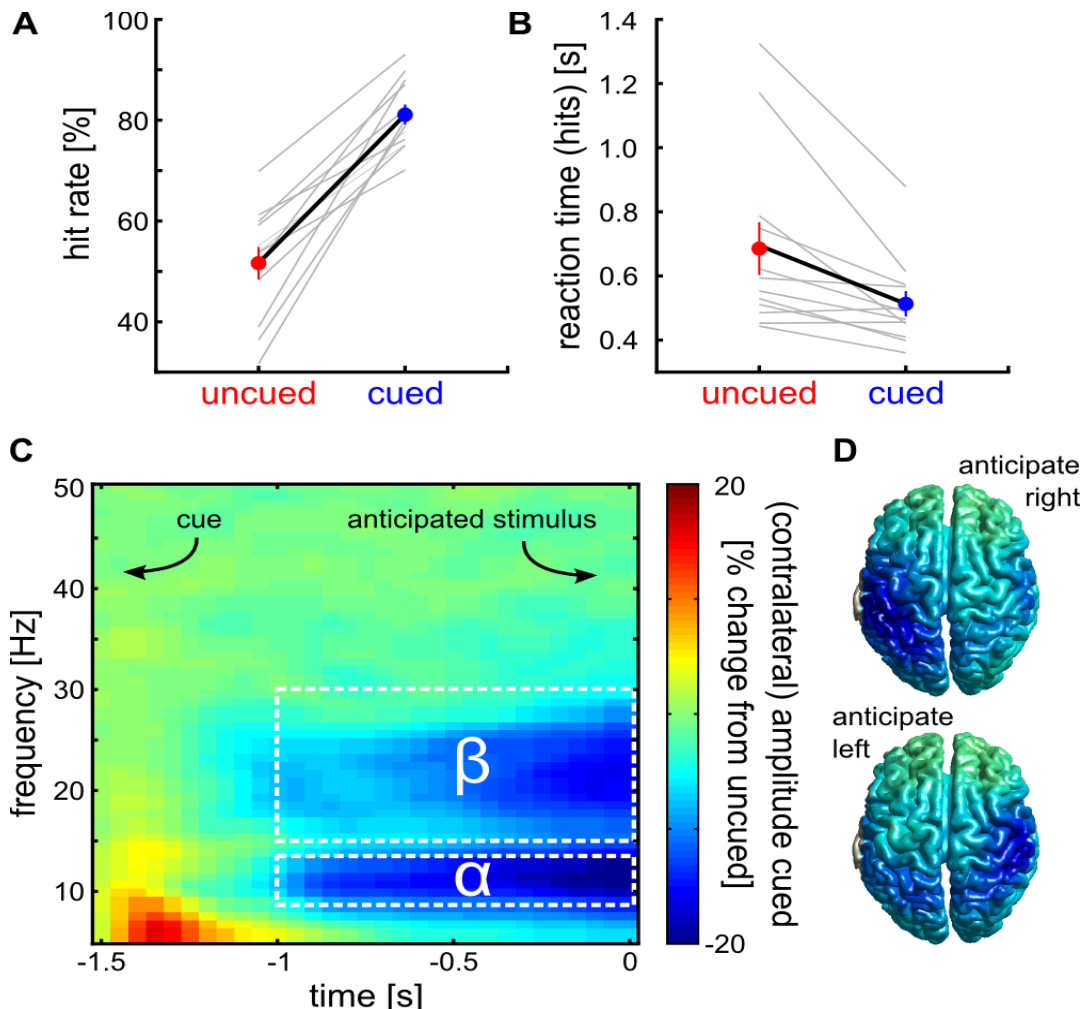


**Fig. 2** Attentional orienting improves perception and involves anticipatory amplitude modulation. **A.** Hit rate in the uncued and cued condition. Colored data points indicate means  $\pm$  SEM. Gray lines show individual subjects. **B.** Same as A, showing reaction time in hit trials. **C.** Time-frequency representation of oscillatory amplitude in somatosensory cortex following a cue to the contralateral side, expressed as percentage change from the uncued condition. White boxes indicate the time-frequency window used in subsequent analyses. **D.** Average source-reconstructed amplitude modulation in anticipation of a left and right hand tactile stimulus, averaged over the alpha- and beta-band in a 1 s prestimulus window.

a decrease in oscillatory amplitude in contralateral sensorimotor cortex. The topography was not qualitatively different for alpha and beta-band (data not shown).

It is unlikely that the observed amplitude modulation is due to motor preparation or execution. First, the response mapping was only given after the stimulus such that subjects could not prepare a specific response (i.e. left or right hand button). Second, we did not observe any bias in response side as a function of expected stimulus side (side congruent - side incongruent responses:  $t(11) = -0.572$ ,  $p = 0.579$ ). Finally, in line with previous work (van Ede et al., 2011), EMG recordings from the muscles of the forearm did not show muscular activity in anticipation of the stimulus. These modulations are unlikely to be caused by the auditory cue because first the auditory cue was presented

bilaterally, while the anticipatory modulation is clearly lateralized (Figure 2D), and second non-cue auditory tones did not result in such a pattern. (Note, however, that the transient increase in low-frequency amplitude immediately after cue-onset likely reflects auditory activity.)

In sum, when subjects know when and where an upcoming stimulus might occur, they orient their attention to this event, facilitating its perception. At the same time, this involves a contralateral suppression of oscillatory alpha- and beta-band amplitude in sensory cortex. Having established these observations we asked how much of the perceptual improvement could be explained by this anticipatory brain response.

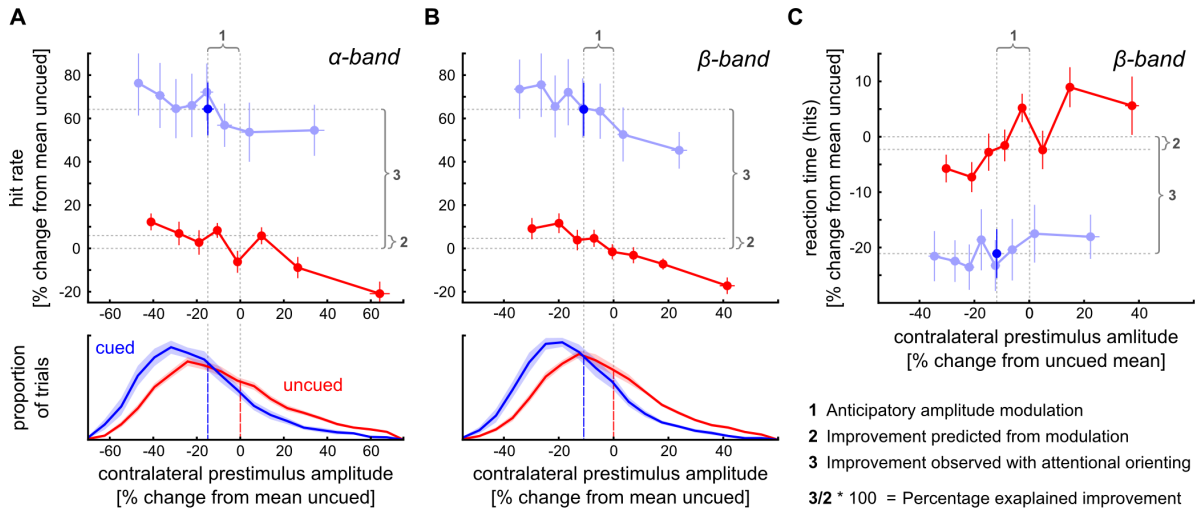


**Fig. 3** Contribution of anticipatory amplitude modulation to the attentional improvement in perception. **A.** Upper panel. hit rate as a function of prestimulus amplitude in the alpha-band. Trials from the uncued (red) and cued (blue) condition were separately sorted by amplitude and grouped into 8 bins. The dark blue data point shows mean amplitude and hit rate in the cued condition. Error bars indicate SEM. Lower panel. distribution of prestimulus amplitude over trials. Data are normalized to percentage change from the mean in the uncued condition and averaged across subjects. Vertical dashed lines indicate mean amplitude. **B.** same as A showing hit rate as a function of beta-band amplitude. **C.** same as A showing reaction time (in hit trials) as a function of beta-band amplitude.

### 3.2 Prestimulus amplitude predicts hit rate and reaction time and explains part of the attentional improvement

Previous studies have shown that naturally occurring fluctuations of oscillatory amplitude in sensory cortex correlates with perceptual performance (see Introduction). We used these naturally occurring fluctuations to investigate the contribution of MEG-recorded amplitude modulations to attentional facilitation.

First, we used data from the uncued condition to establish the relation between prestimulus amplitude and perceptual performance. We sorted trials by amplitude and grouped them into eight non-overlapping bins. For each bin we calculated the mean amplitude, hit rate and median reaction time. To allow averaging over subjects we normalized amplitude, hit rates, and reaction times in each bin as a percentage change from the mean in the uncued condition (see Materials and Methods). The results are depicted by the red lines in Figure 3A, B, C (upper panels) and show that hit rate and reaction time are linearly related to prestimulus amplitude over the contralateral hemisphere, with lower amplitude predicting improved perceptual performance (denoted: amplitude-perception relation). We found a similar relation in the cued condition where subjects were orienting attention towards the upcoming stimulus (light blue lines in Figure 3A, B, C upper

panels). The slope did not differ between conditions (regression coefficients uncued - cued; alpha:  $t(11) = 0.648$ ,  $p = 0.469$ ; beta:  $t(11) = 0.983$ ;  $p = 0.347$ ). Moreover, we found that prestimulus amplitude in the uncued and cued trials was mostly in the same range (Figure 3A, B lower panels).

Next, we used the amplitude-perception relation from the uncued condition to investigate the contribution of the anticipatory amplitude modulation to the perceptual improvement in the cued condition. This involved three steps. First, we quantified the anticipatory amplitude modulation as the difference between the mean of the cued and the uncued condition (blue and red vertical lines in Figure 3A, B lower panels). Second, we used the amplitude-perception relation from the uncued condition to predict the improvement in performance that would follow from the anticipatory amplitude modulation. Third, we calculated the ratio between predicted and actual performance improvement due to the cue. We refer to this ratio (multiplied by 100) as the percentage explained improvement. As illustrated by the vertical distance between the red line (uncued) and the blue data point (cued) in Figure 3A, B, C (upper panels), only a small part of the attentional improvement can be explained by the prestimulus amplitude modulation. In fact, according to the depicted amplitude-perception relation in the uncued condition, the anticipatory modulation in alpha-band amplitude would lead to an improvement

**Table 1.** Contribution of prestimulus amplitude to attentional improvement in hit rate

	Anticipatory modulation	Regression coefficient	P	Percentage explained
Alpha contralateral	-14.9 ± 2.7	-0.0051 ± 0.0013	0.002	5.8 ± 1.5
Alpha ipsilateral	-3.3 ± 3.0	-0.0037 ± 0.0016	0.046	2.0 ± 1.4
Beta contralateral	-10.9 ± 1.5	-0.0087 ± 0.0020	0.001	7.0 ± 1.5
Beta ipsilateral	-1.4 ± 2.1	-0.0069 ± 0.0019	0.005	1.9 ± 0.7

of approximately 5% in hit rate, whereas the actual improvement in hit rate is approximately 65%. The anticipatory shift thus explains  $5/65*100 = 7.7\%$  of the attentional improvement that occurs in the cued condition.

Our calculation of the percentage explained improvement was based on a logistic regression in which we modeled the relationship between prestimulus amplitude and hit rate, separately for every subject (see Materials and Methods). The logistic regression has two major advantages over a procedure based on binning oscillatory amplitudes: First, it does not require an arbitrary choice on the number of bins and second, it can be extended to include multiple predictors (e.g. alpha- and beta-band amplitude together). The results of this analysis, using single predictors for alpha- or beta-band amplitude contralateral or ipsilateral to the side of the stimulus, are summarized in Table 1. In the uncued trials, we observed that both contralateral and ipsilateral alpha- and beta-band amplitude are predictive of subsequent performance, as indicated by the regression coefficients. This is not surprising because in the uncued trials the subject does not know on which hand the stimulus might occur and thus fluctuations in attentional state may very well occur bilaterally. Still, contralateral beta amplitude is the strongest predictor (in line with Jones et al., 2010). A strong anticipatory modulation was observed in the contralateral hemisphere (alpha -15%:  $t(11) = -5.523$ ,  $p < 0.001$ ; beta -11%:  $t(11) = -7.215$ ,  $p < 0.001$ ), but not in the ipsilateral (alpha -3%:  $t(11) = -1.092$ ,  $p = 0.298$ ; beta -1%:  $t(11) = -0.665$ ,  $p = 0.520$ ). Taking the anticipatory modulation and the amplitude-perception relation together, all four predictors explain part of the attentional improvement, with contralateral alpha and beta being the strongest determinants of the attentional improvement. However, the percentage explained improvement was not significantly different for contralateral alpha and beta ( $t(11) = 0.923$ ,  $p = 0.376$ ).

Next, we tested to what extent alpha- and beta-band amplitude in the contra- and ipsilateral

hemisphere contributed independently to the explained improvement. If two predictors are independent (i.e. uncorrelated across trials), then the percentage explained by the combined model should equal the sum of the percentages explained by the two individual models. We found that combining contralateral beta and alpha explained only an additional  $1.7 \pm 0.8\%$  ( $t(11) = 2.065$ ,  $p = 0.063$ ) of the improvement compared to using only contralateral beta. This implies that amplitude fluctuations in the alpha- and beta-band are highly correlated and that their influence on perception is not unique. Combining contralateral and ipsilateral beta also did not add to the percentage explained (additional percentage explained  $-0.1 \pm 0.9\%$ ;  $t(11) = -0.107$ ,  $p = 0.916$ ), and neither did combining contralateral and ipsilateral alpha (additional percentage explained  $0.2 \pm 1.0\%$ ;  $t(11) = 0.219$ ,  $p = 0.831$ ).

For reaction times we used a linear regression model because, in contrast to hit rate, reaction times are not expressed as a probability. Testing the same four predictors as for hit rate we found that only contralateral beta amplitude correlated significantly with reaction times (regression coefficients over subjects;  $t(11) = 2.938$ ,  $p < 0.05$ ) and explained  $12.5 \pm 6.0\%$  of the attentional improvement.

To assess the specificity of our findings, we tested to what extent they depended on the spatial, spectral, and temporal aspects of our predictor variables. First, we considered the spatial location of the somatosensory sources. In our analysis, we had localized somatosensory cortex using post-stimulus data from an independent localizer recording (see Materials and Methods). We might have underestimated the true explained improvement using non-optimal sources that did not reflect the perceptually relevant alpha- and beta-band amplitude. We therefore conducted the same analysis using sources obtained from the anticipatory modulation, thus biasing our source selection in favor of stronger effects. The different selection did not qualitatively affect our results (data not shown). Moreover, instead of unilateral amplitudes, we also

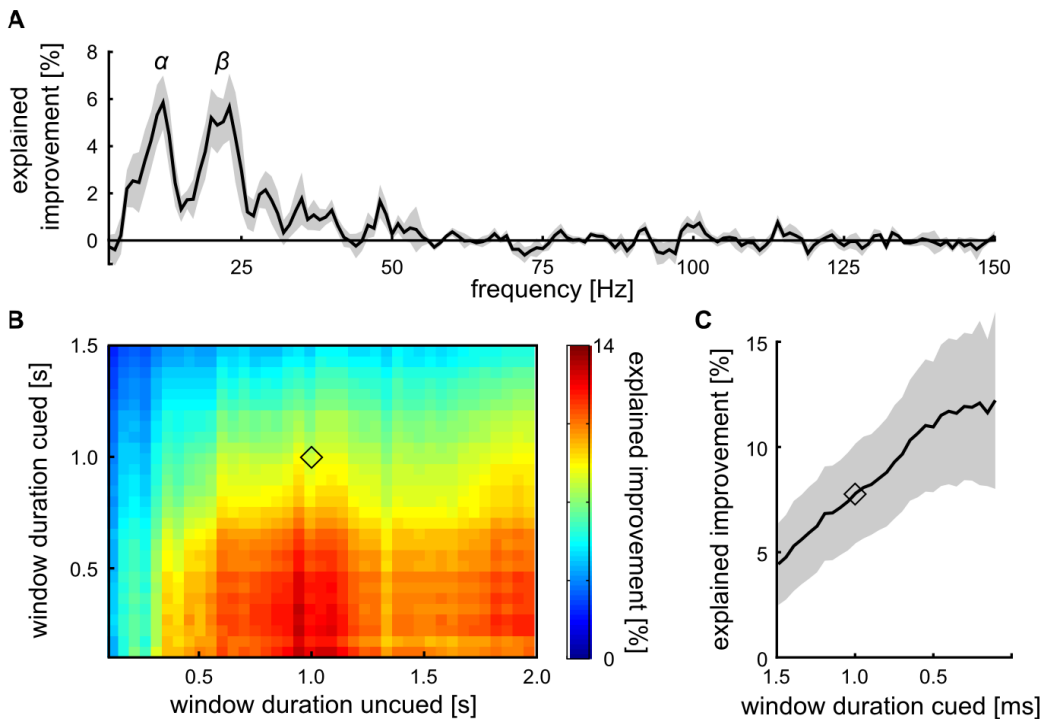


**Fig. 4** Explained perceptual improvement is alpha- and beta-frequency specific and depends on time window duration. **A.** Percentage of the attentional hit rate improvement that can be explained by prestimulus amplitude as a function of frequency. Amplitude was estimated in a 1 s prestimulus window with 4 Hz frequency smoothing. Shading indicates SEM. **B.** Percentage hit rate improvement explained as a function of the time window duration used to estimate amplitude in uncued (horizontal axis) and cued (vertical axis) trials. Contralateral alpha and beta amplitude were used as joint predictors. **C.** Percentage hit rate improvement explained as a function of window duration in the cued trials. Window duration for the uncued trials was fixed to 1 s. The diamond in panels B and C indicates the window durations used in the other analyses. Windows always ended at stimulus onset.

tested amplitude lateralization between contra- and ipsilateral hemisphere (cf. Thut et al., 2006) as a predictor of perceptual performance. However, we did not find a predictive relationship between ongoing fluctuations in amplitude lateralization and performance.

Second, we investigated whether our frequency band selection had been appropriate. We performed a frequency resolved analysis of the percentage explained improvement in hit rate. Results are depicted in Figure 4A and indeed the alpha- and the beta-band are the main predictive frequency bands. In line with previous observations (e.g. van Ede et al., 2010), we did not observe a contribution of gamma-band amplitudes to hit rate.

Third, we investigated the dependence of our results on the time windows that were used to estimate oscillatory amplitude. We had initially used a 1 s prestimulus window for both the cued and the uncued condition (in line with Jones et al., 2010; Linkenkaer-Hansen et al., 2004). In a control analysis, we independently varied the duration of the window (keeping it locked to stimulus onset) used to estimate the regression slope in the uncued trials, and the duration of the window to quantify

the anticipatory modulation in the cued trials. Figure 4B shows the explained improvement in hit rate as a function of both durations (using a combined model with contralateral alpha and beta amplitude as predictors). The relation between amplitude and hit rate in the uncued condition is relatively stable for time windows longer than 600 ms. However, the anticipatory modulation in cued conditions increases with shorter time windows, leading to a higher percentage explained improvement with shorter time windows. The likely cause is that, after a cue, it takes time to shift oscillatory amplitude and therefore, the closer the window is to the actual stimulus, the stronger the estimated modulation. Figure 4C shows that the explained improvement increases almost linearly with shorter windows for estimating the cue shift. Using the best selection of time-windows (950 ms window uncued, 250 ms window cued) and combining contralateral alpha and beta amplitude as predictors, the explained attentional improvement is  $13.1 \pm 4.0\%$ .

## 4. Discussion

Knowing when and where a stimulus will occur allows for orienting of attention towards the upcoming stimulus and improves its perception. There is abundant evidence suggesting that modulations of oscillatory amplitude in sensory cortex are an important mechanism underlying such orienting of attention. Using a somatosensory detection task, we confirmed that orienting attention to an upcoming stimulus involves a modulation of oscillatory amplitude and that spontaneous amplitude fluctuations are related to perceptual performance. Linking these two findings, we have, for the first time, quantified the contribution of MEG recorded amplitude modulations to the perceptual improvement that occurs with attentional orienting. Our results show that anticipatory amplitude modulations in somatosensory cortex explain up to approximately 13% of the hit rate improvement that follows from orienting attention. Moreover, while prestimulus amplitude in both the alpha- and beta-band was predictive of performance and was modulated by attentional orienting, their contributions to the perceptual improvement were largely shared.

These results raise the question what accounts for the remaining 87% of the improvement due to attentional orienting. In the following section, we consider other anatomical regions and physiological mechanisms that are potentially contributing to the improvement and discuss the role of MEG signal quality. Next, we discuss the functional relevance of alpha- and beta-band oscillations in somatosensory perception. Finally, we point out how the experimental paradigm presented here can be extended to other imaging techniques and modalities to investigate the neural substrates of attention.

### 4.1 Limitations concerning anatomical origin, physiological mechanism, and MEG signal quality

#### 4.1.1 Anatomical origin

In our analysis we have used a reconstructed signal which we believe originated from primary somatosensory cortex (S1; see Materials and Methods). However, several other brain regions, both up-stream and down-stream of S1, are involved in processing somatosensory stimuli and are therefore potentially involved in the attentional improvement.

Nevertheless, an actual improvement will only be

observed if activity in those regions is at least partially uncorrelated with the amplitude that we recorded. For example, a frontoparietal control region might be involved in orienting of attention but if its only function was to induce amplitude modulations in sensory cortex, then recording from this area would not improve the prediction of perceptual performance. Indeed, several studies report that activation of frontoparietal controls activity in early sensory cortex (Bressler, Tang, Sylvester, Shulman, & Corbetta, 2008; Capotosto, Babiloni, Romani, & Corbetta, 2009; Gregoriou, Gotts, Zhou, & Desimone, 2009; Moore & Armstrong, 2003; Zhang & Ding, 2010). These areas are also involved in orienting attention to upcoming somatosensory events (Carlsson, Petrovic, Skare, Petersson, & Ingvar, 2000; Langner et al., 2011).

One area that is potentially involved in the attentional improvement is ipsilateral S1. Several previous studies have suggested that differential activity in regions representing the relevant stimulus and regions not representing this stimulus predicts attention and perception (e.g. Drevets et al., 1995; Haegens et al., 2011; Sylvester, Shulman, Jack, & Corbetta, 2007; Thut et al., 2006). In the present study we investigated local oscillatory amplitude and may have overlooked the influence of differential activity in contralateral and ipsilateral S1. Yet, three arguments can be given against this possibility. First, attentional orienting did not significantly modulate ipsilateral amplitude. Second, the relation between ipsilateral amplitude and performance in the uncued condition was of the same rather than the opposite sign as contralateral amplitude. Third, a balanced measure (i.e. contralateral - ipsilateral) did not predict performance.

In addition to S1, the secondary somatosensory cortex (S2) is likely to be involved in the attentional improvement. This is supported by studies showing an attentional modulation spiking activity in S2 in anticipation of (Meftah, Bourgeon, & Chapman, 2009) or during (Roy, Steinmetz, Hsiao, Johnson, & Niebur, 2007; Steinmetz et al., 2000) tactile stimulation. Moreover, Chapman and Meftah (2005) suggested that attentional modulation might be independent between S1 and S2.

Sensory input is routed to S1 via the thalamus. There is converging evidence that the thalamus plays an active role in gating sensory information to the cortex and, accordingly, is modulated by top-down attention (Boly et al., 2007; O'Connor, Fukui, Pinsk, & Kastner, 2002; Sadaghiani, Hesselmann, & Kleinschmidt, 2009; for a review see Saalmann, Pigarev, & Vidyasagar, 2007). This idea is in line with

a study by Boly and colleagues (2007) who showed that ongoing fluctuations in thalamic BOLD activity were predictive of somatosensory detection performance. It is an open question whether thalamic activity could predict somatosensory performance independently of S1 activity, or whether activity in both areas would depend on each other.

#### *4.1.2 Underlying physiological mechanism*

In addition to anatomical restrictions, our analysis was constrained by the physiological signal that we measured. We focused on the amplitude of extracranially recorded alpha- and beta-band oscillations, which are believed to reflect synchronized activity in the underlying neuronal populations (Naruse et al., 2010; Pfurtscheller & Lopes da Silva, 1999). Likely, not all physiologically relevant processes are captured by this signal and we will now discuss some processes that are potentially relevant.

One mechanism that has consistently been implicated in attention is the modulation of gamma-band oscillations. While gamma-band amplitude and spike-filed coherence during stimulus processing is modulated by attention (Bauer, Oostenveld & Peeters, 2006; Fries, Reynolds, Rorie, & Desimone, 2001; Siegel et al., 2008), purely anticipatory gamma-band amplitude modulations are not consistently observed (see also Figure 4A). However, coherence between sensory and parietal regions in the gamma-band has been observed during stimulus anticipation (Siegel et al., 2008) and might, independently from local amplitude modulations, be involved in the attentional improvement.

Furthermore, our analysis focused on oscillatory amplitude and ignored phase information. The phase of ongoing alpha-band oscillations has also been related to perceptual performance in the visual domain (Busch, Dubois, & VanRullen, 2009; Mathewson, Gratton, Fabiani, Beck, & Ro, 2009). However, to our knowledge, there are no reports of alpha or beta phase alignment by attention, making alpha and beta phase unlikely to contribute to attentional orienting. It must be noted that phase alignment has been observed in the delta range (1.5 Hz; Lakatos, Karmos, Mehta, Ulbert, & Schroeder, 2008; Schroeder & Lakatos, 2009). Likewise, the phase of spontaneous infraslow oscillations (0.01 - 0.1 Hz) has been related to somatosensory detection performance (Monto, Palva, Voipio & Palva, 2008). Yet, oscillations on this time scale cannot account for attentional orienting during a 1.5 s cue-target interval.

Finally, the attentional improvement might be mediated by processes on the level of individual neurons, which are at least partially invisible in extracranially recorded oscillatory amplitude. For example, synchronization of local spiking activity has been reported in anticipation (de Oliveira, Thiele, & Hoffmann, 1997) and during stimulus processing (Roy et al., 2007; Steinmetz et al., 2000). Moreover, Meftah and colleagues (2009) report increased firing rates in secondary somatosensory cortex in anticipation of a tactile stimulus and a similar rate increase was found in V2 and V4 in visual anticipation (Luck, Chelazzi, Hillyard, & Desimone, 1997). Moreover, recent experiments suggest that attention decorrelates spike rates between neurons (Cohen & Maunsell, 2009; Mitchell et al., 2009). While these correlations might reflect (partially) the same process that determines the amplitude of local field potential oscillations, it is currently not clear to what extent they are related to MEG recorded oscillatory amplitude.

#### *4.1.3 Signal quality*

In regression analysis, noise added to the independent variable (i.e. amplitude) biases the slope of the regression line (i.e. amplitude-behavior relation) towards zero. This phenomenon is referred to as regression attenuation (cf. Frost & Thompson, 2000). Consequently, noisy amplitude estimates will lead to an underestimation of the predictive relation between amplitude and perceptual performance and hence of the contribution of oscillatory amplitude modulations to behavioral improvement. Given that MEG measurements are inherently noisy due to the nature of the sensors (superconducting quantum interference devices), environmental noise and subject movement, it is likely that we have underestimated the amplitude-behavior relation. Accordingly, the real contribution of anticipatory amplitude modulation to the attentional improvement is likely to be larger than our estimate.

Concluding, it remains an open question to what extend our estimate of the contribution of amplitude modulation is determined by the origin of the signal and to what extend it is determined by the quality of the signal. Nevertheless, we believe these results are revealing since they quantify the behavioral relevance of the MEG recorded amplitude in attentional orienting.

## 4.2 Alpha- and beta-band amplitude contribute non-uniquely to somatosensory perception

The present as well as previous studies have shown that both alpha- and beta-band amplitude are related to somatosensory perception. That is, amplitude in both frequency bands is modulated during anticipation of upcoming stimuli (present study, Anderson & Ding, 2011; van Ede et al., 2011; Jones et al., 2010), and ongoing fluctuations are related to perceptual performance (present study, Jones et al., 2010; Linkenkaer-Hansen et al., 2004; Schubert et al., 2009). However, it remains an open question whether amplitude in the alpha- and beta-band is independently related to somatosensory perception or whether both frequency bands reflect a single underlying process that is related to somatosensory perception. Our observations are in line with the latter hypothesis, because the contributions of alpha- and beta-amplitude to the attentional improvement were largely shared. That is, using alpha and beta amplitude as combined predictors in our regression model did not significantly improve the prediction of perceptual performance as compared to using the predictors individually. This indicates across-trial correlation between alpha and beta amplitude (cf. Scheeringa et al., 2011).

At the same time, several observations suggest a dissociation between alpha- and beta-band oscillations. First, beta oscillations have been localized more anterior than alpha oscillations (Salmelin & Hari, 1994). Second, we have previously shown different temporal flexibility of alpha and beta amplitude modulations in the context of temporal orienting of somatosensory attention (van Ede et al., 2011). Third, after a tactile stimulus the beta rebound of oscillatory amplitude occurs before the alpha rebound (Cheyne et al., 2003). Finally, a computational model by Jones and colleagues (2009) suggests differences in the mechanisms generating alpha- and beta-band oscillations. Given these opposing results, it remains unclear under which circumstances alpha and beta oscillations overlap in their functional role and under which circumstances they function independently.

## 4.3 Combining spontaneous and task-induced fluctuations to study the contribution of specific brain states to attention

In the present study we investigated the contribution of a specific brain state (represented as a neural signal) to the behavioral improvement that occurs with attention. First, we utilized spontaneous fluctuations to model the relation between the ongoing brain state and behavioral performance. Then, we used this relation and the induced attentive brain state to predict the attentional improvement in behavior. Comparing the predicted with the actual improvement, we quantified the contribution of a specific brain state to the attentional improvement.

This approach could be extended in several ways. First, stimuli in different modalities (e.g. visual, auditory) can be used to investigate whether a neural signal is relevant for attention only within a particular modality or whether it is relevant across modalities. Second, the response variable, which was perceptual performance in the present study, can also be a neurophysiological measure that is affected by attention, for example the amplitude of stimulus evoked responses (O'Connor et al., 2002; Jones et al., 2010; Zhang & Ding, 2010). Third, the brain state can be measured during anticipation but also during stimulus processing. Fourth, different signals, such as BOLD or spiking activity, can be used to represent the brain state.

Methods that simultaneously measure activity in multiple regions (e.g. fMRI) are particularly interesting in this context, because the quantitative approach suggested here can be used to compare the relative contribution of multiple brain areas. Moreover, by combining multiple predictors in a regression model and comparing the results to individual predictors, it is possible to test whether signals contribute independently to the response variable. This could be used to investigate, for example, whether frontoparietal and sensory regions contribute independently to the attentional improvement or whether fMRI and simultaneously recorded electroencephalography signals can contribute independently.

## 5. Conclusion

Orienting attention to an upcoming sensory event involves a modulation of oscillatory amplitude within sensory cortex. We have shown that the MEG recorded amplitude modulation can explain up to 13% of the perceptual improvement that occurs with attention in a somatosensory detection task. Both alpha- and beta-band oscillations are predictive of the improvement and their contributions were largely shared. It remains an open question to what extend our estimate is determined by physiological relevance of amplitude modulations within sensory cortex and to what extend it depends on the signal-to-noise ratio of the MEG signal. Nevertheless, given that MEG and electroencephalography are commonly used to study the neural mechanisms underlying attention, these results are important because we have for the first time quantified the behavioral relevance of an MEG recorded signal in the context of attentional orienting. Together with suggested future research, these results will help to explain by which neurophysiological mechanisms attention improves perception.

## Acknowledgments

I am grateful to Eric for making this project possible and being there whenever I needed support. His clear thinking has inspired me. I thank Freek for guiding me at every stage of the project and providing encouragement when I needed it. I could not have had a better colleague. Finally, I thank Claus Hilgetag for introducing me to neuroscience and helping me find my way.

## References

- Anderson, K. L., & Ding, M. (2011). Attentional Modulation of the Somatosensory Mu Rhythm. *Neuroscience, 180*, 165-180.
- Bahramisharif, A., van Gerven, M., Heskes, T., & Jensen, O. (2010). Covert attention allows for continuous control of brain-computer interfaces. *European Journal of Neuroscience, 31*(8), 1501-1508.
- Bauer, M., Oostenveld, R., Peeters, M., & Fries, P. (2006). Tactile spatial attention enhances gamma-band activity in somatosensory cortex and reduces low-frequency activity in parieto-occipital areas. *The Journal of Neuroscience, 26*(2), 490-501.
- Becker, R., Reinacher, M., Freyer, F., Villringer, A., & Ritter, P. (2011). How Ongoing Neuronal Oscillations Account for Evoked fMRI Variability. *The Journal of Neuroscience, 31*(30), 11016-11027.
- Boly, M., Balteau, E., Schnakers, C., Degueldre, C., Moonen, G., Luxen, A., ..., Laureys, S. (2007). Baseline brain activity fluctuations predict somatosensory perception in humans. *Proceedings of the National Academy of Sciences of the United States of America, 104*(29), 12187-12192.
- Brainard, D. H. (1997). The Psychophysics Toolbox. *Spatial vision, 10*(4), 433-6.
- Bressler, S. L., Tang, W., Sylvester, C. M., Shulman, G. L., & Corbetta, M. (2008). Top-down control of human visual cortex by frontal and parietal cortex in anticipatory visual spatial attention. *The Journal of Neuroscience, 28*(40), 10056-10061.
- Busch, N. A., Dubois, J., & VanRullen, R. (2009). The phase of ongoing EEG oscillations predicts visual perception. *The Journal of Neuroscience, 29*(24), 7869-7876.
- Capoto, P., Babiloni, C., Romani, G. L., & Corbetta, M. (2009). Frontoparietal cortex controls spatial attention through modulation of anticipatory alpha rhythms. *The Journal of Neuroscience, 29*(18), 5863-5872.
- Carlsson, K., Petrovic, P., Skare, S., Petersson, K. M., & Ingvar, M. (2000). Tickling expectations: neural processing in anticipation of a sensory stimulus. *Journal of Cognitive Neuroscience, 12*(4), 691-703.
- Cheyne, D., Gaetz, W., Garnero, L., Lachaux, J.-P., Ducorps, A., Schwartz, D., & Varela, F. J. (2003). Neuromagnetic imaging of cortical oscillations accompanying tactile stimulation. *Cognitive Brain Research, 17*(3), 599-611.
- Cohen, M. R., & Maunsell, J. H. R. (2009). Attention improves performance primarily by reducing interneuronal correlations. *Nature Neuroscience, 12*(12), 1594-600.
- van Dijk, H., Schoffelen, J. M., & Oostenveld, R. (2008). Prestimulus oscillatory activity in the alpha band predicts visual discrimination ability. *Journal of Neuroscience, 28*(8), 1816.
- Drevets, W. C., Burton, H., Videen, T. O., Snyder, A. Z., Simpson, J. R., & Raichle, M. E. (1995). Blood flow changes in human somatosensory cortex during anticipated stimulation. *Nature, 373*, 249-252.
- van Ede, F., de Lange, F., Jensen, O., & Maris, E. (2011). Orienting Attention to an Upcoming Tactile Event Involves a Spatially and Temporally Specific Modulation of Sensorimotor Alpha- and Beta-Band Oscillations. *Journal of Neuroscience, 31*(6), 2016-2024.
- van Ede, F., Jensen, O., & Maris, E. (2010). Tactile expectation modulates pre-stimulus [beta]-band oscillations in human sensorimotor cortex. *NeuroImage, 51*(2), 867-876.
- Ergenoglu, T., Demiralp, T., Bayraktaroglu, Z., Ergen, M., Beydagli, H., & Uresin, Y. (2004). Alpha rhythm of the EEG modulates visual detection performance in humans. *Cognitive Brain Research, 20*(3), 376-383.
- Foxe, J. J., Simpson, G. V., & Ahlfors, S. P. (1998). Parieto-occipital ~10 Hz activity reflects anticipatory state of visual attention mechanisms. *Neuroreport, 9*(17), 3929-3933.

- Fries, P., Reynolds, J. H., Rorie, A. E., & Desimone, R. (2001). Modulation of oscillatory neuronal synchronization by selective visual attention. *Science*, 291(5508), 1560-3.
- Frost, C., & Thompson, S. G. (2000). Correcting for regression dilution bias: comparison of methods for a single predictor variable. *Journal of the Royal Statistical Society: Series A (Statistics in Society)*, 163(2), 173-189.
- Gaetz, W., & Cheyne, D. (2006). Localization of sensorimotor cortical rhythms induced by tactile stimulation using spatially filtered MEG. *NeuroImage*, 30(3), 899-908.
- Gould, I. C., Rushworth, M. F., & Nobre, A. C. (2011). Indexing the graded allocation of visuospatial attention using anticipatory alpha oscillations. *Journal of Neurophysiology*, 105(3), 1318-1326.
- Gregoriou, G. G., Gotts, S. J., Zhou, H., & Desimone, R. (2009). High-frequency, long-range coupling between prefrontal and visual cortex during attention. *Science*, 324(5931), 1207-1210.
- Gross, J., Kujala, J., Hamalainen, M., Timmermann, L., Schnitzler, A., & Salmelin, R. (2001). Dynamic imaging of coherent sources: Studying neural interactions in the human brain. *Proceedings of the National Academy of Sciences of the United States of America*, 98(2), 694-699.
- Haegens, S., Handel, B. F., & Jensen, O. (2011). Top-Down Controlled Alpha Band Activity in Somatosensory Areas Determines Behavioral Performance in a Discrimination Task. *The Journal of Neuroscience*, 31(14), 5197-5204.
- Hanslmayr, S., Aslan, A., Staudigl, T., Klimesch, W., Herrmann, C. S., & Bäuml, K. H. (2007). Prestimulus oscillations predict visual perception performance between and within subjects. *NeuroImage*, 37(4), 1465-1473.
- Händel, B. F., Haarmeier, T., & Jensen, O. (2011). Alpha oscillations correlate with the successful inhibition of unattended stimuli. *Journal of Cognitive Neuroscience*, 23(9), 2494-2502.
- Jones, S. R., Kerr, C. E., Wan, Q., Pritchett, D. L., Hamalainen, M., & Moore, C. I. (2010). Cued Spatial Attention Drives Functionally Relevant Modulation of the Mu Rhythm in Primary Somatosensory Cortex. *The Journal of Neuroscience*, 30(41), 13760-13765.
- Kelly, S. P., Lalor, E. C., Reilly, R. B., & Foxe, J. J. (2006). Increases in alpha oscillatory power reflect an active retinotopic mechanism for distracter suppression during sustained visuospatial attention. *Journal of Neurophysiology*, 95(6), 3844-3851.
- Lakatos, P., Karmos, G., Mehta, A. D., Ulbert, I., & Schroeder, C. E. (2008). Entrainment of neuronal oscillations as a mechanism of attentional selection. *Science*, 320(5872), 110-113.
- Langner, R., Kellermann, T., Boers, F., Sturm, W., Willmes, K., & Eickhoff, S. B. (2011). Modality-Specific Perceptual Expectations Selectively Modulate Baseline Activity in Auditory, Somatosensory, and Visual Cortices. *Cerebral Cortex*, 21(12), 2850-2862.
- Linkenkaer-Hansen, K., Nikulin, V., & Palva, S. (2004). Prestimulus oscillations enhance psychophysical performance in humans. *The Journal of Neuroscience*, 24(45), 10186-10190.
- Luck, S. J., Chelazzi, L., Hillyard, S. A., & Desimone, R. (1997). Neural mechanisms of spatial selective attention in areas V1, V2, and V4 of macaque visual cortex. *Journal of Neurophysiology*, 77(1), 24-42.
- Mathewson, K., Gratton, G., Fabiani, M., Beck, D. M., & Ro, T. (2009). To See or Not to See: Prestimulus alpha Phase Predicts Visual Awareness. *The Journal of Neuroscience*, 29(9), 2725-2732.
- Meftah, E. M., Bourgeon, S., & Chapman, C. E. (2009). Instructed Delay Discharge in Primary and Secondary Somatosensory Cortex Within the Context of a Selective Attention Task. *Journal of Neurophysiology*, 101(5), 2649.
- Mitchell, J. F., Sundberg, K. A., & Reynolds, J. H. (2009). Spatial attention decorrelates intrinsic activity fluctuations in macaque area V4. *Neuron*, 63(6), 879-888.
- Monto, S., Palva, S., Voipio, J., & Palva, J. (2008). Very slow EEG fluctuations predict the dynamics of stimulus detection and oscillation amplitudes in humans. *The Journal of Neuroscience*, 28(33), 8268-8272.
- Moore, T., & Armstrong, K. M. (2003). Selective gating of visual signals by microstimulation of frontal cortex. *Nature*, 421(6921), 370-373.
- Naruse, Y., Matani, A., Miyawaki, Y., & Okada, M. (2010). Influence of coherence between multiple cortical columns on alpha rhythm: a computational modeling study. *Human Brain Mapping*, 31(5), 703-715.
- Nolte, G. (2003). The magnetic lead field theorem in the quasi-static approximation and its use for magnetoencephalography forward calculation in realistic volume conductors. *Physics in medicine and biology*, 48(22), 3637-3652.
- de Oliveira, S. C., Thiele, A., & Hoffmann, K. P. (1997). Synchronization of neuronal activity during stimulus expectation in a direction discrimination task. *The Journal of Neuroscience*, 17(23), 9248-9260.
- Oostenveld, R., Fries, P., Maris, E., & Schoffelen, J.M. (2011). FieldTrip: Open source software for advanced analysis of MEG, EEG, and invasive electrophysiological data. *Computational Intelligence and Neuroscience*, 2011, 156869.
- O'Connor, D. H., Fukui, M. M., Pinsk, M. A., & Kastner, S. (2002). Attention modulates responses in the human lateral geniculate nucleus. *Nature Neuroscience*, 5(11), 1203-1209.
- Percival, D. B., & Walden, A. T. (1993). *Spectral analysis for physical applications: multitaper and conventional univariate techniques*. Cambridge: Cambridge University Press.
- Pfurtscheller, G., & Lopes da Silva, F. H. (1999). Event-related EEG/MEG synchronization and desynchronization: basic principles. *Clinical neurophysiology*, 110(11), 1842-1857.
- Posner, M. I., & Petersen, S. E. (1990). The attention system of the human brain. Annual review of neuroscience, 13, 25-42.

- Ritter, P., Moosmann, M., & Villringer, A. (2009). Rolandic alpha and beta EEG rhythms' strengths are inversely related to fMRI-BOLD signal in primary somatosensory and motor cortex. *Human Brain Mapping, 30*(4), 1168-87.
- Romei, V., Brodbeck, V., Michel, C., Amedi, A., Pascual-Leone, A., & Thut, G. (2008). Spontaneous fluctuations in posterior alpha-band EEG activity reflect variability in excitability of human visual areas. *Cerebral Cortex, 18*(9), 2010-2018.
- Romei, V., Gross, J., & Thut, G. (2010). On the role of pre-stimulus alpha-rhythms over occipito-parietal areas in visual input regulation: Correlation or causation? *The Journal of Neuroscience, 30*(25), 8692-7.
- Roy, A., Steinmetz, P. N., Hsiao, S. S., Johnson, K. O., & Niebur, E. (2007). Synchrony: a neural correlate of somatosensory attention. *Journal of Neurophysiology, 98*(3), 1645.
- Saalmann, Y. B., Pigarev, I. N., & Vidyasagar, T. R. (2007). Neural mechanisms of visual attention: how top-down feedback highlights relevant locations. *Science, 316*(5831), 1612-1615.
- Sadaghiani, S., Hessellmann, G., & Kleinschmidt, A. (2009). Distributed and antagonistic contributions of ongoing activity fluctuations to auditory stimulus detection. *The Journal of Neuroscience, 29*(42), 13410-13417.
- Salmelin, R., & Hari, R. (1994). Spatiotemporal characteristics of sensorimotor neuromagnetic rhythms related to thumb movement. *Neuroscience, 60*(2), 537-550.
- Sauseng, P., Klimesch, W., Gerloff, C., & Hummel, F. C. (2009). Spontaneous locally restricted EEG alpha activity determines cortical excitability in the motor cortex. *Neuropsychologia, 47*(1), 284-288.
- Sauseng, P., Klimesch, W., Stadler, W., Schabus, M., Doppelmayr, M., Hanslmayr, S., Gruber, W. R., & Birbaumer, N. (2005). A shift of visual spatial attention is selectively associated with human EEG alpha activity. *European Journal of Neuroscience, 22*(11), 2917-2926.
- Scheeringa, R., Fries, P., Petersson, K.-M., Oostenveld, R., Grothe, I., Norris, D. G., Hagoort, P., & Bastiaansen, M.C.M. (2011). Neuronal dynamics underlying high- and low-frequency EEG oscillations contribute independently to the human BOLD signal. *Neuron, 69*(3), 572-583.
- Schroeder, C., & Lakatos, P. (2009). Low-frequency neuronal oscillations as instruments of sensory selection. *Trends in Neurosciences, 32*(1), 9-18.
- Schubert, R., Haufe, S., Blankenburg, F., Villringer, A., & Curio, G. (2009). Now you'll feel it, now you won't: EEG rhythms predict the effectiveness of perceptual masking. *Journal of Cognitive Neuroscience, 21*(12), 2407-2419.
- Siegel, M., Donner, T. H., Oostenveld, R., Fries, P., & Engel, A. K. (2008). Neuronal synchronization along the dorsal visual pathway reflects the focus of spatial attention. *Neuron, 60*(4), 709-719.
- Snyder, A. C., & Foxe, J. J. (2011). The countervailing forces of binding and selection in vision. *Cortex, 1-8*.
- Steinmetz, P. N., Roy, A., Fitzgerald, P., Hsiao, S., Johnson, K., & Niebur, E. (2000). Attention modulates synchronized neuronal firing in primate somatosensory cortex. *Nature, 404*(6774), 131-133.
- Sylvester, C. M., Shulman, G. L., Jack, A. I., & Corbetta, M. (2007). Asymmetry of anticipatory activity in visual cortex predicts the locus of attention and perception. *The Journal of Neuroscience, 27*(52), 14424-33.
- Tamura, Y., Hoshiyama, M., Nakata, H., Hiroe, N., Inui, K., Kaneoke, Y., Inoue, K., & Kakigi, R. (2005). Functional relationship between human rolandic oscillations and motor cortical excitability: an MEG study. *European Journal of Neuroscience, 21*(9), 2555-2562.
- Thut, G., Nietzel, A., Brandt, S. A., & Pascual-Leone, A. (2006). Alpha-band electroencephalographic activity over occipital cortex indexes visuospatial attention bias and predicts visual target detection. *The Journal of Neuroscience, 26*(37), 9494-9502.
- Ward, L. M. (2008) Attention. *Scholarpedia, 3*(10):1538.
- Worden, M. S., Foxe, J. J., Wang, N., & Simpson, G. V. (2000). Anticipatory biasing of visuospatial attention indexed by retinotopically specific alpha-band electroencephalography increases over occipital cortex. *The Journal of Neuroscience, 20*(6), RC63.
- Wyart, V., & Tallon-Baudry, C. (2008). Neural dissociation between visual awareness and spatial attention. *The Journal of Neuroscience, 28*(10), 2667-2679.
- Yamagishi, N., Callan, D. E., Anderson, S. J., & Kawato, M. (2008). Attentional changes in pre-stimulus oscillatory activity within early visual cortex are predictive of human visual performance. *Brain Research, 1197*, 115-122.
- Yamagishi, N., Goda, N., Callan, D. E., Anderson, S. J., & Kawato, M. (2005). Attentional shifts towards an expected visual target alter the level of alpha-band oscillatory activity in the human calcarine cortex. *Cognitive brain research, 25*(3), 799-809.
- Zhang, Y., & Ding, M. (2010). Detection of a weak somatosensory stimulus: role of the prestimulus mu rhythm and its top-down modulation. *Journal of Cognitive Neuroscience, 22*(2), 307-322.

# Adaptation and Retention of Motor Memories During Self-Motion: The Role of the Vestibular System

Adjmal Sarwary<sup>1</sup>

Supervisors: Luc P.J. Selen<sup>1</sup>, W. Pieter Medendorp<sup>1</sup>

*<sup>1</sup>Donders Institute for Brain, Cognition and Behaviour, Radboud University Nijmegen, The Netherlands*

Retention of motor memories has typically been studied by testing adaptation of planar reaching movements in stationary subjects under different force fields generated by haptic interfaces. Results have shown that a learned motor memory for one field is lost when an opposing field has to be learned. Here we challenge these findings for motor learning and adaptation during lateral linear whole body accelerations. In contrast to previous research, in this dynamic environment the vestibular system is engaged. Using an ABAB scheme, forward and backward reaching movements were performed under two opposite reaching direction dependent accelerations (A and B). In this scheme, both anterograde and retrograde interference were present, creating a challenging context for retention. Our results show retention by an increased learning rate during the second exposure to a force field by a factor of six. Retention also occurred in a further paradigm, in which anterograde interference was reduced using wash-out trials. Next to these results, it has been argued that adaptation is not about minimizing error, but about re-optimizing the movement. Using optimal feedback control theory, we show that also behavior in an accelerating environment can be understood as an optimal strategy, exploiting the environmental dynamics. However, optimal solutions are markedly different for traditional curl-fields and the accelerative environment. Additionally, the amount of time necessary to reach a state of full adaptation is more than twice as long for curl-fields compared to accelerations. These results suggest two important functions of the vestibular system for motor learning: one, it has a facilitating effect on adaptation by providing information of the environmental dynamics; second, it provides strong enough cues to disambiguate the context between the two opposing force fields, which results in retention of motor memories.

*Keywords:* motor learning, adaptation, retention, internal model, interference, contextual cues, optimal control

---

Corresponding author: Adjmal Sarwary, email: a.sarwary@donders.ru.nl

## 1. Introduction

Humans perform countless complex movements on a daily basis. A key component enabling complex movement patterns such as speaking, playing the drums, or dancing is motor learning. That is when the human brain has to constantly adapt current movements to achieve the desired outcome.

In the past decades, motor learning and adaptation have predominantly been studied in arm reaching paradigms with sensory or force perturbations. Force perturbations, directly coupled with either position or velocity of the reaching arm, are called a force field. Such force fields have been generated in two different ways: using a robotic manipulandum, which imposes the perturbation forces directly to the hand (Shadmehr & Mussa-Ivaldi, 1994; Brashers-Krug et al., 1996; Caithness et al., 2004; Nozaki et al., 2006; Cothros et al., 2008; Howard et al., 2010), and by using non-contact coriolis force in rotating platform experiments (Lackner & Dizio, 1994; Dizio & Lackner, 1995).

In the absence of such force fields, simple reaching movements show roughly straight trajectories. When exposed to force fields, subjects initially generate highly curved trajectories that become straighter with practice (Lackner & Dizio, 1994; Shadmehr & Mussa-Ivaldi, 1994). Several models have been proposed to describe the process of motor adaptation (Shadmehr et al., 2010). It has been hypothesized that adaptation tries to reduce the spatial difference between the observed trajectory under force field conditions and the trajectory when no forces are present. On the other hand, others have argued that adaptation is driven by re-optimizing movements in a new environment, here a force field (Izawa et al., 2008). One indication of this is that if a curved path between two points is artificially created to cause minimum resistance, people adapt their reaches to these novel dynamics to follow the curved path and not a straight line (Chib et al., 2006).

This notion of re-optimization is well captured by optimal feedback control theory (OFCT), which is based on the idea that the goal of adaptation is not to cancel the imposed forces, but to find the trajectory that minimizes some cost function for this particular environment (Todorov, 2004; Izawa et al., 2008). Therefore, an optimal trajectory in one environment (no force field) is unlikely to be optimal in another (force field) (Wang et al., 2001; Diedrichsen, 2007). Within this framework, adaptation leads to the acquisition of an internal model of the dynamics of the novel environment (e.g., force field) and results in

reaching movements that exploit the environmental dynamics to minimize the cost associated with the movement plan (Kawato, 1999).

How many of such internal models can we store? Daily life suggests that there is no limit. Multiple forces act upon us constantly, whether we drive a car, ride our bikes, or play sports. We are perfectly capable to compensate for the forces under each of these contexts, suggesting the existence of multiple internal models that are adapted and consolidated automatically and independently (Kawato, 1999).

This introspection is at odds with laboratory findings (Brashers-Krug et al., 1996; Caithness et al., 2004; Cothros et al., 2008). In most of these studies subjects perform reaching movements using a manipulandum with two opposite velocity-dependent force fields (A & B), by applying an ABA scheme. The reasoning behind this schema is if multiple internal models are established, the internal model for force field A is not lost after learning field B. However, results show that during the second exposure to A, prior learned dynamics from the first exposure are forgotten (Caithness et al., 2004).

These findings demonstrate that adapting to novel dynamics is prone to interference. Interference effects can occur in two directions: Retrograde interference characterizes the effect of learning a new task while remembering the old one (field B on A), and anterograde interference denotes the effect of the old task on the new (field A on B). It has been suggested that multiple forward models may be established by reducing the amount of interference. Typically, anterograde interference can be reduced by adding blocks of null trials, so called wash-out trials, between perturbation blocks (Miall et al., 2004). Adding wash-out trials after learning a force field will diminish its effect on learning the subsequent force field (e.g. A on B).

Strikingly, even by interspersing perturbation blocks by wash-out trials no retention of the initially learned internal model of field A seems to occur (Caithness et al., 2004). Additional experiments that tried to reduce the amount of interference by providing contextual cues did not succeed. For example, each force field (i.e. internal model) was then linked to a different color (Osu et al., 2004) or differently shaped handles of a manipulandum (Cothros et al., 2008). These experiments also failed to report the existence of multiple internal models. Only experiments that provided contextual cues that were directly part of the motor act itself could demonstrate retention and thereby the learning of multiple internal models (Nozaki et al., 2006; Howard et al., 2010).

This led us to the question whether the lack of retention in the classic force field studies may be due to the nature of the fields and/or the contextual cues. Previous studies have shown that adaptation to inertial force fields from a rotating room are markedly different from adaptation to contact forces from a robotic manipulandum (Lackner & DiZio, 2005). Second, in the classic force field studies, subjects have to disambiguate both the context and kinematic and dynamic errors from their reaches or from cues that are not directly part of their motor actions. Here we set out to explore whether a rich sensory environment, in which errors and causes can be easily disambiguated, can help learning of multiple inertial force field adaptations.

In this study we are having a close look at motor learning of reaching movements in accelerating environments. Similar to rotating room experiments (Lackner & Dizio, 1994; Dizio & Lackner, 1995), inertial, contact-free forces are created, though not by whole body rotation, but via linear acceleration. The important difference however, is the type of sensory feedback provided by creating inertial forces via acceleration compared to forces created through a robotic manipulandum or a rotating room. In the cases of manipulanda and rotating rooms, only visual and proprioceptive feedback is present. Using acceleration provides additional sensory feedback from the vestibular system. We hypothesize that information from the vestibular system provides an estimate of the imposed forces, as well as a strong contextual signal to disambiguate the force fields, which could make multiple internal model learning possible.

Our results indicate fast adaptation, as in the rotating room experiments, and additionally, a context provided through the vestibular system that makes distinction between two opposing perturbations possible. This results in retention shown by a significant faster relearning of one perturbation after an interference perturbation block. The first paradigm contained both retrograde and anterograde interference fully present and was therefore called full interference paradigm (FIP). In the second paradigm, reduced interference paradigm (RIP), we reduced the amount of anterograde interference by adding null trials. In addition, we used an adapted Optimal Feedback Control Theory model to predict subjects final adaptation to forces in this moving actor environment. Comparing the behavioral data with the model shows that adaptation in this environment is not a process of perturbation cancellation, but rather of re-optimization.

## 2. Materials and methods

### 2.1 Participants

In total, 21 right-handed subjects participated in one of two paradigms. The subjects were naive to the research question and participated after signing a consent form. As reimbursement, course credit or payment was provided. All subjects had normal, or corrected to normal vision, and had no motor deficits. Four subjects were excluded from the analyses, since they used primarily an impedance control strategy instead of adapting to the environmental dynamics (Franklin et al., 2003).

### 2.2 Setup

The setup in both paradigms was equivalent. All subjects performed reaching movements with their right index finger, while sitting in a sled that slided along a magnetic track (Kollmorgen S700 controller). The fingertip and sled position were recorded at 250 Hz and stored for off-line analysis using the Optotrak Certus system (NDI, Northern Digital Instruments, Waterloo, Canada). Both paradigms were performed under dimmed light, to reduce the use of environmental anchoring points and to improve visibility of targets. The start and target position were displayed for the whole duration of a trial using a sled mounted table with a total of 286 integrated LED pairs. The table was mounted on the sled and served as an armrest in between trials. To create a dynamic environment, the sled was accelerated laterally with a bell-shaped velocity profile of 650 ms duration and 30 cm amplitude. Sled movement was triggered by the initiation of the reaching movement, determined by using real-time Optotrak data recorded at 100 Hz (delay ca. 60 ms). The setup was controlled using custom build software written in Delphi.

The procedure was similar in the full interference ( $n = 8$  subjects) and the reduced interference paradigm ( $n = 9$  subjects). Subjects had to perform 35 cm forward reaching and backward reaching movements, while sitting in the sled. Participants' bodies and heads were fixated using a racing belt and sled mounted headphones. The headphones also provided the go cue and auditory feedback during the experiments. Start and target position were indicated using a green (start) and red (target) LED, which were below eye level in the subject's midsagittal plane (Fig. 1).

**Table 1.** Description of the experiment.

Paradigm	Subject Number	Structure
Full Interference (FIP)	8	n A B A B n
Reduced Interference (RIP)	9	n A n B n A n B n

## 2.3 Experimental paradigms

In both paradigms participants initiated a trial by positioning their right index finger onto the green start LED. A go beep was given after the finger had remained stable on the start position and its speed stayed below 25 cm/s for 500 msec.

The reach was considered to start and to end as soon as the finger speed exceeded/underwent 25 cm/s. As soon as the red LED was reached, the participants received auditory feedback, indicating whether their reach time was below ('move faster'), within ('well done'), or above ('move slower') the required time window of 600 - 800 ms. Both start and target position had a circular position tolerance of 1.5 cm radius (Fig. 2).

On some trials, perturbations were generated by sled acceleration perpendicular to the reaching direction. Subjects were instructed to perform reaches as natural as possible and try to stay within the reach time window, as well as not to slide over the table surface.



**Fig. 1** Experimental setup. Subject seated in the sled, fixated with racing belts, headphones, and with the LED table in front performing reaching movements.

Two types of force fields were created by different couplings of the reaching direction and lateral acceleration direction. Field A consists of a forward reach with a leftward acceleration and a backward reach with a rightward acceleration. Field B creates the opposite forces by switching the coupling of reach direction and acceleration direction (Fig. 3).

### 2.3.1 Full interference paradigm (FIP)

In the FIP, subjects performed a familiarization block (50 movement) in which the sled was not moved (null). This block was followed by 4 perturbation blocks (160 movements each) with alternating force fields, beginning with force field A (Table 1). Each perturbation block included 14 catch trials consisting of 7 forward and 7 backward catches, that were randomly given with a 10 trial distance and were equivalent to null trials (Fig. 3). The initial 20 trials of a perturbation block were catch trial free. After the last perturbation block a de-learning block followed (50 movements), which was equivalent to the familiarization block (null).

### 2.3.2 Reduced interference paradigm (RIP)

The RIP differed from the FIP only by interspersing blocks of null trials (null) (40 movements) in between perturbation blocks (Table 1).

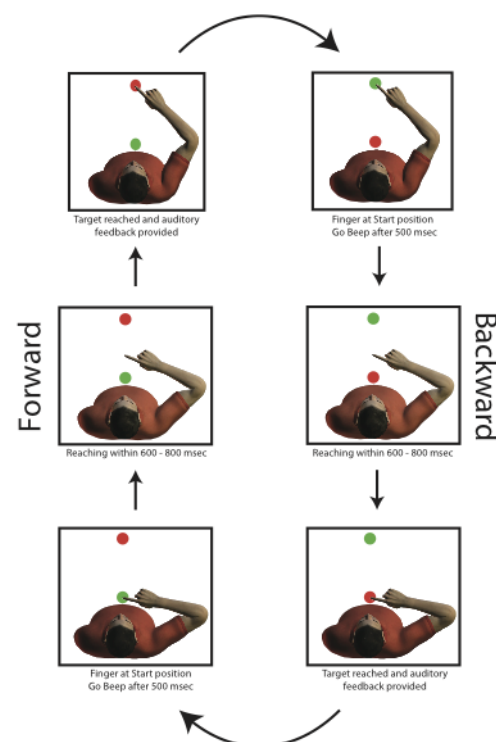


**Fig. 2** Forward and backward reaching trials in a null field. Forward and backward reaches follow after each other. The null field condition is equivalent to a catch trial during a perturbation block.

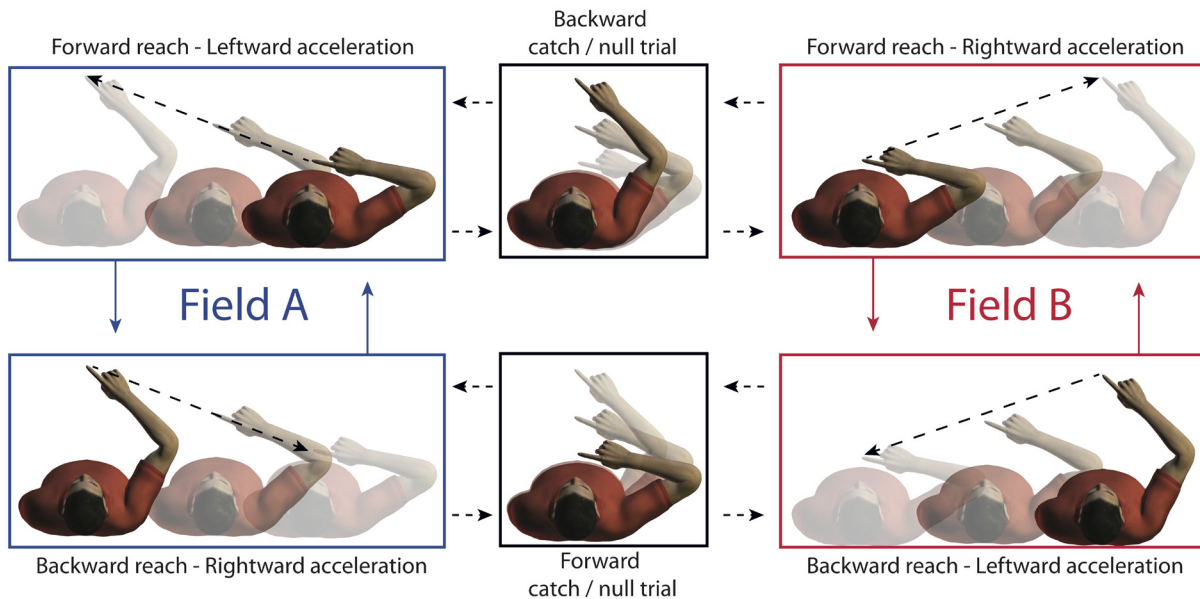


**Fig. 3** Description of the two force fields. Consecutive forward and backward reaches, interspersed with catch trials. Field A consists of a forward reach with leftward acceleration and backward reach with rightward acceleration coupling. Field B entails the opposite couplings.

## 2.4 Analysis

Data of position was first preprocessed following two steps. Missing data points, which were the result of an occlusion of an Optotrak sensor, were interpolated. After interpolation, the position data was filtered using a 12 Hz low-pass filter.

Adaptation to the accelerating environment was quantified by computing the absolute hand-path error of each trajectory. The absolute hand-path error determines the area of the trajectory in perturbation direction x, weighted by its velocity in y direction, relative to a straight line determined from the centers of the start to target position (Franklin, 2003). Compared to the maximum perpendicular distance, this error measure is more robust to outlier trajectories. It takes the entire trajectory into account and weighs most heavily the deviation of the trajectory at peak velocity.

$$E = \int_{t_0}^{t_f} |x(t)| |\dot{y}(t)| dt * c$$

The absolute hand-path error was computed from start of the reach,  $t_0$  (speed of the reach exceeded 25 cm/s) until the end of the reach (speed of the reach went below 25 cm/s) and multiplied by a constant  $c$ . Trials, with a movement time above 1 s or with a final position not at target within a 1.5 cm radius tolerance were excluded from further analysis.

To assess learning over time, hand-path errors from each block of each subject were fitted with the following exponential function:

$$E(t) = A_0 * e^{-t/\tau} + A_{asympt}$$

using least squares. In this function,  $A_0$  refers to the gain of the exponential function,  $\tau$  to the learning rate,  $A_{asympt}$  to the converged adaptation value, and  $t$  to the trial number. For the fitting process, absolute hand-path errors were collapsed in batches of two trials, one forward and one backward reach. If one trial of a batch was discarded based on speed or accuracy criteria, or was a catch trial, the entire batch was ignored in the exponential fitting process.

The exponential fitting process itself is sensitive to converge in local minima. This is affected by the initial values of the  $A_0$ ,  $\tau$ , and  $A_{asympt}$  and is highly influenced by outliers. We tackled these problems via outlier detection, by running 100 fits for each block and subject, with a randomized initial value of  $A_0$  ( $30 \leq A_0 \leq 50 \text{ cm}^2/\text{s}$ ),  $\tau$  ( $1 \leq \tau \leq 20 \text{ batches}$ ), and  $A_{asympt}$  ( $2 \leq A_{asympt} \leq 10 \text{ cm}^2/\text{s}$ ). Out of the 100 fits we selected the exponential function with the smallest residual error. For each block 5% of the values with the largest distance from this exponential function were characterized as outliers. With the outliers removed, we re-fitted exponential functions for each block and subject, and used only these values for statistical testing.

To assess retention of learning in our paradigms we compared the  $\tau$  values of the exponential fits of the first exposure to a force field with the second exposure to the same field using paired parametrical test statistics.

All analyses were implemented using custom written scripts in Matlab (Natick, MA).

## 2.5 Model

To predict optimal reach patterns in an accelerating environment we used a modified stochastic optimal feedback control model (OFC) (Todorov & Jordan, 2002; Todorov, 2005; Izawa et al., 2008) with a simulated sensory delay (Izawa & Shadmehr, 2008). OFC offers a new perspective on how the motor system adapts to imposed forces during reaches. Within this framework, the goal of the motor system is not to cancel the imposed forces, but to perform optimally in the new environment (Izawa et al., 2008). The optimization is based on the structure of the task, the environmental and body dynamics (Diedrichsen et al., 2010). Figure 4 describes the structure of the model, showing each component with the according variable and the pathways that connect the components.

The mathematics in this model follows Izawa et al. (2008). We will only describe the rough outlines of the model and our modifications.

The OFC model consists of three elements: one generates the motor commands (optimal controller), another represents the internal model that predicts sensory consequences of these motor commands, and the third represents a motor plant/environment, which reacts to the sensory consequences from the internal model. The amount of noise present in this model is signal dependent; SD increases with the size of the motor commands (Harris & Wolpert, 1998; Jones et al., 2002).

We used a linear dynamic system where the

vector  $\mathbf{x}_t$  represents the state of the system and  $\mathbf{u}_t$  the control signal input to the system at time  $t$ . The state vector was of the form  $[p_{\text{Hx}}, p_{\text{Hy}}, f_{\text{sx}}, p_{\text{sy}}, f_{\text{sy}}, T_x, T_y]$ , where  $p$  indicates the position of the hand in a body-centered reference frame (H) and the shoulder in a world-centered reference frame (S),  $f$  represents muscle-like force, and  $T$  denotes target position with  $x$  and  $y$  coordinates. Matrices  $A$  and  $B$  represent the system dynamics, which leads to equation (3).

$$\text{Dynamics : } \mathbf{x}_{t+1} = A\mathbf{x}_t + B\mathbf{u}_t + \xi_t$$

$$\text{Observation : } \mathbf{y}_t = H\mathbf{x}_t + \omega_t$$

$$\text{Cost : } 0 \leq \mathbf{x}_t^T Q \mathbf{x}_t + \mathbf{u}_t^T R \mathbf{u}_t$$

Observations made by the system,  $\mathbf{y}_t$ , are embedded in the observation matrix  $H$ . Additive state variability and measurement noise are represented by the Gaussian random variables  $\xi_t$  and  $\omega_t$ , with mean 0 and variance 1. The system dynamics were discretized by  $\Delta = 10$  ms. The costs are determined by the state of the system and the control signal, weighted respectively by the matrix of state cost,  $Q$ , and the matrix of motor cost,  $R$ . The true state of the system  $\mathbf{x}_t$  is not available to the controller, only the estimated state of the actual system state  $\hat{\mathbf{x}}_t$ . The estimated state is updated using a Kalman filter:

Estimated State :

$$\hat{\mathbf{x}}_{t+1} = A\hat{\mathbf{x}}_t + B\mathbf{u}_t + K_t(\mathbf{y}_t - H\hat{\mathbf{x}}_t),$$

where  $K$  is the Kalman gain. The optimal control

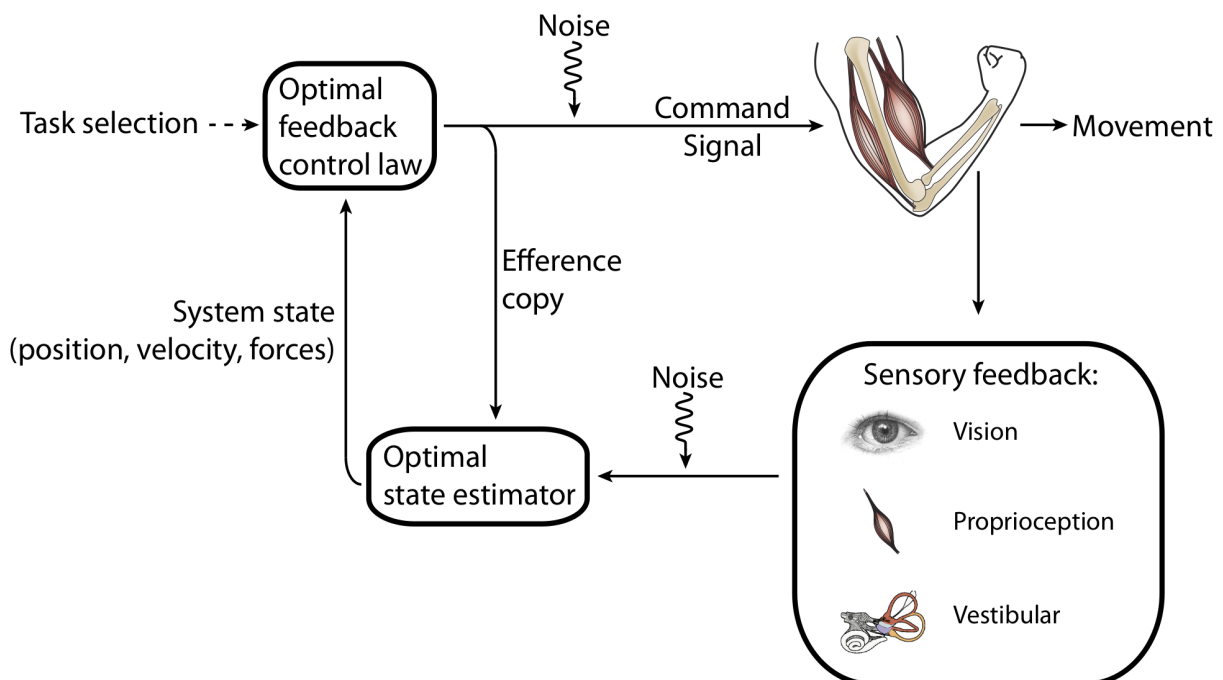


**Fig. 4** Structure of the optimal feedback control model. Mathematical vectors/variables of the model are placed at the associated components.

policy we used to calculate the control signals is given by:

$$\mathbf{u}_t = -L_t \hat{\mathbf{x}}_t$$

Here,  $L_t$  is the time-varying feedback-gain matrix that determines the controller's response. To simulate sensory delay in our model, we used the approach from Izawa (2008), in which an extended state vector is suggested. The extended state vector makes it possible to simulate transmission of information by having multiple states. Information will then travel from one state  $k$  to the next  $k + \delta$ , with  $\delta = 10$  ms, until a delay of 100 ms is reached. Only information from the most delayed state of  $y_t$  is observed by the system. However, information from the estimate  $H\hat{x}_t$  is instantaneous.

We approximated the non-linear dynamics of a two segment arm by introducing the dynamics of the arm as a point mass in Cartesian coordinates. To represent inertia, we used a  $2 \times 2$  mass matrix ( $M$ ) approximating the inertia of the two segments. The additional values  $\alpha$ ,  $\gamma$ , and  $\beta$  were used to represent gains of forces that acted on the finger in  $x$  ( $\alpha = -0.26$ ) and  $y$  ( $\gamma = -0.12$ ) direction due to the acceleration, which was directly coupled with the finger motion during the reach ( $\beta = 0.85$ ). Cost values were set to  $w_{position} = 0.93$ ,  $w_{velocity} = 1.85$ ,  $w_{control} = 8.8 * 10^{-9}$ . Below, all matrices and vectors are summarized:

$$M = \begin{bmatrix} 2.1 & 0 \\ 0 & 1.1 \end{bmatrix}$$

$$A_d = \begin{bmatrix} 1 & \delta & 0 & 0 & 0 & 0 & 0 & 0 & 0 & 0 \\ 0 & 1 & \delta/M & 0 & 0 & 0 & 0 & 0 & 0 & 0 \\ 0 & 0 & 1 - (\delta/\tau) & 0 & 0 & \alpha & 0 & 0 & 0 & 0 \\ 0 & 0 & 0 & 1 & \delta & 0 & 0 & 0 & 0 & 0 \\ 0 & 0 & 0 & 0 & 1 & \delta/M & 0 & 0 & 0 & 0 \\ 0 & 0 & 0 & 0 & 0 & 1 - (\delta/\tau) + \gamma & 0 & 0 & 0 & 0 \\ 0 & 0 & 0 & 0 & 0 & 0 & 1 & \delta & 0 & 0 \\ 0 & 0 & 0 & 0 & 0 & \beta * (\delta/M) & 0 & 1 & 0 & 0 \\ 0 & 0 & 0 & 0 & 0 & 0 & 0 & 0 & 1 & \delta \\ 0 & 0 & 0 & 0 & 0 & 0 & 0 & 0 & 0 & 0 \end{bmatrix}$$

$$A = \begin{bmatrix} A_d & 0 \\ 0 & I_{2 \times 2} \end{bmatrix}$$

$$A_{ext} = \begin{bmatrix} A & 0 & 0 & \dots & 0 & 0 \\ I_{12 \times 12} & 0 & 0 & \dots & 0 & 0 \\ 0 & I_{12 \times 12} & 0 & \dots & 0 & 0 \\ 0 & 0 & I_{12 \times 12} & \dots & 0 & 0 \\ \vdots & \vdots & \vdots & \ddots & \vdots & \vdots \\ 0 & 0 & 0 & \dots & I_{12 \times 12} & 0 \end{bmatrix}$$

### 3. Results

#### 3.1 Full interference paradigm

In the first paradigm we tested how subjects adapt to forces in an accelerating environment and if the additional vestibular signal provides a strong enough cue to help learning multiple force fields at full levels of retrograde and anterograde interference present. Figure 5 shows the average trajectories across subjects for each field and exposure. Subjects show clear adaptation to each force field during the first and second exposure. However, as can be seen in the average trajectory of the first exposure (dashed line) in the first few trials in force field A, initial reaches (blue) match the final adaptation (red), which indicates that subjects tend to stiffen-up. To determine if normal adaptation, learning of an internal model occurred, we used catch trials and looked for the presence of after-effects. During catch trials the force field is unexpectedly removed, hence the sled is not moving. If a subject established an internal model, the reach trajectory will compensate for expected forces that will not be present, which will lead to a mirror image of the trajectory of a perturbed reach. The magnitude of this after-effect, determined by the hand-path error, increases over time during a perturbation block and thereby provides information of learning (Shadmehr

$$B = \begin{bmatrix} 0_{2 \times 2} & & \\ \delta/\tau & 0 & \\ 0 & 0 & \\ 0 & 0 & \\ 0 & \delta/\tau & \\ 0_{6 \times 2}; \end{bmatrix}$$

$$B_{ext} = \begin{bmatrix} B \\ 0_{84 \times 2} \end{bmatrix}$$

$$H_d = \begin{bmatrix} 1 & 0 & 0 & 0 & 0 & 0 & 0 & 0 & 0 & 0 \\ 0 & 1 & 0 & 0 & 0 & 0 & 0 & 0 & 0 & 0 \\ 0 & 0 & 0 & 0 & 0 & 0 & 0 & 0 & 0 & 0 \\ 0 & 0 & 0 & 1 & 0 & 0 & 0 & 0 & 0 & 0 \\ 0 & 0 & 0 & 0 & 1 & 0 & 0 & 0 & 0 & 0 \\ 0 & 0 & 0 & 0 & 0 & 0 & 0 & 0 & 0 & 0 \\ 0 & 0 & 0 & 0 & 0 & 0 & 0 & 0 & 0 & 0 \\ 0 & 0 & 0 & 0 & 0 & 0 & 0 & 0 & 0 & 0 \\ 0 & 0 & 0 & 0 & 0 & 0 & 0 & 0 & 0 & 0 \end{bmatrix}$$

$$H = [H \ 0_{8 \times 2}]$$

$$H_{ext} = \begin{bmatrix} 0_{8 \times 84} \\ H \end{bmatrix}$$

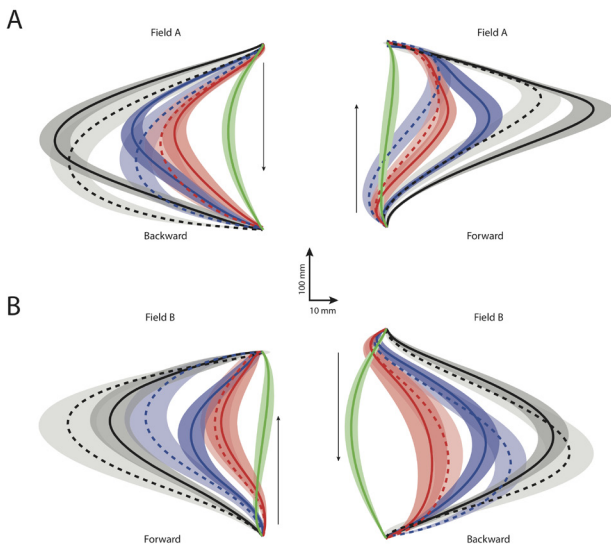


**Fig. 5** Average trajectories across subjects. Black: average of trial 1-4; blue: average of trial 11-15; red: average of last 20 trials. Dashed lines denote the first exposure to a field and solid lines the second. Green lines are the average of trajectories in the null field condition. The height of the shaded areas with the same color code represent  $\pm 1$  SE. **A.** backward and forward trajectories over time for force field A. **B.** forward and backward trajectories over time under the influence of force field B.

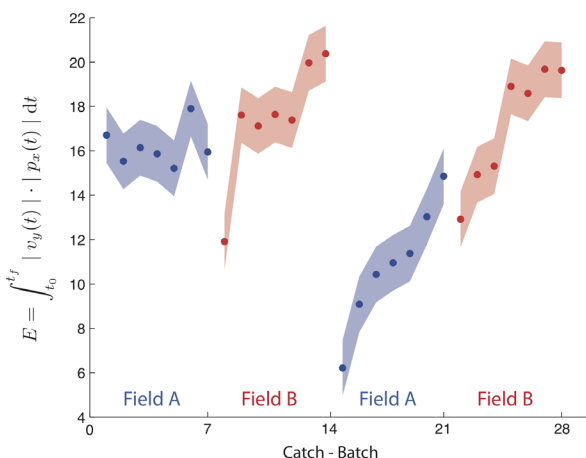


**Fig. 6** Hand-path error of catch trials in batches of 2 of each perturbation block. The height of the shaded areas denote  $\pm 1$  SE.

& Mussa-Ivaldi, 1994). Figure 6 shows the hand-path error across subjects of each perturbation block as a function of batches of catch trials. The magnitude of the after-effects increases during each perturbation block, except the first. This shows no proper learning during the first exposure to field A, which makes a comparison between the first and second exposure of force field A invalid. Another reason to discard a comparison between the two exposures of force field A is the difference between the transitions to force field A in the first and the second exposures. The first transition consists of a null field followed by a perturbation block (first

exposure field A) and the second transition is a direct follow-up of perturbation blocks (field B to field A). Therefore we tested for retention only in force field B (Table 1).

Figure 5B shows the trajectories of force field B, the initial (black) and final trajectories (red) of the first and second exposure do not indicate a clear difference. However, the blue lines from the first and second exposure are fairly different, showing that during the second exposure (solid blue line) the state of adaptation almost reached its final state (red line), indicating faster re-learning compared to the first exposure.

To test for a faster re-learning in the second exposure after an interference block, we calculated the absolute hand-path error of every subject for each trial and fitted an exponential function to the data of each block. Figure 7 shows the average hand-path error across subjects in each force field with exponential fits. We ran tests on the values  $A_0$ , comparable with the first exposure to a field (Fig. 5 black trajectories),  $\tau$  representing the learning rate, and  $A_{\text{asym}}$ , which is comparable with the final adaptation to a field (Fig. 5 red trajectories), of equation 2.

The initial and final values of learning field B in the first and second exposure were not significantly different ( $p_{A_0} = 0.73$ ;  $p_{A_{\text{asym}}} = 0.77$ ; First exposure:  $A_0$ ,  $M=2.85 \text{ cm}^2/\text{s}$ ;  $SE = 0.35$ ;  $A_{\text{asym}}$ ,  $M = 1.07 \text{ cm}^2/\text{s}$ ;  $SE = 0.08$ ; Second exposure:  $A_0$ ,  $M = 2.69 \text{ cm}^2/\text{s}$ ;  $SE = 0.30$ ;  $A_{\text{asym}}$ ,  $M = 1.12 \text{ cm}^2/\text{s}$ ;  $SE = 0.16$ ). Contrary to these observations, the learning rate  $\tau$  was significantly faster ( $p = 0.048$  - one-tailed) for the second exposure ( $M = 2.94$  batches;  $SE = 0.4867$ ) than for the first ( $M = 17.37$  batches;  $SE = 8.08$ ).

The results of the FIP demonstrate that adaptation in an accelerating environment takes place. In addition, and contrary to previous literature (Brashers-Krug et al., 1996; Caithness et al., 2004; Cothros et al., 2008), it shows that subjects are able to retain a previously established internal model after being exposed to an interfering perturbation block, even with both anterograde and retrograde interference fully present.

### 3.2 Reduced interference paradigm

Former studies used paradigms with intermediate blocks of wash-out trials in between perturbation blocks to reduce the amount of anterograde interference. It was argued that this procedure will result in a better performance in showing retention due to less net interference (Miall et al., 2004).

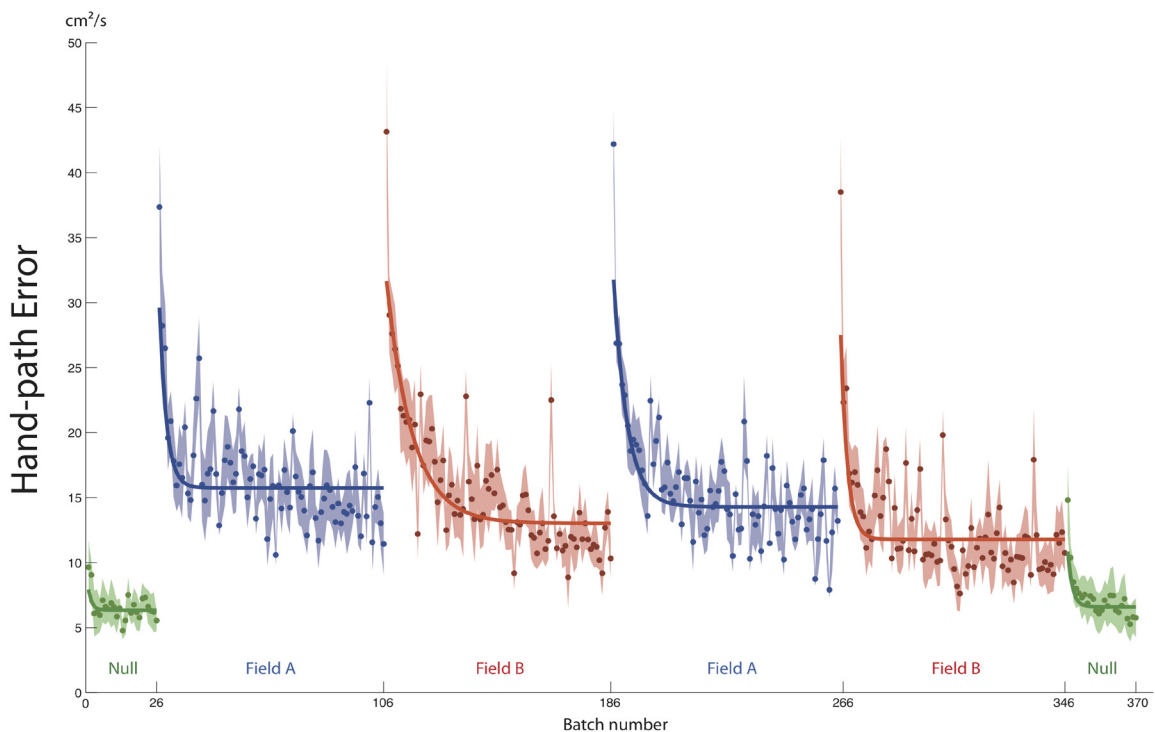


**Fig. 7** Hand-path error of the FIP of each field in batches of 2 with an exponential function fit. The height of the shaded areas denote  $\pm 1$  SE.

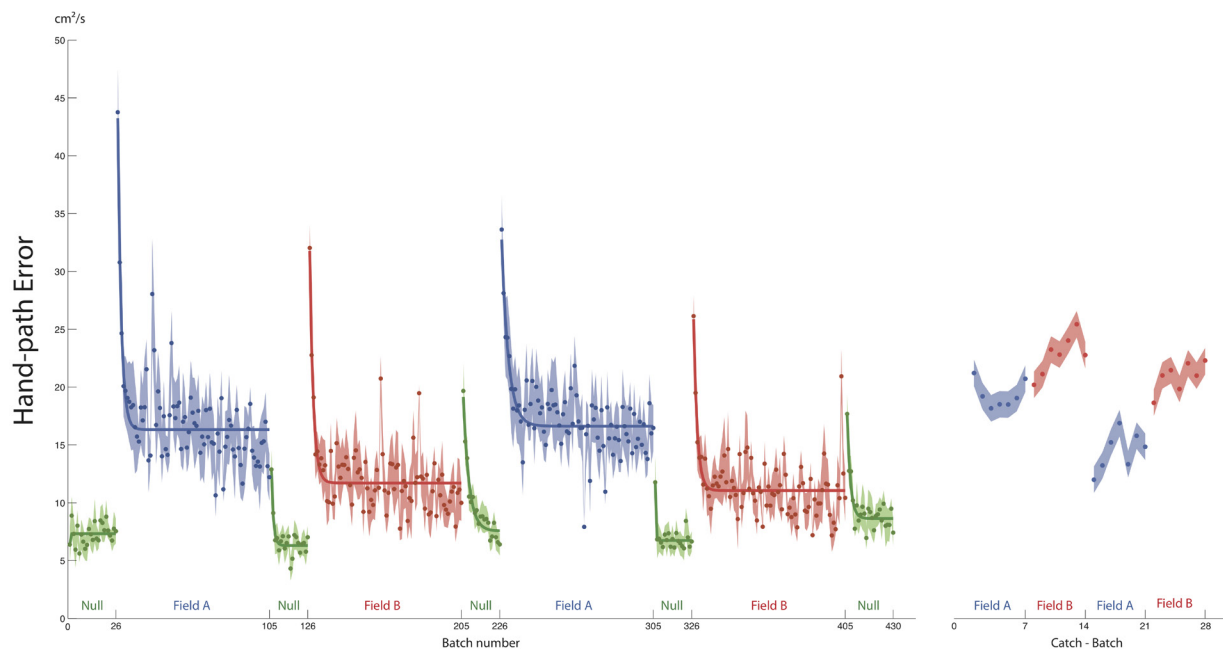


**Fig. 8** Hand-path error of the RIP of each field in batches of 2 with an exponential function fit. On the side are the catch trials in batches of 2 of each field. The height of the shaded areas denote  $\pm 1$  SE.

To determine how the absence of anterograde interference influences retention in an accelerating environment, we conducted an additional paradigm (RIP), which is equivalent to the FIP, with the difference of interspersed blocks of null trials (Table 1). The analyzing procedure is equivalent to the FIP, and Figure 8 shows the batched hand-path error with exponential fits of each block as well as the batches of catch trials. The catch trials confirm the

results from the FIP, where the first perturbation block showed improper learning and thus we only tested field B for retention. Similar to the FIP, the learning rate  $\tau$  of the second exposure to field B ( $M = 1.3$  batches;  $SE = 0.37$ ) was significantly faster ( $p = 0.05$  - one-tailed) than the learning rate of the first exposure to field B ( $M = 5.17$  batches;  $SE = 2.39$ ).

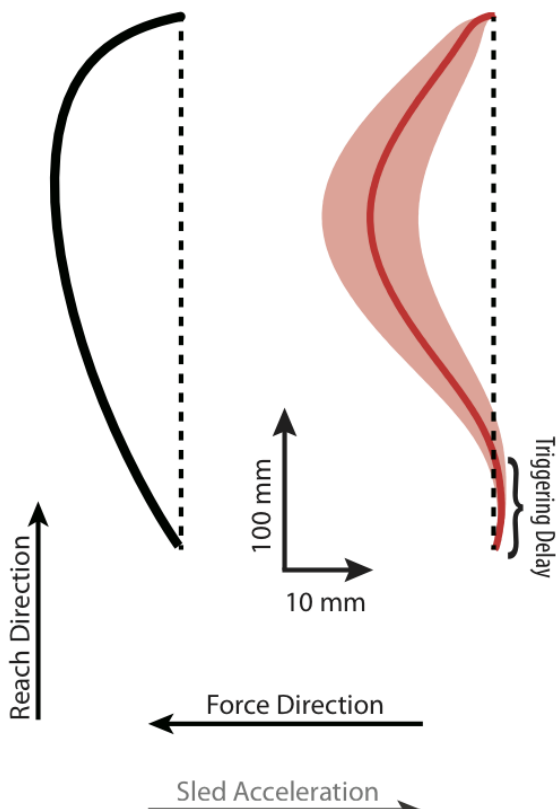


**Fig. 9** Optimal trajectory and mean final adapted trajectory within the created accelerated environment with respect to the optimal trajectory of a null field (dashed black line). Solid black line: optimal trajectory; Red line: average of last 20 trials of force field B's second exposure with a shaded area that represents  $\pm 1$  SE (equivalent to Fig. 5B).

### 3.3 Model

The modified stochastic optimal feedback control model (OFC) with a simulated sensory delay was used to make predictions about the final adaptation of reaches in the accelerating environment. Figure 9 shows the optimal trajectory (solid black line) and the average of the last 20 forward reaches in force field B's second exposure (equivalent to Fig. 5), both relative to a straight line.

We simulated the hand as a point mass and the model indicates the optimal trajectory in this environment to be a curved path. It deviates to the left with respect to the optimal trajectory in a null field. Comparing the optimal trajectory of the model with subjects' final adaptation, they do follow the same strategy under the induced forces (Fig 9). However, the initial path of both trajectories is quite different. This can be explained by the sled triggering delay of  $\sim 60$  ms within the experiment. During this delay, subjects already started their reach but no forces are experienced because the sled has not yet been initiated. In that period subjects' hands do not follow the force direction as they do as soon

as the movement starts. This triggering delay was not included in our model simulation and therefore the model is exposed to immediately induced forces that are followed by the point mass.

Despite the triggering delay, the principle during a rightward acceleration is to follow the forces that pull the hand to the left and to just compensate for some forces. Only at about the center of the movement, at peak velocity, the hand is brought back towards the target. Important to note is that after the point of peak velocity the amount of forces induced by acceleration also decrease until the target is reached. This strategy of exploiting the force field in an accelerating environment by first following and then compensating reflects least total force necessary for performing a reaching movement. These results are quite different from what has been found using robotic manipulanda and a velocity-dependent force field, where subjects' trajectory generally overcompensates for forces and exploits the field mainly in the end to be pulled back to target.

In summary, the model predicted a leftward deviated trajectory with respect to the optimal trajectory in a null field, which is comparable to subjects' trajectory.

## 4. Discussion

We have shown that subjects adapt to forces, induced by an accelerating environment, in an optimal fashion. Additionally, subjects are able to consolidate the learned dynamics after adapting to an opposing force field perturbation, even when being exposed to full levels of interference. Both fast adaptation and retention of motor memories are the result of the incorporation of the vestibular system. This system provides information about the environmental dynamic changes and a strong contextual cue to different types of force fields.

### 4.1 Retention of motor memories

Our findings stand in direct contrast to previous research that failed to show retention when adapting to opposite perturbations in succession (Brashers-Krug et al., 1996; Caithness et al., 2004; Cothros et al., 2008). However, they are consistent with the view of active and inactive memory states (Caithness et al., 2004). When new motor memories are formed, they are in an active memory state. In this state they are still fluid and can be modified. After some time, they turn over to an inactive state that can be reactivated at a later point in time (Nader et

al., 2000; Nader, 2003). To decide when and which motor memory should be reactivated, contextual cues are needed. For example, if you are riding your bicycle the motor memory of that specific skill is automatically recalled due to the unmistakable context. Computer modeling is consistent with the suggestion of active and inactive memory states and can account for most adaptation characteristics (Lee & Schweighofer, 2009). How does the view of active and inactive memory states explain the lack of retention in previous studies?

It has been suggested that previous research failed to show retention because participants had to perform the same reaching task in two different force fields (ABA). In this paradigm the motor memory that is established while adapting to field A is still in use and modified while adapting to field B. The same occurs during the second exposure to field A. Even after reducing anterograde interference, the residual level of interference remains too high. In other words, one memory is formed that is continuously overwritten. Most of these studies did not provide contextual cues to act as a switch between force fields. This switch could have reduced interference further by increasing the possibility that a motor memory is formed of each force field, thus no internal model would have been overwritten. This raises the question of what types of cues are necessary to create a specific context for each field so that multiple internal models are established?

Recent studies tried to answer this question by providing visual- or haptic sensory cues during force field adaptation of a robotic manipulandum (Osu et al., 2004; Cothros et al., 2008). Using the ABA paradigm, both failed to report multiple internal models. This indicates that sensory cues are too weak to provide a rich context for each field and therefore the same memory is overwritten.

However, multiple internal models can be established if cues are incorporated, which are part of the motor act itself (Nozaki et al., 2006; Howard et al., 2010).

If sensory cues are too weak to create a strong enough context and only cues that are a component of the motor act itself are strong enough to create that context, how were subjects able to remember what they learned during the second exposure to the same field in our paradigms? The important difference in our experiment is that reaches were performed under acceleration. This situation provides important information from the vestibular system. This system was not engaged in studies using robotic manipulanda or rotating platforms. Using a robotic manipulandum, reaches are performed in

a stable environment, thus no vestibular signal is provided. In rotating platform experiments reaches were only initiated when the platform was rotating at constant velocity and the vestibular system was in an adapted state.

In our experiment the vestibular system did provide a sensory cue that, in contrast to visual and haptic cues, directly detects the underlying accelerative cause of the perturbing forces. Thus, provides important information about the dynamic environment. Similar to cues that are part of the motor act itself, the vestibular cue was only available after the onset of the reaching movement and was not provided before perturbation. This suggests a direct switch between internal models during the movement.

Taking all findings into account, we can conclude that contextual cues need to be provided to facilitate learning of multiple internal models simultaneously. Cues, either from the sensory or motor domain, have to provide sufficient detectable changes in the task. These cues then substantially reduce interference and boost the formation of multiple memories, internal models. At which level, conscious or subconscious, is it sufficient to detect these changes? How big does the gap between the cues have to be to induce the formation of multiple motor memories? Do cues from the sensory domain have to entail information about the dynamic environment as they do here? These are only a few questions that cannot be answered at this point and need further investigation.

## 4.2 Adaptation in an accelerating environment

Adaptation has widely been studied by looking at trajectory changes over time while exposing subjects to perturbations (Lackner & Dizio, 1994; Shadmehr & Mussa-Ivaldi, 1994; Dizio & Lackner, 1995; Brashers-Krug et al., 1996; Caithness et al., 2004; Nozaki et al., 2006; Cothros et al., 2008; Howard et al., 2010). These perturbations are either induced by contact (robotic manipulandum) or non-contact forces (rotating platform, accelerating environment).

Findings suggest that adaptation is a process of re-optimizing movements based on environmental and body dynamics (Izawa et al., 2008; Diedrichsen et al., 2010). The optimal feedback control framework captures the idea of re-optimization and makes it possible to predict the optimal trajectory of reaches within an altered dynamic environment.

Models of optimal feedback control can account for adaptation results of previous research using robotic manipulanda (Izawa et al., 2008). Our computer model, based on the same framework, also predicted the final adapted trajectory adequately. In both cases, i.e. contact and non-contact forces, an optimal strategy that reduces a cost function seems to be at play. However, the optimal policy in these two environments differs substantially.

In a velocity-dependent curl field created by a manipulandum, the general finding is an adapted trajectory that overcompensates for forces (Izawa et al., 2008). It has been argued that the initial overcompensation is an efficient way to exploit the forces that pull the hand back to target after peak velocity. In contrast to the optimal trajectory to contact forces, the final adapted trajectory to non-contact forces shows no overcompensation (Lackner & Dizio, 1994; Dizio & Lackner, 1995). Trajectories follow the perturbation direction only compensating for little force. Additionally, adapted trajectories from our data demonstrate that only after peak velocity of the reach the direction is adjusted back towards the target. But why after peak velocity and not earlier/later? Important to note is that at the time of peak velocity of the reach, the peak of the sleds velocity profile is reached. After this point the sled starts to de-accelerate. This de-acceleration will create forces based on the inertia of the arm, that pull the hand in the opposite direction of the initial perturbation direction. In other words, acceleration perpendicular to a forward/backward reach will pull the hand away from a straight line, and de-acceleration will pull it back towards it. This strategy exploits the environmental dynamics maximally to minimize costs.

In addition to the differences in control policy, the time scale at which adaptation takes place to non-contact forces is remarkably faster than to contact forces. Lackner & Dizio (2005) showed that full adaptation to forces by a rotating platform requires about 40-45 trials. Adaptation to robot forces however, needs about 80 trials to reach a stable state. This difference may be explained by the nature of the imposed forces. Inertial forces act without any mechanical contact on the entire arm, compared to contact forces, which are applied only locally to the hand or wrist through a robotic arm. Many of the forces experienced in daily life contain such an inertial component, making it likely that our brain is well equipped to compensate for such forces. Furthermore, our results downfall the previously observed time scales even more. For example, the time constant of the first exposure to force field B

of the reduced interference paradigm is 5.17 batches. This time constant indicates that subjects adapt to the non-contact forces in our accelerating environment in only 31 trials ( $\tau * 2$  (forward & backward) \* 3 (for 99% adaptation)). This improvement in adaptation time can be taken as evidence for the incorporation of vestibular signals in the adaptation process. How is the vestibular signal integrated with other sensory information in motor learning? Will a disturbed or malfunctioning vestibular system lead to different adaptation? These are questions to be answered by future research.

## References

- Brashers-Krug, T., Shadmehr, R., & Bizzi, E. (1996). Consolidation in human motor memory. *Nature*, 382, 252–5.
- Caithness, G., Osu, R., Bays, P., Chase, H., Klassen, J., Kawato, M., et al. (2004). Failure to consolidate the consolidation theory of learning for sensorimotor adaptation tasks. *Journal of Neuroscience*, 24, 8662–8671.
- Chib, V. S., Patton, J. L., Lynch, K. M., & Mussa-Ivaldi, F. A. (2006). Haptic identification of surfaces as fields of force. *Journal of Neurophysiology*, 95, 1068–77.
- Cothros, N., Wong, J., & Gribble, P. L. (2008). Distinct haptic cues do not reduce interference when learning to reach in multiple force fields. *PLoS One*, 3, 1990.
- Diedrichsen, J. (2007). Optimal task-dependent changes of bimanual feedback control and adaptation. *Current Biology*, 17, 1675–9.
- Diedrichsen, J., Shadmehr, R., & Ivry, R. B. (2010). The coordination of movement: optimal feedback control and beyond. *Trends in Cognitive Science*, 14, 31–9.
- Dizio, P., & Lackner, J. R. (1995). Motor adaptation to coriolis force perturbations of reaching movements: endpoint but not trajectory adaptation transfers to the nonexposed arm. *Journal of Neurophysiology*, 74, 1787–92.
- Franklin, D. W., Osu, R., Burdet, E., Kawato, M., & Milner, T. (2003). Adaptation to stable and unstable dynamics achieved by combined impedance control and inverse dynamics model. *Journal of Neurophysiology*, 90, 3270.
- Harris, C. M., & Wolpert, D. M. (1998). Signal-dependent noise determines motor planning. *Nature*, 394, 780–4.
- Howard, I. S., Ingram, J. N., & Wolpert, D. M. (2010). Context-dependent partitioning of motor learning in bimanual movements. *Journal of Neurophysiology*, 104, 2082–2091.
- Izawa, J., Rane, T., Donchin, O., & Shadmehr, R. (2008). Motor adaptation as a process of reoptimization. *Journal of Neuroscience*, 28, 2883–91.
- Izawa, J., & Shadmehr, R. (2008). On-line processing of uncertain information in visuomotor control. *Journal of Neuroscience*, 28, 11360–11368.
- Jones, K. E., Hamilton, A. F., & Wolpert, D. M. (2002).

- Sources of signal-dependent noise during isometric force production. *Journal of Neurophysiology*, 88, 1533–44.
- Kawato, M. (1999). Internal models for motor control and trajectory planning. *Current Opinion in Neurobiology*, 9, 718–727.
- Lackner, J. R., & Dizio, P. (1994). Rapid adaptation to coriolis force perturbations of arm trajectory. *Journal of Neurophysiology*, 72, 299–313.
- Lackner, J. R., & DiZio, P. (2005). Motor control and learning in altered dynamic environments. *Current Opinion in Neurobiology*, 15, 653–9.
- Lee, J.-Y., & Schweighofer, N. (2009). Dual adaptation supports a parallel architecture of motor memory. *Journal of Neuroscience*, 29, 10396–404.
- Miall, R. C., Jenkinson, N., & Kulkarni, K. (2004). Adaptation to rotated visual feedback: a re-examination of motor interference. *Experimental Brain Research*, 154, 201–10.
- Nader, K. (2003). Memory traces unbound. *Trends in Neuroscience*, 26, 65–72.
- Nader, K., Schafe, G. E., & LeDoux, J. E. (2000). The labile nature of consolidation theory. *Nature Reviews Neuroscience*, 1, 216–9.
- Nozaki, D., Kurtzer, I., & Scott, S. H. (2006). Limited transfer of learning between unimanual and bimanual skills within the same limb. *Nature Neuroscience*, 9, 1364–6.
- Osu, R., Hirai, S., Yoshioka, T., & Kawato, M. (2004). Random presentation enables subjects to adapt to two opposing forces on the hand. *Nature Neuroscience*, 7, 111–112.
- Shadmehr, R., & Mussa-Ivaldi, F. A. (1994). Adaptive representation of dynamics during learning of a motor task. *Journal of Neuroscience*, 14, 3208–24.
- Shadmehr, R., Smith, M. A., & Krakauer, J. W. (2010). Error correction, sensory prediction, and adaptation in motor control. *Annual Review of Neuroscience*, 33, 89–108.
- Todorov, E. (2004). Optimality principles in sensorimotor control (Vol. 7) (No. 9). Todorov, E. (2005). Stochastic optimal control and estimation methods adapted to the noise characteristics of the sensorimotor system. *Neural Computation*, 17, 1084–108.
- Todorov, E., & Jordan, M. I. (2002). Optimal feedback control as a theory of motor coordination. *Nature Neuroscience*, 5, 1226–35.
- Wang, T., Dordevic, G. S., & Shadmehr, R. (2001). Learning the dynamics of reaching movements results in the modification of arm impedance and long-latency perturbation responses. *Biological Cybernetics*, 85, 437–48.

# Conflict in the Bilingual Brain: The Case of Cognates and False Friends

Flora Vanlangendonck<sup>1</sup>

Supervisors: Ton Dijkstra<sup>1</sup>, Shirley-Ann Rueschemeyer<sup>1</sup>

<sup>1</sup>Donders Institute for Brain, Cognition and Behaviour, Radboud University Nijmegen, The Netherlands

Due to common roots and linguistic borrowing, languages share form and meaning characteristics with each other. As a result, the bilingual brain is faced with the challenge of handling both similarities and differences between languages, while at the same time controlling which language is in use. Here we investigated how bilinguals process words with different levels of cross-linguistic orthographic and semantic overlap. Dutch-English bilinguals performed two English lexical decision tasks on cognates, false friends, English control words and pseudowords. In one of the tasks, half of the pseudowords were replaced with Dutch words. We present behavioral and fMRI evidence that similarities and differences between a bilingual's languages can both facilitate and hinder visual word recognition, depending on the type of overlap and the context in which a word occurs. Our findings indicate that bilinguals cannot completely inhibit a non-target language and that cross-linguistic interference leads to activity in brain areas that are sensitive to linguistic conflict (left inferior frontal gyrus) and response conflict (superior medial frontal cortex, subcortical structures and right inferior frontal gyrus).

*Keywords:* bilingualism, cognates, false friends, lexical decision, fMRI

---

Corresponding author: Flora Vanlangendonck, email: f.vanlangendonck@donders.ru.nl

## 1. Introduction

A central question in psycholinguistic research on bilingualism is how bilinguals succeed at selecting words from the correct language in a given task and context. Words with different levels of form and meaning overlap across languages allow us to consider the interaction and competition between a bilingual's languages. In the current study, we used cognates and false friends to investigate the effects of stimulus-based and response-based conflict in bilingual visual word recognition. By collecting both reaction time (RT) and functional MRI data for the same stimulus materials, we aimed to better understand how the bilingual brain handles these different types of conflict.

Below, we first review existing research on cognates and false friends, focusing on the effects of stimulus list composition and task demands on their recognition. Next, we discuss the process of bilingual word selection and in particular, the role of stimulus-based and response-based conflict in the recognition of cognates and false friends. Finally, we introduce our RT and fMRI experiments and formulate hypotheses for both dependent variables.

### 1.1 Access to the bilingual mental lexicon

How are bilinguals capable of reading words or utterances in one language without constant interference from the non-target language? One proposal is that bilinguals can completely filter out the non-target language through language-selective access (Rodríguez-Fornells, Rotte, Heinze, Nössel, & Münte, 2002) or by accessing language-specific lexicons (Gerard & Scarborough, 1989). In contrast, other authors (e.g., Dijkstra & van Heuven, 2002) have proposed that words in the bilingual mental lexicon are accessed in a language non-selective manner. In this view, bilinguals activate word candidates in both languages while reading, and these representations compete for selection. Although there is some evidence supporting the former proposal (e.g., Scarborough, Gerard, & Cortese, 1984), the majority of behavioral and neuroimaging research supports the notion that the non-target language cannot be switched off and remains active (Dijkstra & van Heuven, 2002; van Heuven & Dijkstra, 2010). Much of this evidence comes from behavioral studies on words with different levels of form and meaning overlap across languages, such as false friends and cognates.

False friends or interlingual homographs are

words with similar forms but different meanings across languages. In this study, we consider false friends that share identical orthographical forms in different languages. Examples of such false friends between Dutch and English are kind (Dutch meaning: child), glad (Dutch meaning: slippery) and brand (Dutch meaning: fire). False friends are typically recognized as fast as or slower than control words (Dijkstra, 2007).

Cognates are words with similar forms and meanings across languages. They can be described on a spectrum ranging from identical cognates with identical orthographical forms in different languages over non-identical cognates with similar orthographical forms across languages to words with little or no cross-linguistic orthographic overlap. Examples of cognates between English and Dutch include hotel, tent, silver (Dutch: zilver), ocean (Dutch: oceaan) and olive (Dutch: olijf).

In contrast to false friends, bilinguals often recognize and produce cognates faster than control words. This cognate facilitation effect has been observed in visual word recognition (Cristoffanini, Kirsner, & Milech, 1986; de Groot & Nas, 1991; Dijkstra, Grainger, & van Heuven, 1999; Lemhöfer & Dijkstra, 2004), auditory word recognition (Marian & Spivey, 2003) and word production (Costa, Caramazza, & Sebastian-Galles, 2000; Kroll & Stewart, 1994). The effect has been found in first language (Van Hell & Dijkstra, 2002), second language (Lemhöfer & Dijkstra, 2004), and third language processing (Lemhöfer, Dijkstra, & Michel, 2004), but it is typically strongest in non-native languages.

A recent study by Dijkstra, Miwa, Brummelhuis, Sappelli, and Baayen (2010) showed that the cognate facilitation effect is modulated by the degree of cross-linguistic orthographic overlap. Reaction times in an English lexical decision task decreased gradually with increasing orthographic overlap. A sudden drop in RTs was found for identical cognates, suggesting that identical cognates are processed differently from non-identical cognates and control words.

However, in another English lexical decision experiment, Van Assche, Drieghe, Duyck, Welvaert, and Hartsuiker (2011) found a linear trend in reaction times as the degree of cross-linguistic orthographic similarity increases without a discontinuity for identical cognates. It thus remains an open question whether identical cognates have a special status in the bilingual mental lexicon.

## 1.2 The role of task demands and stimulus list composition

The results obtained in reaction time experiments using false friends and cognates greatly depend on task demands. For example, van Heuven, Schriefers, Dijkstra, and Hagoort (2008) found no difference in reaction times between false friends and English control words in a generalized lexical decision task. In an English lexical decision task, they observed a significant inhibitory effect for false friends. Similarly, Dijkstra et al. (2010) found that Dutch-English bilinguals recognize cognates faster than English control words in an English lexical decision task. In a language decision task, cognates showed an inhibitory effect compared to controls, as the Dutch and English readings of a cognate become linked to different responses.

In addition to task demands, stimulus list composition can affect the recognition of false friends. Dijkstra, Van Jaarsveld, and Ten Brinke (1998) found no difference in reaction times between false friends and English control words in an English lexical decision task when only English control words were included. When Dutch words were added to the stimulus list, a considerable inhibitory effect was observed for false friends. The effect of stimulus list composition on cognate recognition in adults has not been studied yet. It is unclear whether adding Dutch words to the stimulus list of an English lexical decision experiment can cause cognates to behave similar to false friends, possibly even resulting in a cognate inhibition effect. Furthermore, identical cognates (e.g., Dutch-English film) and non-identical cognates (e.g., Dutch tomaat and English tomato) might be affected differently by this type of stimulus list manipulation, because identical cognates are ambiguous with respect to their language membership. Non-identical cognates unambiguously belong to only one language and may therefore be less affected by the presence of Dutch words in the stimulus list. Adding Dutch words to the stimulus list could therefore affect the cognate facilitation effect more strongly for identical cognates than for non-identical cognates.

## 1.3 Conflict in the bilingual brain

How do bilinguals select the lexical representations corresponding to the input letter strings if representations from both languages are activated in parallel? The Bilingual Interactive Activation model (BIA+; Dijkstra & van Heuven, 2002) distinguishes between a word identification and

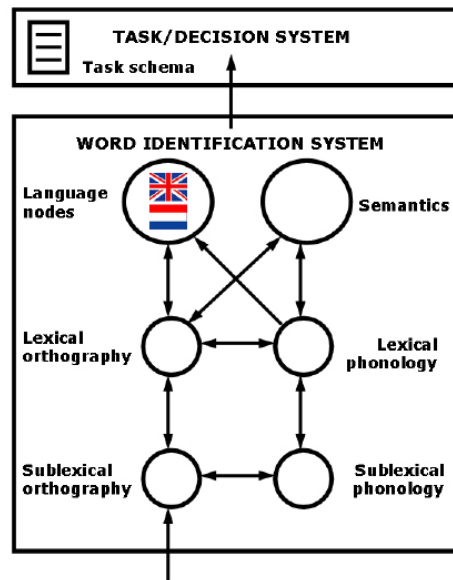


**Fig. 1** The BIA+ model consisting of a word identification and a task/decision system. Conflict can occur in both systems.

a task/decision system (Figure 1). When bilinguals are presented with a visual letter string, they activate the phonological, orthographic, and semantic representations of words with similar forms in the word identification system, and these representations compete for selection. The task/decision system contains task schemas that allow bilinguals to select the appropriate response for a given task or context. This system receives continuous input from the word identification system, but cannot directly influence the word identification system.

Conflict can arise in both the word identification and the task/decision systems. For instance, when Dutch-English bilinguals read a false friend, they will activate the orthographic, phonological, and semantic representations of both the Dutch and the English readings of the false friend. The activated linguistic representations compete for selection in the word identification system, resulting in stimulus-based conflict. In addition, conflict can occur in the task/decision system. For example, in an English lexical decision task, a bilingual is asked to press the YES-button when the word they see is an existing English word and the NO-button when it is not. In this case, the Dutch and the English readings of a false friend are linked to different responses and the bilingual will experience response conflict.

The reaction time results observed for cognates and false friends can be explained as the result of the presence or absence of stimulus- and response-based conflict. For example, take the stimulus list manipulation by Dijkstra et al. (1998). The

addition of Dutch words to the stimulus list of an English lexical decision task turned the null results observed for false friends into an inhibitory effect. According to the BIA+ model, false friends activate the lexical representations associated with both the Dutch and the English readings of the word. These representations are linked to different responses: a YES-response for the English reading and a NO-response for the Dutch reading of false friends. By adding the Dutch words to the stimulus list, the connection between the Dutch readings of the false friends and the NO-response will be strengthened, resulting in more response conflict and therefore slower decisions.

Similarly, when Dutch-English bilinguals read a non-identical cognate such as tomato, they will automatically co-activate the orthographic representation of the Dutch word tomaat. These representations compete in the word identification system and feed activation forward to a shared semantic representation. This semantic representation provides feedback to the orthographic representations, resulting in a higher level of activation and a faster crossing of the activation threshold for cognates in comparison to control words. The picture for identical cognates is less clear-cut. The BIA+ model currently does not specify whether identical cognates have one or two orthographic representations, but assumes that they have a special representation (Dijkstra & van Heuven, 2002).

How does the bilingual brain resolve stimulus-based and response-based conflict? Van Heuven, Schriefers, Dijkstra, and Hagoort (2008) investigated the neural correlates of stimulus-based and response-based conflict induced by false friends. Dutch-English bilinguals performed an English lexical decision task or a generalized lexical decision task in the fMRI scanner. False friends were expected to cause conflict in the word identification system in both tasks, as they activate competing Dutch and English representations. Response-based conflict was only expected in the English lexical decision task, because the Dutch and English readings of a false friend are linked to different responses in this task. Stimulus-based conflict resulted in activity in an anterior and a posterior cluster in the left inferior frontal gyrus (IFG). Van Heuven et al. proposed that this pattern of activity could reflect the selection of information among competing alternatives (Thompson-Schill et al. 1997), phonological retrieval (Gold & Buckner, 2002), or controlled semantic retrieval (Gold & Buckner, 2002; Badre et al., 2005). However, since false friends differ in phonology and

## Task 2

### Task 1

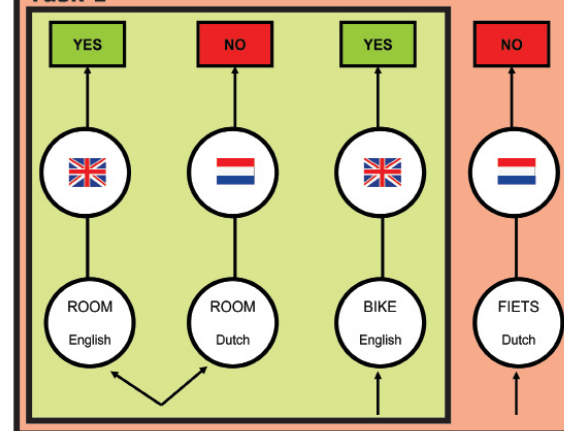


**Fig. 2** Sources of response conflict in the current experiment. In both tasks, the Dutch and the English readings of a false friend are linked to a different response. In the first task, the link between the Dutch reading of a false friend and the NO-response is relatively weak. In the second task, this response binding is strengthened by the presence of Dutch words in the stimulus list requiring a NO-response.

semantics across languages, it was not possible to distinguish between these explanations. Response-based conflict was mainly associated with activity in the pre-supplementary motor area (pre-SMA) and the anterior cingulate cortex (ACC). The authors proposed that the ACC signals response conflict, while the pre-SMA is involved in executive control.

## 1.4 The current study

In the current study, we set out to answer a number of open questions about the effects of stimulus-based and response-based conflict in bilingual visual word recognition. First, we aimed to test whether identical cognates have a special status in the bilingual mental lexicon in comparison to non-identical cognates and English control words. Due to their cross-linguistic form and meaning overlap, they may have a special representation that can lead to more or less conflict in the word identification and the task/decision systems. We aimed to test whether identical cognates have such a special representation and what the processing consequences of this type of representation are.

Second, we aimed to investigate the effects of stimulus list manipulation on the recognition of cognates and false friends. Van Heuven et al. (2008) found effects of task demands on the recognition of false friends, but stimulus list effects may be more subtle and possibly of a different nature. False friends show a large inhibitory effect when Dutch

words are added to the stimulus list (Dijkstra et al., 1998). However, it is as yet unclear whether, applying the same manipulation, cognates will reveal a similar inhibition effect in reaction times, and whether identical and non-identical cognates will be affected to the same extent. By using fMRI, we aimed to test whether this stimulus list manipulation mainly affects processing in the task/decision system, as predicted by the BIA+ model.

Third, we aimed to investigate how stimulus- and response-based conflict affect the recognition of cognates and false friends, and what the neural correlates of these types of conflict are. Van Heuven et al. (2008) successfully separated stimulus- and response-based conflict in the recognition of false friends, but a number of unanswered questions remain. For example, it is unclear what type of stimulus-based conflict causes the activity in the left IFG, given that false friends have different meanings and pronunciations across languages. By looking at cognates in addition to false friends, we aimed to better understand the role of stimulus- and response-based conflict in bilingual visual word recognition.

We conducted a reaction time experiment and an fMRI experiment in proficient Dutch-English bilinguals. Each experiment consisted of two English lexical decision tasks. We used a stimulus list manipulation to induce response conflict in a way similar to the study by Dijkstra et al. (1998), as presented in Figure 2. The first English lexical decision task was performed on a list of cognates, false friends, English control words, and pseudowords. In the second task, half of the pseudowords were replaced by Dutch words. Based on previous research (Dijkstra et al., 1998; van Heuven, 2008), we expected false friends to suffer from stimulus-based and response-based conflict in both tasks, resulting in activity in the IFG and superior medial frontal gyrus (MFG). Response conflict was expected to increase in the second task due to the presence of Dutch words in the stimulus list.

In the first task, we expected to observe a cognate facilitation effect in reaction times (Dijkstra et al., 2010), but we did not have any strong a priori predictions about the neural basis of this effect. The existing PET and fMRI research on cognates is limited to production studies that typically found more brain activity for non-cognates in comparison to cognates (De Bleser et al., 2003; Raboyeau, Marcotte, Adrover-Roig, & Ansaldi, 2010), so we may find a very limited pattern of activity when comparing cognates to English control words in the first task. Based on the BIA+ model, we expected

cognates to induce response conflict in the second task when their Dutch reading becomes linked to a NO-response. We expected this response conflict to affect the cognate facilitation effect, possibly even resulting in a cognate inhibition effect. In the fMRI experiment, we expected cognates to cause activity in areas related to response conflict in the second task. In particular, we expected to find superior medial frontal activity.

## 2. Behavioral experiment

### 2.1 Methods

#### 2.1.1 Participants

Twenty-four Dutch-English bilinguals participated in the study, which consisted of two subsequent lexical decision tasks (excluding or including Dutch words). Data from four participants were excluded from the analyses because they had exceptionally high overall error rates (above 15%). The remaining participants consisted of 4 men and 16 women with a mean age of 22.2 years (SD 2.3). All participants were right-handed and had normal or corrected-to-normal vision. They gave written informed consent before the start of the experimental session and received 10 euro or course credit for participating.

Participants' language background and English proficiency were assessed by means of a self-rating questionnaire. All participants were native speakers of Dutch who on average came into contact with English at the age of 11.0 (SD 1.6). They rated their English reading experience as 5.5 (SD 1.2) on a scale from 1 (very little experience) to 7 (very much experience).

#### 2.1.2 Stimulus materials

The total stimulus set consisted of 300 English words, 30 Dutch words, and 90 pseudowords. All words were nouns and adjectives made up of one or two syllables and four to six letters. The English words consisted of 60 false friends, 60 identical cognates, 120 non-identical cognates, and 60 English control words. The Levenshtein distance (LD) was used to quantify the degree of cross-linguistic orthographic overlap between the non-identical cognates and their Dutch translation equivalents. The Levenshtein distance refers to the number of characters that have to be replaced, added, or deleted to transform one string of characters into another string. The false friends had a Levenshtein distance of at least three to their Dutch translation equivalents.

The English words were matched item-by-item across conditions based on their length and English word form frequency, as available from the SUBTLEXus database (Brysbaert & New, 2009). The pseudowords were created by replacing one letter in existing English words. The Dutch words were low-frequency words with a Dutch word form frequency between 2 and 10 occurrences per million, as available from the SUBTLEX-NL database (Keuleers, Brysbaert, & New, 2010). The Dutch words did not include any false friends or cognates. The pseudowords and Dutch words were matched item-by-item with the English words for length. Table 1 contains examples of the matched stimuli used in the two tasks.

The 300 English words were allocated to two lists, which were matched for English word form frequency and word length (Table 2). Half of the participants were presented with the first list in the first task, the other half saw it in the second task. In the first task, 60 pseudowords were added to the English words. In the second task, 30 pseudowords and 30 Dutch words were included in addition to the English words. As a result, the stimulus lists for each lexical decision task consisted of 210 stimuli, 150 of which were existing English words. Each stimulus was presented once to each participant over the course of the two tasks. The stimuli were pseudorandomized to create a different list for each participant. Each pseudorandomized list contained no more than four English words in a row and stimuli were never succeeded by an item from the same condition. In addition to the stimuli, 30 null events were included in the design for each task.

### 2.1.3 Procedure

Participants received written instructions before the start of the experiment. They were asked to indicate as quickly as possible whether a presented letter string was an existing English word or not by pressing the appropriate button. YES-responses were given with the right index finger, NO-responses were given with the left index finger. Participants were informed of the presence of words existing in both Dutch and English in the stimulus list. The same instructions were used for both tasks.

Participants completed a series of 14 practice trials before the start of each task. The practice trials contained the same proportion of stimuli from each condition as the actual experiment. The experiment was run using Presentation software. Participants were seated in a normally lit room at approximately 60 cm from the computer screen. Stimuli were presented in white 20-point Arial font on a black screen. Each trial began with a variable jitter of 0, 500, 1000, or 1500 ms. Next, a fixation cross was presented in the centre of the screen for 400 ms. The fixation cross was immediately followed by the presentation of the stimulus in the centre of the screen. The stimulus remained visible until the participant pressed a button or until the maximum response time of 2000 ms was reached. Between trials a blank screen appeared for 2000 ms. In total, each task took no more than 25 minutes.

Each participant completed both tasks. The two tasks were scheduled on different days, between 1 and 14 days apart. The order of the tasks was kept constant to ensure that the presence of Dutch words

**Table 1.** Examples of stimuli used in the two lexical decision tasks.

False friends	Identical cognates	Non-identical cognates LD1	Non-identical cognates LD2	English control words	Pseudo-words	Dutch words
blank	blond	stiff	handy	cloud	pread	snoer
brave	alarm	ocean	wheel	shape	jorce	pruik
ramp	duel	calf	cork	cone	mift	bijl
vast	echo	crab	bean	leap	tond	geel
mode	yoga	mint	text	leaf	mipe	boef

**Table 2.** Average English word form frequency per million and number of letters per condition. False friends, cognates and English control words were matched item-by-item for length and English word form frequency. Dutch words (occurring only in the second task) and pseudowords were matched with the other items for length.

	False friends	Identical cognates	Non-identical cognates LD1	Non-identical cognates LD2	English control words	Pseudo-words	Dutch words
English word form frequency	53.78	52.17	51.61	47.44	51.67		
Number of letters	4.43	4.43	4.47	4.50	4.43	4.42	4.47

would not affect participants' expectations during the second session. After the first experiment, participants filled out a written questionnaire assessing their language background and English proficiency. Apart from this, experimental procedures were identical during both sessions.

## 2.2 Results

Responses to 15 items (gown, moan, arts, bout, gist, rake, stem, stout, vast, beak, plight, wasp, grin, heap, and wart) that elicited at least 40% errors over the two tasks were removed. The removal of these data points did not create any significant differences in the matching between conditions. In addition, all responses that were faster than 300 ms or slower than 1500 ms were discarded. Finally, we removed data points that were 2.5 standard deviations removed from both the participant and the item mean per task. This outlier analysis was performed separately for the English words and the Dutch words/pseudowords. In total, we removed 5.71% of data points in the first task and 5.24% of data points in the second task. Error rates in the remaining data were 3.76% in the first task and 4.82% in the second task.

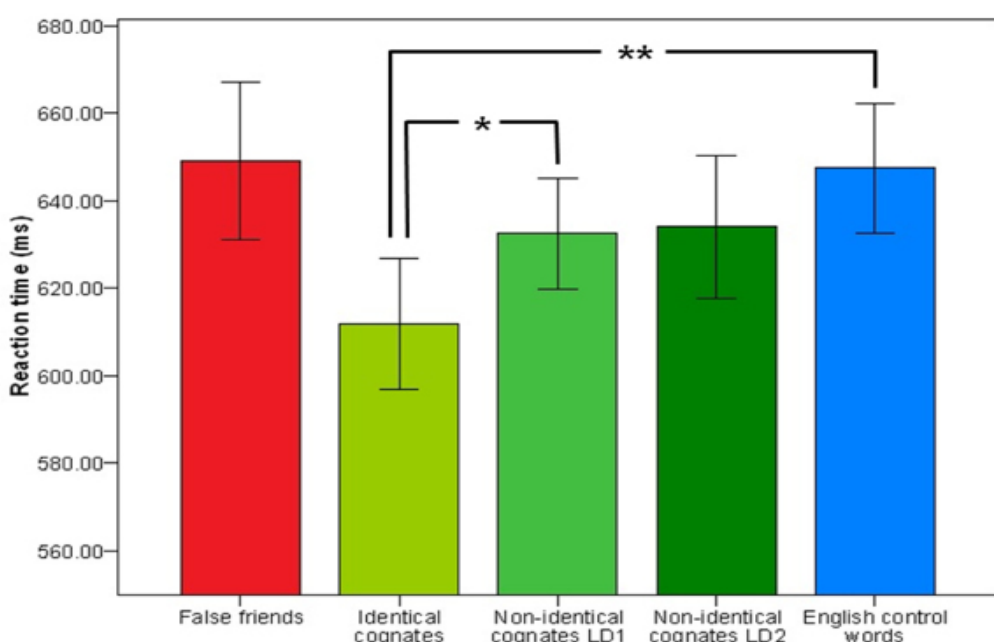
The reaction time analysis was performed on the correct responses only. We conducted a one-way repeated measures ANOVA per task and a  $2 \times 5$  (task  $\times$  condition) factorial repeated measures ANOVA across both tasks. Planned comparisons were run comparing the false friends, identical cognates, non-identical cognates with Levenshtein distance 1, and

**Table 3.** Reaction time results, standard deviations and error rates for the different conditions in each task.

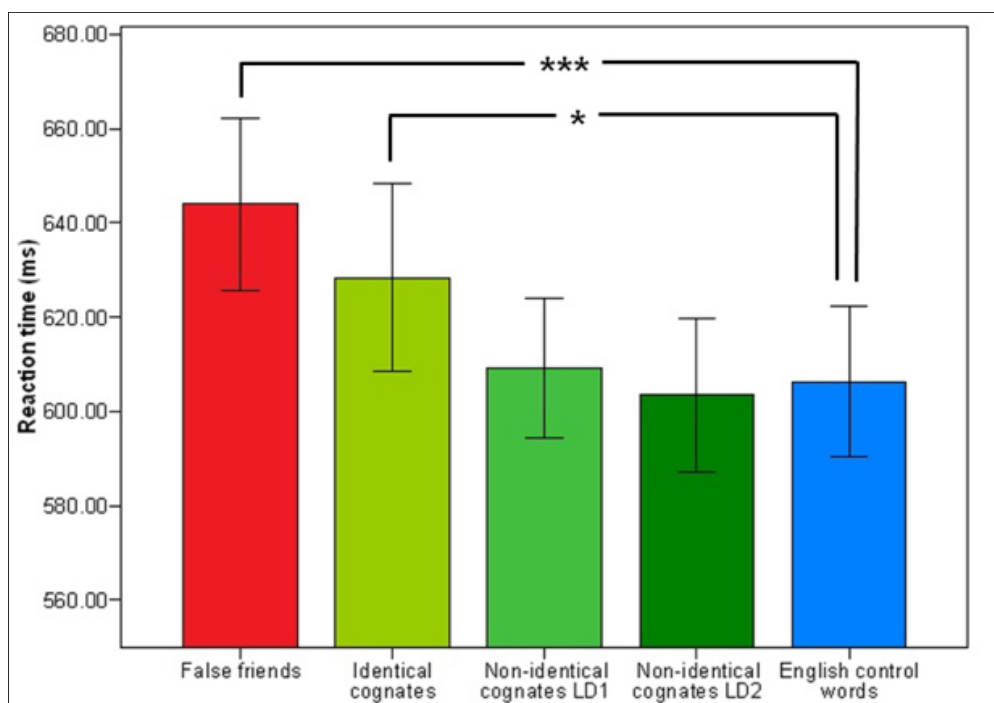
<b>Task 1</b>			
<b>Condition</b>	<b>RT</b>	<b>SD</b>	<b>% Error</b>
False friends	649.14	80.54	5.81
Identical cognates	611.86	66.82	2.36
Non-identical cognates LD1	632.55	56.85	4.64
Non-identical cognates LD2	634.05	73.15	4.11
English control words	647.45	65.71	4.23
Pseudowords	735.40	85.42	2.75

<b>Task 2</b>			
<b>Condition</b>	<b>RT</b>	<b>SD</b>	<b>% Error</b>
False friends	644.01	81.47	6.92
Identical cognates	628.38	59.06	4.24
Non-identical cognates LD1	609.10	66.70	3.74
Non-identical cognates LD2	603.50	72.77	5.67
English control words	606.35	71.52	4.35
Pseudowords	733.80	86.97	4.59
Dutch words	718.96	100.35	4.48



**Fig. 3** Reaction time results for the first lexical decision task that did not include Dutch words. Error bars indicate the standard error of the mean.



**Fig. 4** Reaction time results for the second lexical decision task that included Dutch words. Error bars indicate the standard error of the mean.

non-identical cognates with Levenshtein distance 2 to the English control words. In addition, we compared the identical cognates to the non-identical cognates with Levenshtein distance 1 per task to investigate whether identical cognates have a special status in comparison to non-identical cognates. All results are listed in table 3.

### 2.2.1 Task 1: English lexical decision task

The reaction time results for the first task are presented in Figure 3. The analysis of this task revealed a significant main effect of condition on reaction times,  $F(4,76) = 3.93$ ,  $p < 0.01$ , partial  $\eta^2 = 0.17$ . Planned contrasts revealed that responses to identical cognates were significantly faster than to English control words,  $F(1,19) = 15.08$ ,  $p < 0.01$ , partial  $\eta^2 = 0.41$ . In addition, identical cognates were recognized significantly faster than non-identical cognates with Levenshtein distance 1,  $F(1,19) = 7.84$ ,  $p < 0.05$ , partial  $\eta^2 = 0.29$ .

### 2.2.2 Task 2: English lexical decision task with Dutch words

The reaction time results for the second task are presented in Figure 4. A significant main effect of condition was also found in the second task,  $F(4,76) = 9.84$ ,  $p < 0.001$ , partial  $\eta^2 = 0.34$ . Planned comparisons showed that identical cognates were recognized significantly slower than English control

words,  $F(1,19) = 8.06$ ,  $p < 0.05$ , partial  $\eta^2 = 0.30$ , and that false friends were recognized significantly slower than English control words,  $F(1,19) = 20.46$ ,  $p < 0.001$ , partial  $\eta^2 = 0.52$ . The difference between identical cognates and non-identical cognates with Levenshtein distance 1 was only marginally significant,  $F(1,19) = 4.38$ ,  $p = 0.05$ , partial  $\eta^2 = 0.19$ .

### 2.2.3 Overall results: comparing the two tasks

A significant main effect of condition was found across tasks,  $F(4,76) = 5.62$ ,  $p < 0.01$ , partial  $\eta^2 = 0.23$ . The main effect of task failed to reach significance,  $F(1,19) = 2.02$ ,  $p = 0.17$ , partial  $\eta^2 = 0.10$ . A significant task x condition interaction effect was found,  $F(4,76) = 6.46$ ,  $p < 0.001$ , partial  $\eta^2 = 0.25$ . In order to break down this interaction effect, we performed planned contrasts comparing task 1 to task 2 and all experimental conditions to the English control words. Significant interaction effects were found when comparing task 1 to task 2 both for false friends compared to English control words,  $F(1,19) = 5.76$ ,  $p < 0.05$ , partial  $\eta^2 = 0.23$ , for identical cognates compared to English control words,  $F(1,19) = 34.56$ ,  $p < 0.001$ , partial  $\eta^2 = 0.65$ , and for identical cognates compared to non-identical cognates with Levenshtein distance 1,  $F(1,19) = 18.81$ ,  $p < 0.001$ , partial  $\eta^2 = 0.50$ . As is evident from a comparison of Figures 5 and 6, the interaction effect found for false friends reflects that

the non-significant difference between false friends and English control words in the first task became a significant inhibitory effect in the second task. The interaction effects for identical and non-identical cognates reflect the reversal of the directionality of the cognate effect from the first task to the second task: relative to the English control words, facilitation turned into inhibition.

### 2.3 Discussion

The results of the first task show that identical cognates are recognized faster than non-identical cognates and English control words. The two types of non-identical cognates could not be distinguished from each other and did not differ significantly from the English control words. These findings indicate that the transition from complete orthographic overlap to even the smallest cross-linguistic orthographic difference results in a large and non-linear slowing down of reaction times, in line with the findings of Dijkstra et al. (2010). Non-identical cognates with Levenshtein distance 1 were recognized 15 ms faster than control words, but this difference failed to reach significance. Reaction times to false friends did not differ significantly from control words. This finding differs from the results of van Heuven et al. (2008), who observed slower reaction times for false friends. Possible causes for this difference will be discussed in the general discussion.

In the second task, including Dutch words, the pattern of results for identical cognates reversed: we obtained a large inhibitory effect in comparison to control words. This is the first time a cognate inhibition effect is found in a lexical decision task in adults. An even larger inhibitory effect was found for false friends. The presence of Dutch words in the stimulus list appears to have mainly affected the recognition of words that have complete orthographic overlap between Dutch and English. The behaviour of non-identical cognates did not differ from control words.

Overall, reaction times in the second task were faster than in the first task, indicating that participants' performance improved with practice. At the same time, the reaction time patterns across test and control conditions in both the first and second task are in line with earlier research. For instance, the addition of Dutch words to lexical decision has been shown to induce inhibition effects for false friends (e.g., Dijkstra et al., 1998). Cognate inhibition dependent on stimulus list composition has been observed in children (Brenders, Van

Hell, & Dijkstra, 2011). Our study is the first to show these cognate inhibition effects in adults; it further demonstrates that the reversal of cognate effects across tasks is dependent on cross-linguistic orthographic similarity. An important conclusion on the basis of our data is that the effect of stimulus list manipulation on the recognition of cognates and false friends appears to be similar to the effects of task demands reported in previous research (e.g., Dijkstra et al., 2010; Van Heuven et al., 2008).

## 3. fMRI experiment

### 3.1 Methods

#### 3.1.1 Participants

Nineteen Dutch-English bilinguals participated in the experiment. Data from one participant was excluded from the analyses due to chance-level performance on the pseudoword condition. The remaining participants were nine men and nine women with a mean age of 23.9 years (SD 2.3). All participants were right-handed and had normal or corrected-to-normal vision. They gave written informed consent before the start of the experiment and received 20 euro or course credit for participating. None of the participants had any neurological impairments.

Participants' language background and English proficiency were assessed by means of a self-rating questionnaire. All participants were native speakers of Dutch who on average came into contact with English at the age of 10.3 (SD 2.7). They rated their English reading experience as 6.1 (SD 1.0) on a scale from 1 (very little experience) to 7 (very much experience).

#### 3.1.2 Stimulus materials

The same stimulus lists were used as in the behavioral experiment.

#### 3.1.3 Procedure

Participants received written instructions before the start of the experiment. They were asked to press a button when a presented letter string was not an existing English word. All responses were given with the right index finger. The lexical decision task used in the RT experiment was adapted in this way to avoid motor artifacts on critical trials. Participants were informed of the presence of words existing in both Dutch and English in the stimulus list. The same instructions were used for both tasks.

Participants completed a series of 14 practice trials outside the scanner before the start of each task. The practice trials contained the same proportion of stimuli from each condition as the actual experiment. The two tasks were run using Presentation software. Stimuli were presented in white 20-point Arial font on a black screen. Each trial began with a variable jitter of 0, 500, 1000 or 1500 ms to improve the temporal resolution of the fMRI signal. Then a fixation cross was presented in the centre of the screen for 400 ms. The fixation cross was immediately followed by the presentation of the stimulus in the centre of the screen. The stimulus remained visible until the participant pressed the button or until the maximum response time of 2000 ms was reached. A blank screen then appeared for a variable period of time so that each trial lasted 8 s. In total, participants spent approximately 45 minutes in the scanner per session.

Each participant completed both tasks. The two tasks were scheduled on different days. The order of the tasks was kept constant. After the first experiment, participants filled out a written questionnaire assessing their language background and English proficiency. Apart from this, experimental procedures were identical during both sessions.

### *3.1.4 Image acquisition and analysis*

fMRI data were acquired on a Siemens 3T MAGNETOM Trio MRI scanner using a single-shot FID-EPI sequence (TR = 2000 ms, TE = 30 ms, flip angle = 90°, 31 axial slices in ascending order, voxel size = 3.5 x 3.5 x 3 mm). Structural images were acquired using a MPRAGE sequence (TR = 2300 ms, TE = 3.03 ms, 192 sagittal slices, voxel size = 1 x 1 x 1 mm).

The functional scans were preprocessed and analyzed using SPM8 (Statistical Parametric Mapping, [www.fil.ion.ucl.ac.uk/spm](http://www.fil.ion.ucl.ac.uk/spm)). The first three volumes per session were discarded to allow for T1 equilibration effects. All volumes were realigned to correct for small head movements and slice timing correction was applied by temporally realigning the time course for each voxel to the 16th slice. The mean functional images per subject were co-registered to their anatomical T1 images and structural images were then segmented into grey and white matter. Functional images were spatially normalized to the MNI template provided by SPM, resampled to 2 x 2 x 2 mm voxels and smoothed using a 8-mm FWHM Gaussian filter kernel.

The resulting fMRI time series were analyzed

as an event-related design using the general linear model. A design matrix was constructed for each subject and session that contained 6 regressors modelling the presentation of each of the conditions (false friends, identical cognates, non-identical cognates LD1, non-identical cognates LD2, English control words, and pseudowords/Dutch words) and a regressor modelling the incorrect responses. All regressors were convolved with the hemodynamic response function and its temporal derivative. In addition, 6 movement parameters from the realignment algorithm were included in the model as effects of no interest.

Contrast images of the main effects of the conditions of interest (false friends, identical cognates, non-identical cognates LD1, non-identical cognates LD2, and English control words) were generated per session and participant. In addition, contrast images directly comparing the experimental conditions to the English control word condition were generated. These first-level contrast images were then entered into a second-level random effects analysis per contrast. A one-sample t-test was performed to look whether the differences between conditions at the group level for each task were significantly different from zero. Below, we only report the brain regions showing significantly more activation for the conditions of interest in comparison to the English control words. The results of the inverse contrasts can be found in the supplementary materials online (<http://www.ru.nl/master/cns/journal>). In addition, we created contrast images to test the task x condition interaction between false friends and English control words and between identical cognates and English control words in both tasks. A one-sample t-test was then performed to look whether the interaction effects at the group level were significantly different from zero. A Monte Carlo simulation (Slotnick, Moo, Segal, & Hart, 2003) with 1000 iterations was run to correct for multiple comparisons at  $p < 0.05$  with an individual voxel type I error of  $p \leq 0.001$ . Based on this procedure, the cluster extent threshold was set at 46 resampled voxels (368 mm<sup>3</sup>). Only clusters exceeding this threshold are reported. All reported coordinates are Montreal Neurological Institute (MNI) coordinates.

### 3.2 Results

#### 3.2.1 Whole-brain analyses

All significant activations obtained in the first task are listed in Table 4. Comparisons between the conditions of interest and the English control words in the first task yielded only significant differences for the contrast between false friends and English control words (Figure 5). We found a large cluster covering the left IFG, and a left superior medial frontal cluster extending to the pre-SMA.

All significant activations obtained in the second task are listed in Table 5. The contrast between the false friends and the English control words yielded a significant cluster covering the pre-SMA and superior MFC (Figure 6). In addition, a large cluster was found in the left IFG. Finally, the contrast between false friends and English control words yielded a cluster in the right IFG, extending into the insula. Eleven clusters were found when comparing the activation patterns of the identical cognates and the English control words in the second task (Figure 7). The largest cluster was found on the medial surface of the frontal lobe, covering the left and right pre-SMA

**Table 4.** Brain regions showing significantly more activity for the experimental conditions than for the English control word condition in the first task ( $p < 0.001$ ,  $k > 46$  voxels).

<b>Task 1</b>						
Brain region	Cluster	Zmax	MNI coordinates			
			Extent (voxels)	x	y	
<b>False friends &gt; English control words</b>						
Left inferior frontal gyrus	2025	5.06	-54	38	6	
Left inferior frontal gyrus		4.87	-52	36	16	
Left inferior frontal gyrus		4.47	-50	20	24	
Left superior medial frontal gyrus	339	4.64	-6	30	40	
Left supplementary motor area		3.72	-6	18	50	
<b>Identical cognates &gt; English control words</b>						
No suprathreshold clusters						
<b>Non-identical cognates LD1 &gt; English control words</b>						
No suprathreshold clusters						
<b>Non-identical cognates LD2 &gt; English control words</b>						
No suprathreshold clusters						

and part of the middle cingulate gyrus. Two more significant clusters were found in the right IFG, and one cluster in the left IFG. Subcortical clusters were found in the left and right caudate and the thalamus

All significant task x condition interactions are listed in Table 6. No interaction effect was found when comparing task 2 to task 1 for the contrast between false friends and English control words. A significant task x condition interaction effect was found when comparing task 2 to task 1 for the contrast between identical cognates and English control words in the right IFG.



**Fig. 5** Brain regions showing significantly more activation for false friends than for English control words in the first task ( $p < 0.001$ ,  $k > 46$  voxels).

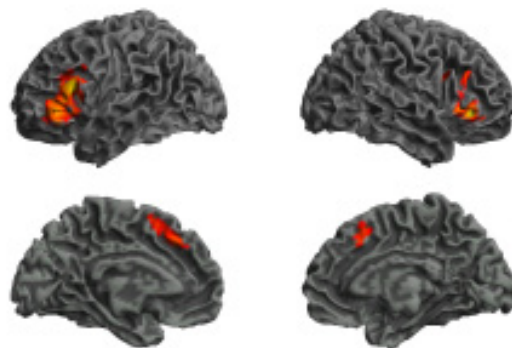


**Fig. 6** Brain regions showing significantly more activation for false friends than for English control words in the second task ( $p < 0.001$ ,  $k > 46$  voxels).

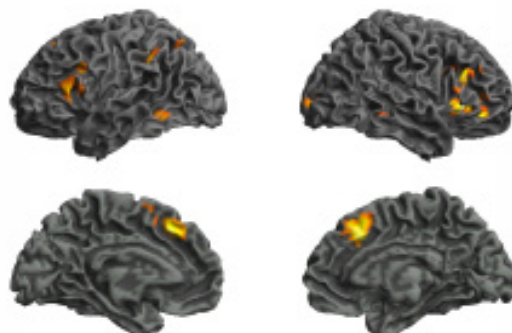


**Fig. 7** Brain regions showing significantly more activation for identical cognates than for English control words in the second task ( $p < 0.001$ ,  $k > 46$  voxels).

**Table 5.** Brain regions showing significantly more activity for the experimental conditions than for the English control word condition in the second task ( $p < 0.001$ ,  $k > 46$  voxels).

Task 2					
Brain region	Cluster Extent (voxels)	Zmax	MNI coordinates		
			x	y	z
<b>False friends &gt; English control words</b>					
Right inferior frontal gyrus	1172	5.69	46	32	-2
Right insula lobe		4.54	34	26	-2
Right inferior frontal gyrus		3.90	54	30	28
Left inferior frontal gyrus	2990	5.20	-50	20	18
Left inferior frontal gyrus		4.67	-54	34	-2
Left inferior frontal gyrus		4.60	-36	28	-2
Left superior medial frontal gyrus	608	4.09	-8	26	40
Right superior medial frontal gyrus		3.88	8	22	44
Left supplementary motor area		3.80	-6	16	52
<b>Identical cognates &gt; English control words</b>					
Right inferior frontal gyrus	849	5.38	32	30	-6
Right inferior frontal gyrus		4.58	40	38	-6
Right putamen		4.56	26	22	-2
Right superior medial frontal gyrus	1207	4.98	6	24	42
Right supplementary motor area		4.21	12	16	52
Left supplementary motor area		3.65	-4	4	62
Right inferior frontal gyrus	517	4.60	52	30	22
Right inferior frontal gyrus		3.81	38	12	30
Right inferior frontal gyrus		3.66	58	18	12
Right cerebral white matter	92	4.58	48	-38	-10
Right middle temporal gyrus		3.26	58	-38	-6
Right cerebral white matter		3.26	44	-42	-2
Left caudate nucleus	485	4.26	-14	0	18
Left thalamus		4.08	-10	-12	2
Left caudate nucleus		3.68	-14	6	10
Left inferior frontal gyrus	766	4.13	-50	20	10
Left precentral gyrus		3.85	-42	12	30
Left inferior frontal gyrus		3.64	-34	10	30
Right cerebral white matter	346	4.10	14	-10	-6
Right thalamus		3.92	18	-12	6
Right caudate nucleus		3.56	10	10	6
Left inferior parietal lobule	117	4.09	-48	-40	38
Supramarginal gyrus		3.29	-42	-42	32
Left inferior temporal gyrus	161	4.07	-54	-52	-8
Left fusiform gyrus		3.17	-46	-56	-18
Right calcarine gyrus	137	3.82	24	-94	0
Sub-gyral white matter		3.36	28	-84	2
Left superior parietal lobule	117	3.70	-30	-70	52
Left inferior parietal lobule		3.39	-32	-60	40
<b>Non-identical cognates LD1 &gt; English control words</b>					
Right inferior frontal gyrus	61	3.84	44	16	24
Left thalamus	55	3.46	-8	-12	6
Left thalamus		3.29	-10	-16	-2
<b>Non-identical cognates LD2 &gt; English control words</b>					
Right cerebral white matter	172	5.05	44	-44	-4
Right cerebral white matter		4.51	40	-36	-8
Right cerebral white matter		3.37	38	-44	6

**Table 6.** Brain regions showing significant interaction effects when comparing task 2 to task 1 for the contrast between false friends and English control words and the contrast between identical cognates and English control words ( $p < 0.001$ ,  $k > 46$  voxels).

Task x condition interaction					
Brain region	Cluster	Zmax	MNI coordinates		
			x	y	z
Extent (voxels)					
<b>False friends &gt; English control words</b>					
No suprathreshold clusters					
<b>Identical cognates &gt; English control word</b>					
Right inferior frontal gyrus	108	3.90	40	34	-2
Right inferior frontal gyrus		3.34	34	32	-8

### 3.3 Discussion

In the first task, we only observed significant clusters for the contrast between false friends and English control words. The clusters were located in the left IFG and the superior MFC. These findings largely replicate the results van Heuven et al. (2008) found in an English lexical decision task when comparing false friends to English control words. Van Heuven et al. (2008) linked activity in these regions to conflict in the word identification system and conflict in the task/decision system. Possible explanations for the absence of significant clusters for the other contrasts will be given in the general discussion.

In the second task, we found a similar pattern of activity for the contrast between false friends and English control words. In addition, activity was found in the right IFG. Comparing identical cognates to English controls resulted in an extensive pattern of activity that partly overlapped with the activation pattern found for false friends. In line with the results of van Heuven et al. (2008), identical cognates and false friends both showed increased activity when compared to English control words in the left inferior frontal and medial frontal cortex. Small clusters of activity were also found when comparing non-identical cognates to English controls.

## 4. General discussion

We investigated the effects of stimulus-based and response-based conflict on bilingual visual word recognition by considering the processing of words with different degrees of cross-linguistic form and meaning overlap. We collected behavioral and fMRI

evidence that bilinguals cannot block a non-target language, even when it is irrelevant for responding or even hinders task performance. In addition, our results support the notion that identical cognates have a special status in the bilingual mental lexicon due to their complete cross-linguistic orthographic and semantic overlap and their language membership ambiguity. Finally, we separated the effects of stimulus-based and response-based conflict on the recognition of cognates and false friends, and identified the brain regions that are involved in resolving these types of conflict.

### 4.1 Language non-selective lexical access

Participants in our study were instructed to indicate whether presented visual letter strings were English words, a task that did not require them to use their knowledge of Dutch. In fact, blocking the non-target language would even have benefited task performance, especially in the second task including non-target language words. Yet, under all task conditions we found behavioral evidence that word candidates from both languages become activated. A large cognate facilitation effect arose for identical cognates in the first task, suggesting that the combination of cross-linguistic form and meaning overlap can facilitate task performance. In the second task, the inclusion of Dutch words in the stimulus list caused considerable inhibitory effects for identical cognates and false friends. Combined, these behavioral results suggest that word candidates from both languages are co-activated and compete for selection during visual word recognition.

### 4.2 The special status of identical cognates

We investigated whether identical cognates have a special status in the bilingual mental lexicon. First, it was an open question whether the cognate facilitation effect shows a discontinuity between non-identical and identical cognates (Dijkstra et al., 2010; Van Assche et al., 2011). In the first task, identical cognates were recognized faster than non-identical cognates with Levenshtein distance 1 and English control words. Reaction times to the two groups of non-identical cognates did not differ. These results provide additional evidence for the discontinuity between non-identical and identical cognates observed by Dijkstra et al. (2010). Combined with shared semantics, complete cross-linguistic orthographic overlap appears to provide a considerable processing advantage over partial

orthographic overlap in the standard English lexical decision task.

Second, we investigated whether identical cognates and non-identical cognates are affected differently by our stimulus list manipulation. We expected that the addition of Dutch words to the stimulus list might affect identical and non-identical cognates differently due to their different levels of orthographic overlap. Identical cognates have exactly the same orthographical form in different languages and are therefore ambiguous with respect to their language membership. In contrast, non-identical cognates and English control words unambiguously belong to only one language. We therefore expected that the addition of Dutch words to the stimulus list would especially affect the recognition of identical cognates. In line with this expectation, the reaction time pattern for identical cognates in the second task reversed relative to the first task. Responses to identical cognates were considerably slower relative to non-identical cognates and control words, while the behavior of non-identical cognates was indistinguishable from control words. This is the first evidence of a cognate inhibition effect in a lexical decision task in adults. Brenders, van Hell, and Dijkstra (2011) previously reported a cognate inhibition effect in an English lexical decision task in children, but their stimulus list did not contain any Dutch words.

The fMRI results provide additional support for the special status of identical cognates. Interestingly, no difference was observed between identical cognates and English control words in the first task. In the second task, the recognition of identical cognates led to an extensive activation pattern including the bilateral inferior frontal gyri, the medial frontal gyrus, and subcortical structures. In contrast, non-identical cognates only showed minor neural differences relative to the English control words. Combined, the results of our experiments support the idea that identical cognates have a special status in the bilingual mental lexicon due to their form and meaning overlap and their ambiguous language membership. However, based on our findings it is difficult to specify what the representation of identical cognates looks like, and how it differs from the representations of non-identical cognates and false friends.

#### 4.3 Conflict in the task/decision system

The BIA+ model distinguishes a word identification system and a task decision system. Conflict in the task/decision system is thought

to be caused by competition between response alternatives. In the current study, we expected to find evidence of response conflict for false friends in the first task and for identical cognates and false friends in the second task. Identical cognates and false friends have identical orthographical forms in Dutch and English and are therefore ambiguous with respect to their language membership. The presence of Dutch words in the stimulus list in the second task was expected to strengthen the connection between the Dutch readings of these words and the NO-response, resulting in response conflict. The effect of the stimulus list manipulation on non-identical cognates was expected to be smaller, as these words are unambiguously English. In line with our expectations, we found inhibitory effects for identical cognates and false friends in reaction times. The behavior of non-identical cognates did not differ from control words.

Based on van Heuven et al. (2008), we expected to find activity supporting the resolution of response conflict in the medial frontal cortex and the basal ganglia. In the first task, we found a cluster of activity in the superior MFG and pre-SMA for the contrast between false friends and English control words. The MFC plays an important role in performance monitoring (Ridderinkhof, Ullsperger, Crone, & Nieuwenhuis, 2004). One of its functions is to resolve high response conflict situations to allow a correct response to be given (Ridderinkhof et al., 2004). In both experiments, the majority of responses in the second task were correct, although the large inhibitory effects in the behavioral data suggest that response conflict slowed down decision-making considerably. The pre-SMA supports the selection of rules for stimulus-response mappings (Rushworth, Walton, Kennerley, & Bannerman, 2004), response selection, and response inhibition (Mostofsky & Simmonds, 2008).

In the second task, we again found clusters of activity in the superior MFC and pre-SMA for the contrasts between identical cognates and controls and between false friends and controls. In addition, we found large clusters of activity in the right IFG. This area supports response inhibition, especially in go/no-go paradigms (Chikazoe, Konishi, Asari, Jimura, & Miyashita, 2007; Aron, Fletcher, Bullmore, Sahakian, & Robbins, 2003). A task x condition interaction effect for identical cognates was observed in this region, suggesting that response conflict increased considerably in the second task. Finally, we found subcortical activity in the caudate nucleus and thalamus for the contrast between identical cognates and English control words. The caudate nucleus is

part of a cortico-subcortical loop connecting the striatum to the prefrontal cortex (Lehéricy, Ducros, Van De Moortele, Francois, Thivard, Poupon, & Swindale, 2004) and plays a role in response selection and control in language processing (Duffau, 2008; Robles, Gatignol, Capelle, Mitchell, & Duffau, 2005). In bilinguals, this structure is involved in language control, monitoring and switching (Crinion et al., 2006; Abutalebi et al., 2007).

#### 4.4 Conflict in the word identification system

Conflict in the word identification system is caused by competition between linguistic representations. Van Heuven et al. (2008) found evidence of this type of conflict for false friends in an English lexical decision task. We therefore expected to find evidence of conflict in the word identification system for false friends in both tasks. It was less clear what to expect for cognates. Van Heuven et al. (2008) proposed that conflict in the word identification system activates the left IFGs. They proposed three possible roles of this region in the recognition of false friends, namely (1) the selection of information among competing alternatives (Thompson-Schill et al., 1997), (2) phonological retrieval (Gold & Buckner, 2002) or (3) controlled semantic retrieval (Gold & Buckner, 2002; Badre et al., 2005). Van Heuven et al. could not distinguish between these accounts, as false friends differ in phonology and semantics across languages. In the current study, we varied both semantic and orthographic overlap, allowing us to investigate the role of this region in more detail.

In line with the study by van Heuven et al., we found left inferior frontal activity for the contrast between false friends and English control words in both tasks. In addition, a smaller cluster of activity was found in this region when comparing identical cognates to English controls in the second task. In the first task, no activity was found in the left IFG for identical cognates and non-identical cognates. What role does the IFG play in the recognition of cognates and false friends? A phonological account seems unlikely, as both word types have different phonological forms in Dutch and English. Similarly, a purely semantic account cannot account for this pattern of results, as the activation pattern of cognates did not differ from English control words in the first task. A more general cognitive function for the left IFG probably offers the best explanation of the observed pattern of results.

One proposal is that the left IFG supports cognitive control and regulates conflict between

competing characterizations of linguistic stimuli (January, Trueswell, & Thompson-Schill, 2009; Novick, Trueswell, & Thompson-Schill, 2005). Left inferior frontal activity has been reported in tasks that involve phonetic decision making (Blumstein, Myers, & Rissman, 2005), semantic ambiguity (Bedny, Hubert, & Thompson-Schill, 2007; Rodd, Davis, & Johnsrude, 2005), syntactic ambiguity (Mason, Just, Keller, & Carpenter, 2003), and syntactic and spelling violations (van de Meerendonk, Indefrey, Chwilla, & Kolk, 2011). Combined, these results suggest that the left IFG is not involved in a particular aspect of language processing such as syntax (Grodzinsky, 2000). Instead, this region appears to play a more general role in cognitive control at the representational level by biasing attention towards the correct representation when several representations are activated (January et al., 2009). This type of conflict resolution is not restricted to purely linguistic representations (January et al., 2009) and can be separated from response conflict.

A more general account of cognitive control at the representational level can account for the pattern of results we observed in the left IFG. In the first task, we only found activity in this area for false friends, but not for cognates. The main difference between these two word types is that cognates activate a shared semantic representation across languages, while false friends activate a different semantic representation in each language. These activated semantic representations compete for selection in the word identification system and cognitive control is required to select the appropriate meaning. The left inferior frontal activity observed for false friends in the first task can thus be explained as the resolution of representational conflict at the semantic level. This hypothesis is supported by monolingual literature on semantic ambiguity (Bilenko, Grindrod, Myers, & Blumstein, 2009; Grindrod, Bilenko, Myers & Blumstein, 2008; Hargreaves, Pexman, Pittman, & Goodyear, 2010).

The activation pattern in the second task can be explained as the result of semantic and language membership ambiguity. As in the first task, false friends are expected to create semantic ambiguity. Furthermore, the addition of Dutch words to the stimulus list can cause language membership ambiguity. In the first task, bilinguals did not need language membership information to respond correctly. Participants could response accurately by using a general lexical decision criterion (is it a word or not?). In contrast, in the second task, participants were required to verify the language membership of the presented letter strings due to the presence

of the Dutch words. As a result of their identical orthographical forms, identical cognates and false friends are ambiguous with respect to their language membership. Bilinguals require cognitive control to resolve this ambiguity, resulting in left inferior frontal activation for identical cognates and false friends. According to this account, stimulus-based conflict resolution should be most demanding for false friends in the second task, as these elicit both semantic and language membership ambiguity. Our behavioral finding that false friends are an additional 16 ms slower than identical cognates supports this view.

Interestingly, we find neural evidence of stimulus-based conflict for false friends in the first task without any behavioral differences in reaction times. In a previous study using a similar English lexical decision task, van Heuven et al. (2008) found activity in the left IFG as well as an inhibitory effect in reaction times. A possible explanation for this discrepancy is that the reaction times collected in the study by van Heuven et al. were on average at least 350 ms slower than in our study. However, those response times were collected in the scanner during the fMRI recording. Slow responding may have led to an increased spreading of activation in the word identification system, resulting in more conflict. Alternatively, stimulus list or task demand differences may have caused the difference in reaction times. We collected reaction time data in a separate behavioral experiment outside the scanner, so we do not know how fast participants would have responded in the scanner environment. Also, our stimulus list contained cognates in addition to false friends. The presence of cognates may have led participants to accept potentially ambiguous words more readily than in the study by van Heuven et al. (2008).

#### 4.5 Implications of our study

Our results have a number of theoretical implications for models of bilingual language processing. First, we found behavioral and neuroimaging evidence that the non-target language cannot be blocked, providing support for models with language non-selective access to the mental lexicon. Second, we found support for the distinction between a word identification system and a task/decision system. Conflict can be found in both systems. The resolution of stimulus-based conflict is supported by the left IFG, while response-based conflict is supported by the MFC and basal ganglia. Our stimulus list manipulation appears to mainly

affect conflict in the task/decision system. Finally, our results support a special status for identical cognates in the bilingual mental lexicon, but on the basis of this study we cannot specify whether identical cognates have one or two orthographic representations.

### 5. Conclusion

In this lexical decision study, we investigated how bilinguals deal with stimulus- and response-based conflict in bilingual visual word recognition by looking at cognates and false friends. Behaviorally, we showed that the processing of these word types is influenced greatly by stimulus list composition and we found evidence of a special status for identical cognates in the bilingual mental lexicon. By means of fMRI, we separated the effects of stimulus-based and response-based conflict. The resolution of conflict in the word identification system caused activity in the left IFG, while conflict in the task/decision system was supported by medial frontal, right inferior frontal, and subcortical structures. Our findings provide evidence for the predictions of the BIA+ model that bilinguals cannot block the non-target language and that a distinction should be made between a word identification and a task/decision system.

### Acknowledgements

I would like to thank my supervisors Ton Dijkstra and Shirley-Ann Rueschemeyer for their enthusiasm and support throughout the project, the members of the Language Division at the DCC for their advice and my fellow interns for their helpful suggestions and good times.

### References

- Abutalebi, J., Annoni, J. M., Zimine, I., Pegna, A. J., Seghier, M. L., Lee-Jahnke, H., Lazeyras, F., et al. (2008). Language control and lexical competition in bilinguals: an event-related fMRI study. *Cerebral Cortex*, 18(7), 1496–1505.
- Aron, A. R., Fletcher, P. C., Bullmore, E. T., Sahakian, B. J., & Robbins, T. W. (2003). Stop-signal inhibition disrupted by damage to right inferior frontal gyrus in humans. *Nature Neuroscience*, 6(2), 115–116.
- Badre, D., Poldrack, R. A., Paré-Blaogev, E. J., Insler, R. Z., & Wagner, A. D. (2005). Dissociable controlled retrieval and generalized selection mechanisms in ventrolateral prefrontal cortex. *Neuron*, 47(6), 907–918.
- Bedny, M., McGill, M., & Thompson-Schill, S. L. (2008). Semantic Adaptation and Competition during Word

- Comprehension. *Cerebral Cortex*, 18(11), 2574–2585.
- Bilenko, N. Y., Grindrod, C. M., Myers, E. B., & Blumstein, S. E. (2009). Neural correlates of semantic competition during processing of ambiguous words. *Journal of Cognitive Neuroscience*, 21(5), 960–975.
- Blumstein, S. E., Myers, E. B., & Rissman, J. (2005). The perception of voice onset time: An fMRI investigation of phonetic category structure. *Journal of Cognitive Neuroscience*, 17(9), 1353–1366.
- Brenders, P., van Hell, J. G., & Dijkstra, T. (2011). Word recognition in child second language learners: Evidence from cognates and false friends. *Journal of Experimental Child Psychology*, 109(4), 383–396.
- Brett, M., Anton, J., Valabregue, R., & Poline, J. (2002). Region of interest analysis using an SPM toolbox [abstract]. 8th International Conference on Functional Mapping of the Human Brain June 26 2002 Sendai Japan.
- Brysbaert, M., & New, B. (2009). Moving beyond Kučera and Francis: A critical evaluation of current word frequency norms and the introduction of a new and improved word frequency measure for American English. *Behavior Research Methods*, 41(4), 977–990.
- Chikazoe, J., Konishi, S., Asari, T., Jimura, K., & Miyashita, Y. (2011). Activation of Right Inferior Frontal Gyrus during Response Inhibition across Response Modalities. *Journal of Cognitive Neuroscience*, 19(1), 69–80.
- Crinion, J., Turner, R., Grogan, A., Hanakawa, T., Noppeney, U., Devlin, J. T., Aso, T., Urayama, S., Fukuyama, H., Stockton, K., Usui, K., Green, D. W., & Price, C. J. (2006). Language control in the bilingual brain. *Science*, 312(5779), 1537–1540.
- Cristoffanini, P., Kirsner, K., & Milech, D. (1986). Bilingual lexical representation: The status of Spanish–English cognates. *The Quarterly Journal of Experimental Psychology A: Human Experimental Psychology*, 38(3), 367–393.
- Costa, A., Caramazza, A., & Sebastian-Galles, N. (2000). The cognate facilitation effect: Implications for models of lexical access. *Journal of Experimental Psychology: Learning, Memory, and Cognition*, 26(5), 1283–1296.
- de Bleser, R., Dupont, P., Postler, J., Bormans, G., Speelman, D., Mortelmans, L., & Debrock, M. (2003). The organisation of the bilingual lexicon: a PET study. *Journal of Neurolinguistics*, 16(4–5), 439–456.
- de Groot, A. M. B., & Nas, G. L. J. (1991). Lexical representation of cognates and noncognates in compound bilinguals. *Journal of Memory and Language*, 30(1), 90–123.
- Dijkstra, T., Grainger, J., & van Heuven, W. J. (1999). Recognition of cognates and interlingual homographs: The neglected role of phonology. *Journal of Memory and Language*, 41(4), 496–518.
- Dijkstra, T., Miwa, K., Brummelhuis, B., Sappelli, M., & Baayen, H. (2010). How cross-language similarity and task demands affect cognate recognition. *Journal of Memory and Language*, 62(3), 284–301.
- Dijkstra, T., & van Heuven, W. J. (2002). The architecture of the bilingual word recognition system: From identification to decision. *Bilingualism: Language and Cognition*, 5(03), 175–197.
- Dijkstra, T., Van Jaarsveld, H., & Ten Brinke, S. (1998). Interlingual homograph recognition: Effects of task demands and language intermixing. *Bilingualism: Language and Cognition*, 1(01), 51–66.
- Dijkstra, T., Timmermans, M., & Schriefers, H. (2000). On Being Blinded by Your Other Language: Effects of Task Demands on Interlingual Homograph Recognition. *Journal of Memory and Language*, 42(4), 445–464.
- Duffau, H. (2008). The anatomo-functional connectivity of language revisited: New insights provided by electrostimulation and tractography. *Neuropsychologia*, 46(4), 927–934.
- Gerard, L. D., & Scarborough, D. L. (1989). Language-specific lexical access of homographs by bilinguals. *Journal of Experimental Psychology: Learning, Memory, and Cognition*, 15(2), 305–315.
- Gold, B. T., & Buckner, R. L. (2002). Common Prefrontal Regions Coactivate with Dissociable Posterior Regions during Controlled Semantic and Phonological Tasks. *Neuron*, 35(4), 803–812.
- Grindrod, C. M., Bilenko, N. Y., Myers, E. B., & Blumstein, S. E. (2008). The role of the left inferior frontal gyrus in implicit semantic competition and selection: An event-related fMRI study. *Brain Research*, 1229, 167–178.
- Grodzinsky, Y. (2000). The neurology of syntax: Language use without Broca's area. *Behavioral and brain sciences*, 23(1), 1–21.
- Hargreaves, I. S., Pexman, P. M., Pittman, D. J., & Goodyear, B. G. (2011). Tolerating ambiguity: Ambiguous words recruit the left inferior frontal gyrus in absence of a behavioral effect. *Experimental Psychology (formerly Zeitschrift für Experimentelle Psychologie)*, 58(1), 19–30.
- January, D., Trueswell, J. C., & Thompson-Schill, S. L. (2009). Co-localization of stroop and syntactic ambiguity resolution in Broca's area: implications for the neural basis of sentence processing. *Journal of Cognitive Neuroscience*, 21(12), 2434–2444.
- Keuleers, E., Brysbaert, M., & New, B. (2010). SUBTLEX-NL: A new frequency measure for Dutch words based on film subtitles. *Behavior Research Methods*, 42(3), 643–650.
- Lehéritier, S., Ducros, M., Van De Moortele, P., Francois, C., Thivard, L., Poupon, C., & Swindale, N. (2004). Diffusion tensor fiber tracking shows distinct corticostriatal circuits in humans. *Annals of Neurology*, 55(4), 522–529.
- Lemhöfer, K., & Dijkstra, T. (2004). Recognizing cognates and interlingual homographs: Effects of code similarity in language-specific and generalized lexical decision. *Memory & Cognition*, 32(4), 533–550.
- Lemhöfer, K., Dijkstra, T., & Michel, M. (2004). Three languages, one ECHO: Cognate effects in trilingual word recognition. *Language and Cognitive Processes*, 19(5), 585–611.

- Marian, V., & Spivey, M. (2003). Competing activation in bilingual language processing: Within-and between-language competition. *Bilingualism Language and Cognition*, 6(2), 97–116.
- Mason, R. A., Just, M. A., Keller, T. A., & Carpenter, P. A. (2003). Ambiguity in the Brain: What Brain Imaging Reveals About the Processing of Syntactically Ambiguous Sentences. *Journal of Experimental Psychology: Learning, Memory, and Cognition*, 29(6), 1319–1338.
- Mostofsky, S. H., & Simmonds, D. J. (2008). Response inhibition and response selection: Two sides of the same coin. *Journal of Cognitive Neuroscience*, 20(5), 751–761.
- Novick, J. M., Trueswell, J. C., & Thompson-Schill, S. L. (2010). Broca's area and language processing: Evidence for the cognitive control connection. *Language and Linguistics Compass*, 4(10), 906–924.
- Raboyeau, G., Marcotte, K., Adrover-Roig, D., & Ansaldi, A. (2010). Brain activation and lexical learning: The impact of learning phase and word type. *NeuroImage*, 49(3), 2850–2861.
- Ridderinkhof, K. R. (2004). The Role of the medial frontal cortex in cognitive Control. *Science*, 306(5695), 443–447.
- Robles, S., Gatignol, P., Capelle, L., Mitchell, M., & Duffau, H. (2005). The role of dominant striatum in language: a study using intraoperative electrical stimulations. *Journal of Neurology, Neurosurgery, and Psychiatry*, 76(7), 940–946.
- Rodd, J. M., Davis, M. H., & Johnsrude, I. S. (2005). The neural mechanisms of speech comprehension: fMRI studies of semantic ambiguity. *Cerebral Cortex*, 15(8), 1261–1269.
- Rodríguez-Fornells, A., Rotte, M., Heinze, H. J., Nösselt, T., & Münte, T. F. (2002). Brain potential and functional MRI evidence for how to handle two languages with one brain. *Nature*, 415(6875), 1026–1029.
- Rushworth, M. F. S., Walton, M. E., Kennerley, S. W., & Bannerman, D. M. (2004). Action sets and decisions in the medial frontal cortex. *Trends in Cognitive Sciences*, 8(9), 410–417.
- Scarborough, D. L., Gerard, L., & Cortese, C. (1984). Independence of lexical access in bilingual word recognition. *Journal of Verbal Learning and Verbal Behavior*, 23(1), 84–99.
- Slotnick, S.D., Moo, L.R., Segal, J.B., Hart J. (2003). Distinct prefrontal cortex activity associated with item memory and source memory for visual shapes. *Cognitive Brain Research*, 17, 75–82.
- Thompson-Schill, S.L., D'Esposito, M., Aguirre, G. K., & Farah, M.J. (1997). Role of left inferior prefrontal cortex in retrieval of semantic knowledge: A reevaluation. *Proceedings of the National Academy of Sciences*, 94(26), 14792–14797.
- van Assche, E., Drieghe, D., Duyck, W., Welvaert, M., & Hartsuiker, R. J. (2011). The influence of semantic constraints on bilingual word recognition during sentence reading. *Journal of Memory and Language*, 64(1), 88–107.
- van de Meerendonk, N., Indefrey, P., Chwilla, D. J., & Kolk, H. H. (2011). Monitoring in language perception: Electrophysiological and hemodynamic responses to spelling violations. *NeuroImage*, 54(3), 2350–2363.
- van Hell, J. G., & Dijkstra, T. (2002). Foreign language knowledge can influence native language performance in exclusively native contexts. *Psychonomic Bulletin & Review*, 9(4), 780–789.
- van Heuven, W. J., & Dijkstra, T. (2010). Language comprehension in the bilingual brain: fMRI and ERP support for psycholinguistic models. *Brain research reviews*, 64(1), 104–122.
- van Heuven, W. J., Schriefers, H., Dijkstra, T., & Hagoort, P. (2008). Language Conflict in the Bilingual Brain. *Cerebral Cortex*, 18(11), 2706–2716.

# The Tactile Speller: An ERP-based Brain-Computer Interface for Communication

Marjolein van der Waal<sup>1</sup>

Supervisors: Jeroen Geuze<sup>1</sup>, Marianne Severens<sup>1,2</sup>, Peter Desain<sup>1</sup>

<sup>1</sup>Donders Institute for Brain, Cognition and Behaviour, Radboud University Nijmegen, The Netherlands

<sup>2</sup>Sint Maartenskliniek, RDE&E, Nijmegen, The Netherlands

In the present study, a tactile speller was developed and compared with existing visual speller paradigms in terms of classification performance and elicited ERPs. The fingertips of healthy participants were stimulated with short mechanical taps while EEG activity was measured. The fingers represented the letters of the alphabet and subjects could select one of the fingers by silently counting the number of taps on that finger. The offline and online performance of the tactile speller was compared to the overt and covert attention matrix speller and the covert attention Hex-o-Spell speller. For the tactile speller binary target versus non-target classification accuracy was 67% on average. Classification and decoding accuracies of the tactile speller were lower than for the overt matrix speller, but higher than for the covert matrix speller, and similar to Hex-o-Spell. The average information transfer rate of the tactile speller was 7.8 bits/minute, with the best subject reaching a bit-rate of 27 bits/minute. An increased amplitude of the P300 ERP component was found in response to attended stimuli versus unattended stimuli in all speller types. In addition, the tactile and overt matrix speller also used the N2 component for discriminating between targets and non-targets. Overall, this study showed that it is possible to use a tactile speller for communication. The tactile speller seems a useful alternative for the visual speller, especially for people whose eye gaze is impaired. Patient studies will have to show whether the results generalize to the patient population.

*Keywords:* brain-computer interface, speller, somatosensory, visual, event-related potential, P300

---

Corresponding author: Marjolein van der Waal, e-mail: m.vanderwaal@donders.ru.nl

## 1. Introduction

For patients who suffer from severe paralysis as a result of diseases like amyotrophic lateral sclerosis (ALS) or spinal cord injury, brain-computer interfaces (BCIs) constitute a way of communicating with the outside world. In general, a BCI records a physiological (e.g. electrophysiological or hemodynamic) signal from the user's brain and transforms the recorded signal into an output command. Output commands can range from the movement of a cursor on a computer screen to the control of a wheelchair.

A well-known BCI for communication purposes is the visual matrix speller (Figure 1A), first designed by Farwell and Donchin (1988). A matrix containing the letters of the alphabet is shown on a computer screen. The rows and columns of the matrix are then intensified in random order. The most common type of intensification is a short luminance increase, perceived as a flash. Subjects direct their attention to the letter they want to select by silently counting the number of times this letter flashes. As a result, the brain response to flashes of the attended letter is different from the brain response to flashes of unattended letters. A computer algorithm can detect this difference and determine which letter the subject is attending to. It has been found that the majority of healthy people can control the visual speller with high accuracy (Guger et al., 2009). In addition, severely disabled ALS patients were able to use the visual speller to communicate (Nijboer et al., 2008).

Initially, it was assumed that the visual speller primarily used the P300 component of the event-related potential (ERP) to discriminate between attended and unattended letters. The P300 component is characterized as a positive-going deflection in the time window of 250-500 ms after a stimulus. The amplitude of this component can be modulated by attention (Kok, 1997; Polich, 2007). For the visual speller, this means that the P300 amplitude is larger for target (attended) than for non-target (unattended) letter flashes (Wolpaw et al., 2002).

However, there is evidence that other ERP components are involved as well. In most visual speller experiments, subjects are fixating their eye gaze on the target letter. As a result, target letters are always presented in the fovea, whereas non-target stimuli are presented in the periphery. Previous research has shown that stimuli elicit smaller visual evoked responses as they are presented farther away from the fovea (Meredith & Celia, 1982; Schlykowa

et al., 1993).

Consequently, the amplitude of the visual evoked response is larger for target than non-target stimuli. It has been shown that the visual speller indeed uses these differences on early ERP components for classification, and that performance decreases substantially when subjects are looking at a central fixation point instead of the target letter (Brunner et al., 2010; Treder & Blankertz, 2010).

To distinguish the two ways of using the visual speller, we will speak of overt attention when eye gaze is directed towards the target letter, whereas we will speak of covert attention when eye gaze is directed at a central fixation point.

When the visual speller is used with covert attention, the task of counting target letter intensifications is more difficult, especially for targets farther away from the point of fixation. Reasons for this are the reduction of visual acuity at greater distance from fixation (Westheimer, 1965) and the phenomenon of visual crowding (Whitney & Levi, 2011). As a solution to these problems, Treder and Blankertz (2010) developed the Hex-o-Spell visual speller. This speller consists of six circles that are positioned in a hexagonal configuration around a central fixation point (Figure 1B). Thus, all circles have the same distance to the point of fixation. The circles increase in size in random order and the subject counts the number of times the circle containing the target letter is enlarged. An increase in size rather than an increase in luminance is used because the latter can induce perceptual fading of the non-highlighted elements. In contrast to the matrix speller, selecting a letter consists of two steps. In the first step, the circle with the desired group of letters is selected. In the second step, the six letters are redistributed over the circles and the target letter is selected. It was found that when both spellers were used with overt attention, the Hex-o-Spell speller performed equally well as the matrix speller, but when both spellers were used with covert attention, Hex-o-Spell performed better (Treder & Blankertz, 2010).

As mentioned before, the target group of the visual speller consists of patients who have minimal to no voluntary motor control. Some of these patients eventually lose the ability to control eye gaze. For patients who are unable to move their eyes, the Hex-o-Spell seems a better option than the matrix speller. However, a number of patients lose their vision completely, and are therefore unable to use any type of visual speller. For these patients, a speller that relies on information from another sensory modality could allow them to keep communicating with their

environment. One option is to use the auditory modality. A number of auditory spellers have been developed. In these spellers, the rows and columns of the letter matrix are usually represented by different sounds, such as spoken numbers (Furdea, Halder, Krusienski, Bross, Nijboer, Birbaumer, & Kübler, 2009) or environmental sounds (Klobassa, Vaughan, Brunner, Schwartz, Wolpaw, Neuper, & Sellers, 2009), or by different spatial locations (Belitski, Farquhar, & Desain, 2011). When presented with a stream of these auditory stimuli, subjects attend to the stimuli representing the desired row and column. Performance of the auditory spellers was found to be lower than performance of the overt attention visual speller, but high enough for communication purposes.

The purpose of the present study is to investigate whether it would also be possible to build a speller based on tactile stimulation. An advantage of tactile stimulation is that it is relatively unobtrusive to others. Whereas the flashing rows and columns of the visual speller or the sounds of the auditory speller will be noticeable to other people, tactile stimuli could be private for the user. Additionally, in contrast to visual and auditory spellers, a tactile speller does not prevent users from seeing and hearing the person with whom they are communicating. This advantage could make a tactile speller also convenient for patients who are not visually impaired.

BCIs based on somatosensory stimulation have

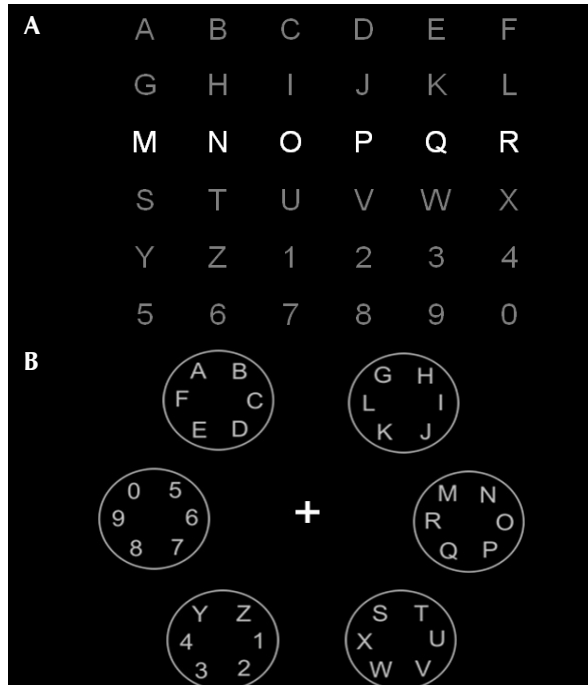


**Fig. 1 A.** Matrix speller: rows and columns are intensified in random order **B.** Hex-o-Spell speler: circles are intensified in random order.

been described before. Müller-Putz et al. (2006) applied steady-state somatosensory stimuli of different frequencies to the left and right index fingers. Subjects directed their attention to one of the fingers, so that in the EEG, the stimulation frequency of this finger was stronger than the other frequency. In two subjects, it was possible to correctly identify which finger was attended in 70–80% of the cases.

Brouwer and van Erp (2010) presented short vibrotactile stimuli to different locations around the waist. Subjects counted the number of times a certain location was being stimulated. A larger amplitude of the ERP P300 component was found in response to stimuli at the target location than stimuli at other locations, and classification accuracies above chance level were obtained.

In the present study, a tactile speller was developed. Stimuli were applied to six fingers that represented the letters of the alphabet (Figure 2A) and subjects could select letters by counting the number of stimuli on the corresponding finger. Figure 2 shows that, similar to the Hex-o-Spell speller, selecting a letter is a two-step process. In the first step, a group of letters is selected and in the second step, one letter from this group is selected.

The primary goal of this study was to assess the performance of the newly developed tactile speller. The second purpose of this study was to compare the new tactile speller with the overt and covert

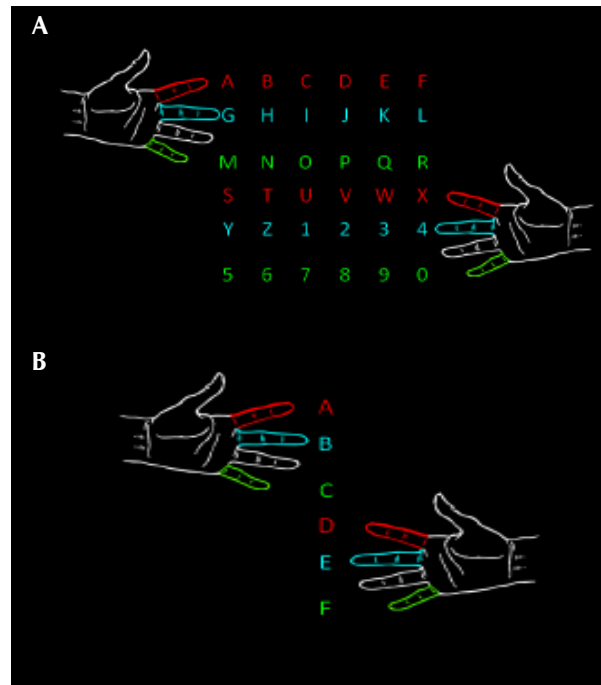


**Fig. 2** The tactile speller. Selecting a letter consists of **A.** Step 1: the fingers represent groups of letters. **B.** Step 2: the fingers represent the letters of the row that was selected in step 1.

attention matrix speller and with the covert attention Hex-o-Spell speller in terms of spelling performance and underlying ERP features.

## 2. Methods

### 2.1 Participants

12 subjects (6 male), aged 19-54 (mean=27) years, participated in the experiment. One of them received course credits, the others volunteered. Four subjects had used the visual speller before and three of these subjects had also participated in other tactile BCI experiments. All other subjects were naïve with regard to BCI experiments. Subjects did not have any neurological abnormalities, reported normal or corrected to normal vision, and did not use medication. All subjects gave informed consent prior to the experiment. Due to excessive eye movements, one subject had to be excluded from the analyses.

### 2.2 Apparatus

EEG was recorded with 64 sintered Ag/AgCl active electrodes (BioSemi), placed according to the international 10-20 system. Additionally, 4 electrodes were used to record horizontal and vertical EOG. These were placed on the outer canthi of the eyes and below and above the left eye.

In order to measure grasp strength, EMG activity was recorded by placing one electrode on the elbow (lateral epicondyle of the humerus) as a reference and another one on the m.flexor digitorum superficialis, an underarm muscle involved in grasping. The sampling rate was 2048 Hz.

Visual stimuli were presented on a 17" TFT screen with 800 x 600 pixel resolution and a refresh rate 60 Hz. Tactile stimuli were presented using piezoelectric Braille stimulators, built into two graspable devices (one for each hand), so that each fingertip rested on



**Fig. 3** Braille stimulator.

a separate Braille cell (Figure 3). One cell consists of two rows of four pins that can be pushed out for short time periods, which subjectively feels like a short tap on the finger. The stimulators were each placed inside a soundproof box to mask the sounds of the Braille cells accompanying the tactile stimuli.

Subjects were seated in front of a table. The screen was in the middle of the table at a distance of approximately 70 cm from the subject. The boxes with the tactile stimulators were placed 30 cm left and right of the body midline. Whenever subjects had to give responses, they used foot pedals to do so, in order to minimize movement of the arms and upper body.

### 2.3 Conditions

The experiment consisted of four conditions, in which subjects used the overt and covert attention matrix spellers, the Hex-o-Spell, and the tactile speller. In every condition, the goal was to copy-spell twelve random letters. In the visual conditions, the spellers were used offline. The tactile condition consisted of an offline and an online copy-spelling part. Each subject participated in all conditions, with the order of conditions randomized between subjects.

In two of the conditions the subjects used the matrix speller, once with overt and once with covert attention. In the overt attention condition, subjects were allowed to fixate on the target letter, while in the covert attention condition, they were instructed to keep looking at the fixation cross and only direct attention at the target letter. The size of each character was 1.0x0.8 cm (0.82x0.65° visual angle) and the entire matrix was 20x20 cm (16x16° visual angle). Stimuli consisted of intensifications of the rows and columns in random order. Intensification was achieved by increasing the size of all characters in the row or column with a factor 1.5 for 100 ms.

The third condition was the Hex-o-Spell condition. Subjects were instructed to look at the fixation cross and only direct attention to the target. So, in this condition, covert attention was used. The Hex-o-Spell circles had a diameter of 4.2 cm (3.4° visual angle) and the distance between the fixation cross and the center of each circle was 10.3 cm (8.4° visual angle). Stimuli consisted of the circles and the letters inside them increasing to 1.5 times their original size for 100 ms.

Finally, subjects used the tactile speller. Most subjects needed some time to get used to the tactile stimulation, and found the task of counting target stimuli more difficult and less intuitive than in the

visual spellers. Therefore, the tactile condition started with a short practice block of six stimulation sequences. Each sequence started with the instruction which finger was the target finger. When the subject pressed a foot pedal, the tactile stimulation began. After the stimulation subjects were asked how many taps they had felt and three answer alternatives were presented. Subjects selected one out of three answer alternatives with the foot pedal, and their response was followed by feedback (“correct” or “wrong”). In contrast to the main experiment, the number of target stimuli in a sequence was varied, so that the correct answer would not always be the same.

After the practice block, the tactile speller was first used offline and then online. The dataset collected during the offline block was used to train the classifier for the online block.

Tactile stimuli consisted of raising four pins of one Braille cell for 100 ms. Stimuli were applied to six fingers (index, middle and little finger of both hands). During tactile stimulation, only a fixation cross was shown on the screen.

Finally, when subjects had completed all four conditions, they were given the opportunity to use the online tactile speller to spell anything they liked. Although this was not compulsory, 8 subjects used this opportunity.

## 2.4 Trials

A trial is defined here as spelling one letter. All trials started with the speller being displayed on the screen, together with the instruction which letter to select. When subjects had localized this letter, they pressed a foot pedal to start the visual or tactile stimulation. For the matrix speller, one stimulation sequence lasted 36 seconds and consisted of 120 stimuli, 20 of which were target stimuli. The stimulus onset asynchrony (SOA) was 300 ms. Each sequence was built up of smaller subseries in which all fingers, circles, or rows and columns were stimulated once in random order, with the restriction that the unit that was stimulated last in one subseries could not be stimulated first in the next. Thus, the same unit was never stimulated twice in a row.

As described in the introduction, in both the Hex-o-Spell and tactile speller, selecting one letter is a two-step procedure. Therefore, after the subject had pressed the foot pedal, there were two stimulation sequences, separated by a pause in which the subject could localize the new target. Each sequence lasted 18 seconds and consisted of 60 stimuli, 10 of which were target stimuli. The SOA was 300 ms. Note that selecting one letter involves the same number

of stimuli and takes the same amount of time in all spellers.

At the end of each stimulation sequence, there was feedback on the screen showing which letter or group of letters was selected. In the visual conditions and the offline part of the tactile condition, feedback always showed that the correct unit was selected. In the online part of the tactile condition, which finger was selected was calculated online. On four occasions throughout the tactile block, the feedback about letter selection was replaced by the question how many taps were felt on the target finger. This was done in order to remind the subjects to keep counting target stimuli, because this task is less intuitive in the tactile condition.

## 2.5 Signal processing

The data was temporally down-sampled to 256 Hz and sliced into sequences, each with a different target unit. A sequence lasted 36 (matrix speller) or 18 (Hex-o-Spell and tactile speller) seconds. Linear detrending was applied to remove slow drifts in the signal and the data was re-referenced using a common average reference (CAR). Bad trials and bad channels (determined by an amplitude of > 3.5 times the standard deviation) were removed, followed by the calculation of a new CAR without the rejected channels and the removal of any remaining outlying trials. The data was spectrally filtered with a band-pass filter of .5-12 Hz and further down-sampled to 32 Hz. Finally, the sequences were sliced further into individual epochs of 0-600 ms after stimulus onset and linear detrending was applied to the individual epochs.

## 2.6 Classification

Prior to classification, the number of target and non-target epochs was balanced by randomly selecting the same number of epochs from the non-target class as the number of epochs in the target class. In addition, the data was spatially whitened. Then a linear classifier was trained on a binary problem (target versus non-target stimulus) using an L2 regularized linear logistic regression algorithm (Bishop, 2006). Leave-one-sequence-out cross validation was used to find the optimal regularization settings.

The binary classification was followed by a decoding step. For each stimulation sequence the binary decision values were compared with the stimulation code. The stimulation unit (e.g. finger or

Hex-o-Spell circle) that had the highest correlation between decision values and stimulus code was predicted to be the target unit in this sequence.

For the tactile and Hex-o-Spell spellers, one out of six units can be the target in each sequence. In contrast, for the matrix speller, each of thirty-six units can be the target. In order to make the results of the decoding procedure comparable, the 120 stimuli of one matrix stimulation sequence were divided in two sets, one containing 60 row intensifications and the other containing 60 column intensifications. In each of the subsets was determined which row (out of 6) or which column (out of 6) contained the target. So, for each of the spellers the decoding procedure consisted of solving a six-class problem.

In addition, the information transfer rate or bit-rate of each speller type was computed as described in Wolpaw (1998). The bit-rate of a BCI indicates how much information can be communicated per time unit. The bit-rate is dependent on classification accuracy, the number of classes, and the time it takes to make a classification.

## 2.7 Statistical analyses

One-way repeated measures ANOVAs were used to compare the different spellers in terms of classification accuracies of the binary classification problem and the decoding problem. In the latter case, the input for the ANOVA was the decoding accuracy at the end of the stimulation sequence, i.e. after 60 stimuli or 18 seconds. If an ANOVA yielded a significant result, pairwise comparisons were made comparing the tactile speller with the three visual spellers. The alpha level for these

pairwise comparisons was Bonferroni corrected to  $0.05/3=0.017$ . For these analyses the PASW Statistics 18.0 software package was used.

For all ERP analyses, the data was preprocessed as described before, with the exception that the data was down-sampled to 128 instead of 32 Hz. ERPs were baseline corrected relative to the 200 ms prior to stimulus onset. Grand-average ERPs were obtained by averaging over epochs and subjects.

Cluster-based permutation tests (Maris & Oostenveld, 2007) were used to assess differences between ERP waveforms. This nonparametric test finds clusters of electrodes and time points where ERP waveforms are different while controlling the false alarm rate. Two different permutation tests were performed. In the first test, for each condition the target and non-target ERPs were compared. Secondly, for the tactile offline and online conditions a difference waveform was computed by subtracting the non-target ERP from the target ERP, and these difference waveforms were compared to each other. Cluster-based permutation tests were performed with FieldTrip (Oostenveld, Fries, Maris & Schoffelen, 2011).

The magnitude of the P300 amplitude difference between targets and non-targets was compared across the different speller types. For each speller type, the time window of significant P300 amplitude modulation was determined based on the results of the cluster-based randomization tests. More specifically, it was defined as the time window of the cluster of significant differences at Cz, around or closest to 300 ms. For each speller type, this time window is indicated with an asterisk in Figure 6A. For each subject, the area between the target and

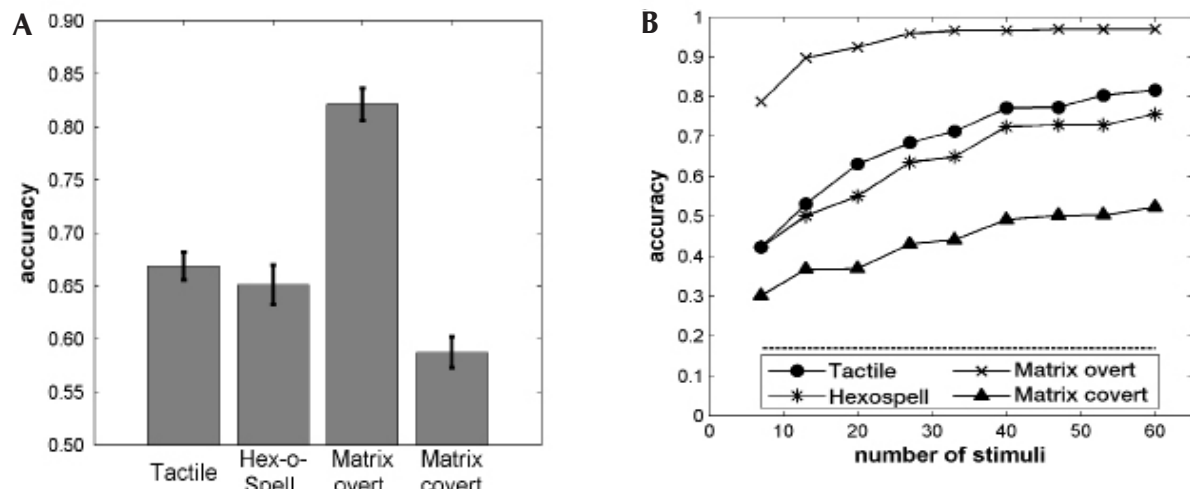


**Fig. 4 A.** Binary (target vs. non-target) classification. Error bars show standard error of the mean. **B.** 6-class decoding accuracy as a function of number of stimuli used for the decoding decision. The dashed line indicates chance level.

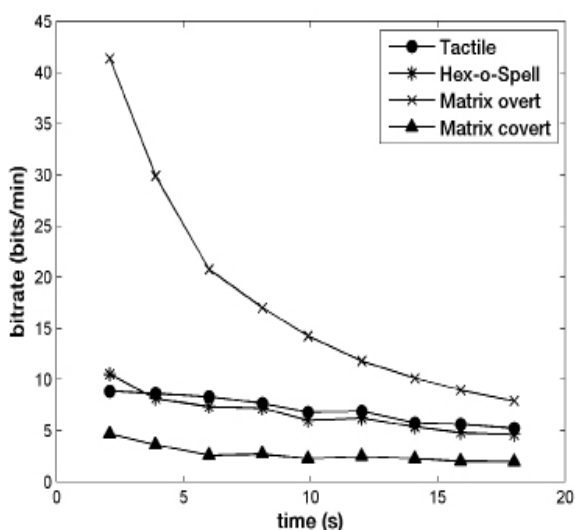


**Fig. 5** Bit-rates. The amount of information that can be communicated with the different speller types as a function of time. As the time until making a classification (horizontal axis) increases, bit-rates decrease. Information transfer rate is highest for the overt matrix speller, lowest for the covert matrix speller and intermediate for the tactile and Hex-o-Spell spellers.

non-target ERP at Cz in the speller-specific time window was estimated using the trapezoid method and divided by the length of the time window. The P300 modulation was compared across the different speller types using a one-way repeated measures ANOVA followed by pairwise comparisons between the tactile and the three visual spellers.

### 3. Results

Unless otherwise indicated, tactile speller results are based on the offline block.

#### 3.1 Classification

After the artifact rejection procedure, a similar number of trials remained in each condition. On average, classification was based on 225 to 240 epochs per class.

The results of the binary (target versus non-target) classification are shown in Figure 4A. It can be seen that classification performance was above chance level (0.5) for all spellers. Results of the repeated measures ANOVA indicated significant differences between the conditions ( $F(4,40)=69.3$ ,  $p<0.001$ ,  $\eta^2=0.874$ ). Pairwise comparisons showed that performance of the tactile speller ( $M=0.67$ ,  $SD=0.046$ ) was significantly lower than performance of the overt attention matrix speller ( $M=0.82$ ,  $SD=0.053$ ),  $p<0.001$ ,  $d=-2.42$ , but higher than the covert attention matrix speller ( $M=0.58$ ,  $SD=0.051$ ),

$p<0.001$ ,  $d=1.61$ . Classification performance of the tactile speller did not significantly differ from the Hex-o-Spell speller.

Figure 4B shows the results of the 6-class decoding procedure. At fixed moments throughout the stimulation sequence, all binary classifications up to that moment are combined to make a decoding decision concerning which unit of stimulation (e.g. finger or circle) is most likely to be the target in this sequence. The figure shows the accuracy of this decoding decision as a function of the number of stimuli included in the decoding decision. Performance was above chance level (0.17) for all spellers. The ANOVA on the accuracy at the end of the stimulation sequence, i.e. after 60 stimuli or 18 seconds, showed significant differences between the conditions ( $F(4,40)=22.1$ ,  $p<.001$ ,  $d=0.688$ ). The pattern of decoding accuracies across spellers was similar to the pattern of classification accuracies. Performance of the tactile speller ( $M=0.82$ ,  $SD=0.14$ ) was significantly lower than performance of the overt attention matrix speller ( $M=0.97$ ,  $SD=0.053$ ),  $p<0.025$ ,  $d=-1.24$ , but higher than the covert attention matrix speller ( $M=0.52$ ,  $SD=0.20$ ),  $p<0.01$ ,  $d=1.54$ . Decoding accuracies of the Hex-o-Spell and tactile speller were not significantly different.

#### 3.2 Information transfer rates

The information transfer rate or bit-rate of a BCI indicates how much information can be communicated per time unit. The bit-rates of the different speller types as a function of time can be seen in Figure 5.

The average peak bit-rate of the tactile speller was 7.8 bits/min. However, the best subject reached a bit-rate of 27 bits/min using the tactile speller, and in fact his classification performance was better for the tactile than the overt matrix speller. This indicates that there are individual differences in how well people can use different speller types.

#### 3.3 ERP results

For all speller types, the cluster-based permutation tests showed significant differences in P300 amplitude between target and non-target ERPs (Figure 6, panel A, B). This amplitude difference follows a typical P300 topography. The classifier weights indicate that for the tactile speller, the Hex-o-Spell and the overt matrix speller, the P300 difference is indeed of importance for classification

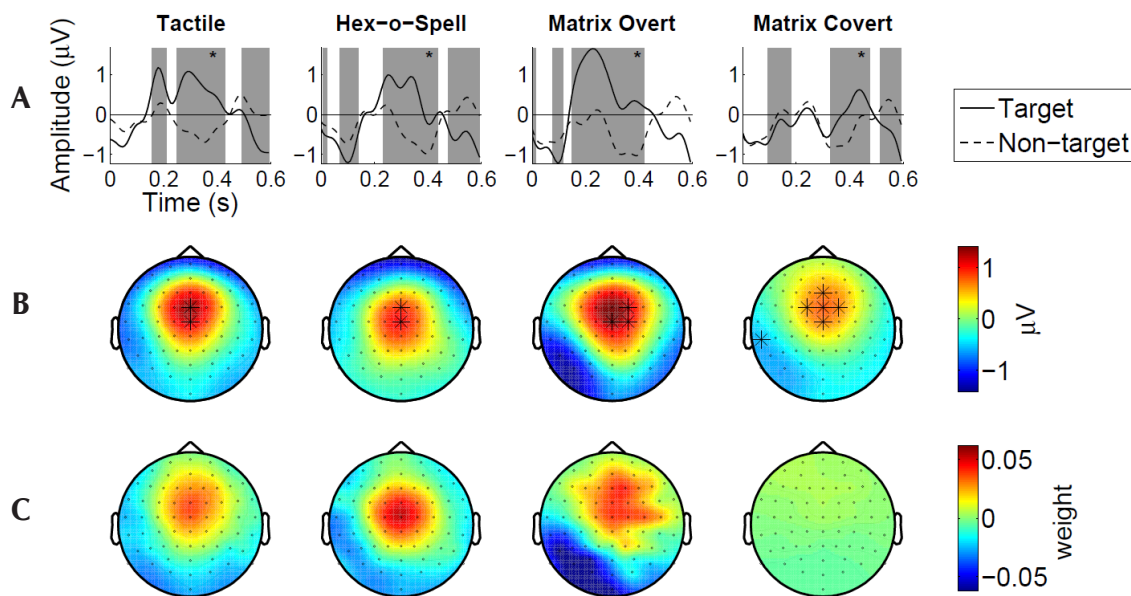


**Fig. 6** P300 results. **A.** Grand-average target and non-target ERPs at Cz. Shaded areas indicate significant differences between the two ERPs. **B.** Topoplots of the target – non-target difference in the time window of the cluster indicated by an asterisk in panel a. Asterisks in the topoplots indicate electrodes where the target – non-target difference is significant in this time window. **C.** Topoplots of the classifier weights, averaged over subjects, in the time window of the significant P300 cluster.

(Figure 6C). Although in the covert matrix speller the grand-average P300 difference between targets and non-targets is significant, the difference seems less useful for the classifier in this speller type.

The difference in P300 amplitude between targets and non-targets at Cz was compared between conditions using a repeated measures ANOVA. The results indicated that the P300 modulation is indeed different across speller types ( $F(4,40)=3.38$ ,  $p=0.018$ ,  $\eta^2=0.25$ ). Subsequent pairwise comparisons of the tactile versus the three visual conditions showed that the P300 amplitude is modulated more strongly for the tactile than for the covert matrix speller ( $p=0.013$ ,  $d=0.91$ ). No significant differences in P300 modulation were found for the tactile versus the overt matrix speller or the tactile versus the Hex-o-Spell speller.

In addition to the P300 component, the N2 amplitude also seemed informative for distinguishing between target and non-target stimuli in the tactile as well as the overt matrix speller.

For the overt matrix speller, a significant N2 amplitude modulation is found over posterior electrodes (Figure 7, left hand side). The positive amplitude difference at central and frontal electrodes reflects the early stage of the P300 modulation. The classifier weights indicate that the posterior N2 difference is very informative for distinguishing target and non-target stimuli in the overt matrix speller, perhaps even more so than the P300

difference.

For the tactile speller, a significant N2 difference is found as well (Figure 7, right hand side). However, this amplitude difference is located at electrodes over the somatosensory cortex. The negative amplitude difference at temporal electrodes is accompanied by a positive difference at frontal electrodes. In this case the frontal difference most probably does not reflect P300 modulation, because in the tactile speller, the P300 modulation appears after the time window used for these topoplots. Rather, the temporal and frontal amplitude differences may reflect activity from the same source, as in the specified time window, the signals measured at electrodes TP7 (temporal) and AFz (frontal) are negatively correlated with  $r = -0.97$  (for the visual speller, the correlation between PO7 and AFz is 0.24 in this time window). Figure 7C shows that both the temporal and frontal amplitude differences appear to be of importance for the classifier, though not as important as the N2 difference for the visual speller.

For the Hex-o-Spell and covert attention matrix speller, no significant amplitude differences were found at any electrode in the 150–250 ms time window.

### 3.4 Online results of the tactile speller

The grand-average ERPs of the tactile speller were very similar in the offline and online parts of

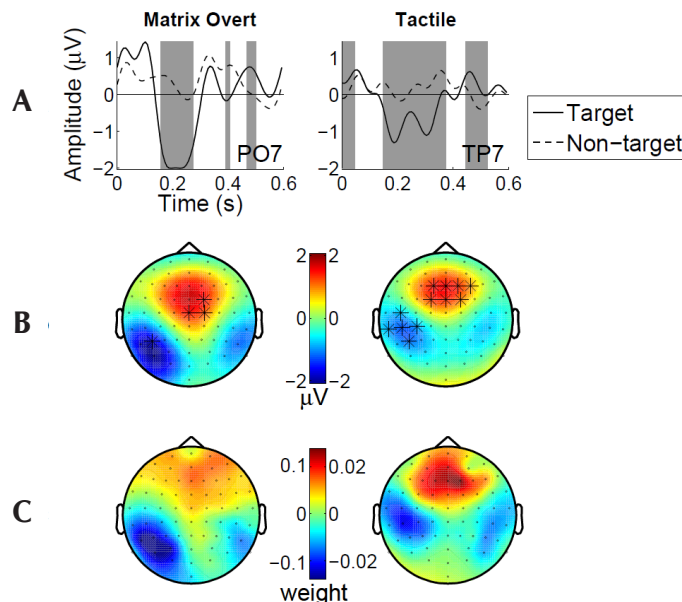


**Fig. 7** N2 results. **A.** Grand-average target and non-target ERPs at PO7 (visual speller) and TP7 (tactile speller). The shaded areas indicate significant differences between the two ERPs. **B.** Topoplots of the target – non-target difference in the time window from 150 to 250 ms post stimulus. Asterisks indicate electrodes where the target – non-target difference is significant in this time window. **C.** Topoplots of the classifier weights in the time window from 150 to 250 ms. Scales on the left side of the color bars correspond to the plots on the left and scales on the right side of the color bars correspond to the plots on the right.

the experiment. The cluster-based permutation test on the target – non-target difference waveforms revealed no significant differences between offline and online speller (all cluster p-values  $>0.05$ ).

Moreover, the online performance of the tactile speller did not differ significantly from its offline performance in terms of binary classification (online:  $M=0.66$ ,  $SD=0.046$ ) or 6-class decoding accuracy (online:  $M=0.79$ ,  $SD=0.14$ ).

## 4. Discussion

The primary goal of this study was to develop a tactile speller. The results showed that it is possible to build a speller based on selective attention to somatosensory stimuli on the fingertips. In addition, the classification performance of the newly developed tactile speller was compared with the performance of existing visual spellers. The performance of the tactile speller was lower than the overt matrix speller, higher than the covert matrix speller and similar to the Hex-o-Spell speller. This pattern was observed for the binary classification as well as the 6-class decoding problem.

Furthermore, the performance of the tactile speller was found to be sufficiently high for effective communication. The mean bit-rate of the tactile speller was 7.8 bits/min, and the maximum bit-rate observed in the best subject was 27 bits/min. This is low compared to bit-rates that are typically reported

for (overt attention) visual spellers. However, it is higher than the bit-rates that were reported for auditory spellers, namely 1.54 bits/min in Furdea et al. (2009) and 2 bits/min in Klobassa et al. (2009). The bit-rate of the tactile speller is also higher than the bit-rate of the tactile BCI described in Brouwer and van Erp (2010), which was 3.71 bits/min. Finally, a more informal indication of the tactile speller's practical applicability is the fact that those subjects who decided to spell a word of their own choice succeeded in doing so. Together, the classification results suggest that for patients with impaired eye gaze, the tactile speller could be a useful alternative for the visual speller.

In addition, a comparison was made between the ERPs that were elicited in the different speller types. The amplitude of the P300 component is significantly larger for target (attended) than non-target (unattended) stimuli in all speller types. This effect has been shown before for visual spellers (Farwell & Donchin, 1988; Treder & Blankertz, 2010) as well as a tactile BCI (Brouwer & Van Erp, 2010). The size of the P300 amplitude modulation in the tactile speller was compared with the modulation in the other speller types. It was found that the P300 amplitude difference of the tactile speller is larger than the amplitude difference of the covert matrix speller, but not significantly different from the Hex-o-Spell or overt matrix speller. This might indicate that the task of counting target stimuli is

more difficult with the covert matrix speller, as the amplitude of P300 generally becomes smaller when task difficulty increases (Kok, 1997; Polich, 2007).

Although it was not statistically tested, the latency of the P300 component appeared to differ across conditions as well. In particular, the latency seemed larger for the covert matrix speller than for the other speller types. In the covert matrix speller stimuli are often presented in the visual periphery, where visual acuity is reduced (Westheimer, 1965). As the latency of the P300 component is related to stimulus evaluation timing (Kok, 1997; Polich, 2007), an increased latency in the covert matrix speller might indicate that it takes longer to identify stimuli as targets or non-targets in this speller type.

In addition to modulations of the P300 component, significant modulations of the N2 component were found in the overt matrix speller and the tactile speller. For the overt matrix speller, modulation of the N2 component at posterior electrodes has been reported before (Treder & Blankertz, 2010). As explained in the introduction, this effect may be caused in part by the fixation of eye gaze on the target. For the tactile speller, an N2 effect was found as well. It has been shown before that selective attention can enhance the amplitude of the tactile N2 (Michie, 1984). However, in this speller type the effect was found at electrodes located over the somatosensory cortex.

A significant difference on grand-average ERPs does not necessarily mean that this difference is useful for classification. The difference between a target and non-target response should reliably occur on the single trial level in order to be of use for the classifier. The classifier weights indicate that the P300 component plays a role in the classification procedure in the tactile, overt matrix and Hex-o-Spell speller. In addition, with the tactile and overt matrix speller, the classifier uses the N2 component as well. The N2 amplitude modulation seems more informative for the overt matrix speller than for the tactile speller. Overall, the results show that neither the visual nor the tactile speller appears to be exclusively based on the P300 component.

We could not verify directly whether subjects were indeed directing their eye gaze towards the target letter in the overt attention condition and towards the fixation cross in the covert attention conditions. However, the large difference in classification between overt and covert visual spellers indicates that this was the case. In addition, modulation of the N2 component of the visual evoked potential, assumed to result from fixation on the target letter, was found in the overt but not in the covert attention

spellers. In addition, it is more likely that subjects would use overt attention when they should use covert attention than vice versa. This would result in an overestimation of performance in the covert attention conditions. If the performance of the covert visual spellers is overestimated, the advantage of the tactile speller over the covert visual spellers would be even greater than reported here.

Possibly, changes in the stimulation paradigm could increase the performance of the tactile speller. In this experiment, we stimulated the index, middle and little fingers of each hand, while the hand was in a fist-like posture. Participants reported that it was sometimes difficult to distinguish taps on index and middle fingers of the same hand. Previous research indicates that the location of somatosensory stimuli is represented in the brain relative to an external, rather than a somatotopic, frame of reference (Azañón et al., 2010; Azañón & Soto-Faraco, 2008; Kitazawa, 2002). Accordingly, it was found that stimuli on adjacent fingers could be discriminated more easily if the distance between the fingers was larger (Riemer et al., 2010) and interference between two tactile stimuli at fixed somatotopic locations was reduced if the stimuli were farther apart in external space (Soto-Faraco et al., 2004). Therefore, to improve discriminability of stimuli on different fingers, it might be beneficial to maximize the distance between the stimulated fingers. This suggests that the performance of the tactile speller might be improved by stimulating fingers that are farther apart, for example thumb, middle finger and little finger, or by spreading the fingers during stimulation. Possibly, stimulating different body parts might also be better than only stimulating fingers.

Another possibility for further improvement might be to design a speller combining visual and tactile stimulation. Recently, a speller with concurrent auditory and visual stimuli has been developed (Belitski et al., 2011). The performance of the audiovisual speller was higher than the performance of the speller with stimulation in either single modality. In addition, it has been shown that there are strong cross-modal links between the visual and tactile modalities in spatial attention (Eimer et al., 2001; Macaluso & Maravita, 2010; Spence et al., 2000). These results suggest that a tactile-visual speller might yield even better results than a speller with only tactile stimulation. However, possible performance benefits would come at the cost of an increased dependence on eye gaze.

As mentioned before, one of the reasons for developing alternatives for the visual matrix speller

is because the visual speller does not work well for patients who suffer from a loss of eye gaze control. Previously, it has been shown that the Hex-o-Spell speller performs better than the matrix speller when subjects are not fixating on the target letter (Treder & Blankertz, 2010). In the current experiment the performance of the tactile speller was similar to the performance of the Hex-o-Spell speller. Thus, for patients who are unable to control their eye gaze, the tactile speller seems a good alternative for the visual speller.

Moreover, the tactile speller does not need the visual modality at all, and can therefore also be used by patients who have lost their vision completely. In this study, we used the visual modality to inform users which finger represented which letter and which letter was selected at the end of each stimulation sequence. However, it is not necessary to present this information visually. For example, instructions and feedback could be given in the auditory modality, although this could slow down the spelling process. Alternatively, if patients were to use the tactile speller some time before vision is lost, they might learn the finger-to-letter associations by heart.

The tactile speller could also be a convenient option for patients who are not visually impaired. Since the tactile speller does not constantly require the visual or auditory modalities, users will be able to look at and listen to the person with whom they communicate.

In conclusion, the present study shows that it is possible to use a tactile speller for communication. The tactile speller might be especially useful for patients who cannot control their eye gaze, but also has advantages for people who are not visually impaired. However, only healthy subjects participated in this experiment. Future studies with patients will have to show whether these findings generalize to the patient population.

## References

- Azañón, E., & Soto-Faraco, S. (2008). Changing reference frames during the encoding of tactile events. *Current Biology*, 18, 1044-1049.
- Azañón, E., Longo, M. R., Soto-Faraco, S., & Haggard, P. (2010). The posterior parietal cortex remaps touch into external space. *Current Biology*, 20, 1304-1309.
- Belitski, A., Farquhar, J., & Desain, P. (2011). P300 audio-visual speller. *Journal of Neural Engineering*, 8, art.nr. 025022.
- Bishop, C. (2006). Pattern recognition and machine learning. Springer.
- Brouwer, A. & van Erp, J. B. F. (2010). A tactile P300 brain-computer interface. *Frontiers in Neuroscience*, 4, 1-11.
- Brunner, P., Joshi, S., Briskin, S., Wolpaw, J. R., Bischof, H. & Schalk, G. (2010). Does the 'P300' speller depend on eye gaze? *Journal of Neural Engineering*, 7, 1-9.
- Eimer, M., Cockburn, D., Smedley, B., & Driver, J. (2001). Cross-modal links in endogenous spatial attention are mediated by common external locations: evidence from event-related potentials. *Experimental Brain Research*, 139, 298-411.
- Farwell, L. A. & Donchin, E. (1988). Talking off the top of your head: toward a mental prosthesis utilizing event-related brain potentials. *Electroencephalography and Clinical Neurophysiology*, 70, 510-523.
- Furdea, A., Halder, S., Krusienski, D. J., Bross, D., Nijboer, F., Birbaumer, N., & Kübler, A. (2009). An auditory oddball (P300) spelling system for brain-computer interfaces. *Psychophysiology*, 46, 617-625.
- Guger et al. (2009). How many people are able to control a P300-based brain-computer interface (BCI)? *Neuroscience Letters*, 462, 94-98.
- Kitazawa, S. (2002). Where conscious sensation takes place. *Consciousness and Cognition*, 11, 475-477.
- Klobassa, D. S., Vaughan, T. M., Brunner, P., Schwartz, N. E., Wolpaw, J. R., Neuper, C., & Sellers, E. W. (2009). Toward a high-throughput auditory P300-based brain-computer interface. *Clinical Neurophysiology*, 120, 1252-1261.
- Kok, A. (1997). Event-related-potential (ERP) reflections of mental resources: a review and synthesis. *Biological Psychology*, 45, 19-56.
- Macaluso, E., & Maravita, A. (2010). The representation of space near the body through touch and vision. *Neuropsychologia*, 48, 782-795.
- Maris, E. & Oostenveld, R. (2007). Nonparametric statistical testing of EEG- and MEG-data. *Journal of Neuroscience Methods*, 164, 177-190.
- Meredith, J. T. & Celesia, G. G. (1982). Pattern-reversal visual evoked potentials and retinal eccentricity, *Electroencephalography and Clinical Neurophysiology*, 53, 243-253.
- Michie, P. T. (1984). Selective Attention Effects on Somatosensory Evoked Potentials. *Annals of the New York Academy of Sciences*, 425, 250-255.
- Müller-Putz, G. R., Scherer, R., Neuper, C., & Pfurtscheller, G. (2006). Steady-state somatosensory evoked potentials: Suitable brain signals for brain-computer interfaces? *IEEE Transactions on Neural Systems and Rehabilitation Engineering*, 14, 30-37.
- Nijboer, F., Sellers, E. W., Mellinger, J., Jordan, M. A., Matuz, T., Furdea, A., Halder, S., Mochty, U., Krusienski, D. J., Vaughan, T. M., Wolpaw, J. R., Birbaumer, N., & Kübler, A. (2008). A P300-based brain-computer interface for people with amyotrophic lateral sclerosis. *Clinical Neurophysiology*, 119, 1909-1916.
- Oostenveld, R., Fries, P., Maris, E., Schoffelen, J. M. (2011). FieldTrip: Open Source Software for Advanced Analysis of MEG, EEG, and Invasive

- Electrophysiological Data. Computational Intelligence and Neuroscience, Volume 2011, doi:10.1155/2011/156869
- Polich, J. (2007). Updating P300: An integrative theory of P3a and P3b. *Clinical Neurophysiology*, 118, 2128-2148.
- Riemer, M., Trojan, J., Kleinböhl, D. & Hölzl, R. (2010). Body posture affects tactile discrimination and identification of fingers and hands. *Experimental Brain Research*, 206, 47-57.
- Schlykowa, L., van Dijk, B. W., & Ehrenstein, W. H. (1993). Motion-onset visual-evoked potentials as a function of retinal eccentricity in man. *Cognitive Brain Research*, 1, 169-174.
- Soto-Faraco, S., Ronald, A., & Spence, C. (2004). Tactile selective attention and body posture: Assessing the multisensory contributions of vision and proprioception. *Perception and Psychophysics*, 66, 1077-1094.
- Spence, C., Pavani, F., & Driver, J. (2000). Crossmodal links between vision and touch in covert endogenous spatial attention. *Journal of Experimental Psychology: Human Perception and Performance*, 26, 1298-1319.
- Treder, M. & Blankertz, B. (2010). (C)overt attention and visual speller design in an ERP-based brain-computer interface. *Behavioral and Brain Functions*, 6, 1-13.
- Westheimer, G. (1965). Visual acuity. *Annual Review of Psychology*, 16, 359-380.
- Whitney, D. & Levi, D. M. (2011). Visual crowding: a fundamental limit on conscious perception and object recognition. *Trends in Cognitive Sciences*, 15, 160-168.
- Wolpaw, J. R. (1998). EEG-based communication: improved accuracy by response verification. *IEEE Transactions on Rehabilitation Engineering*, 6, 326-333.
- Wolpaw, J. R., Birbaumer, N., McFarland, D. J., Pfurtscheller, G. & Vaughan, T. M. (2002). Brain-computer interfaces for communication and control. *Clinical Neurophysiology*, 113, 767-791.

## Abstracts

Proceedings of the Master's Programme of Cognitive Neuroscience is committed to publishing all submitted theses. Given the number of submissions we select certain articles under the recommendation of the editors for our printed edition. To interested readers, we have provided the abstracts of all other articles of which the full versions are available on our website: [www.ru.nl/master/cns/journal](http://www.ru.nl/master/cns/journal).

### **Tracking Bouncing Balls: Default Linear Motion Extrapolation and Bounce Anticipation**

Jeroen Atsma, Rob van Lier, Arno Koning

We investigated motion extrapolation in object tracking in two experiments. In Experiment 1, we used a Multiple-Object-Tracking (MOT) task (3 targets, 3 distractors) combined with a probe detection task to map the attentional spread around a target object. We showed an increased probe detection rate at locations where a target is heading to. In Experiment 2, we introduced a black line ('wall') in the centre of the screen and block-wise manipulated the object's motion with respect to this wall: in one condition objects realistically bounced against the wall, whereas in the other condition objects went through. Just before a target object coincided with the wall, a probe could appear either on the bounce path or on the straight path. In addition to MOT, we included a Single-Object-Tracking (SOT) task (1 target, 5 distractors) for control purposes. We found that in both tasks, straight-path probes were detected more often than bounce-path probes for both motion conditions. This supports the idea that (retinal) linear motion extrapolation, which was also found in Experiment 1, is an automatic, stimulus-driven process. In SOT, bounce-path probes were detected more often in the bounce-motion condition compared to the straight-motion condition. In MOT, this bounce anticipation was not observed, presumably because of the high attentional load that is involved in tracking multiple objects. We conclude that tracking mechanisms seem to be primarily stimulus-driven and only when attentional load is low, top-down predictions are used.

### **Behavioral and Neuronal Headstart Effects in Visual Chinese Phonogram Recognition**

Cheng-hua Bai, Robert Schreuder, Ole Jensen, Jonathan Levy

Chinese phonograms are composed by a semantic radical and a phonetic radical, which provide naturalistic language materials to study the different levels of the processes involved in visual character recognition. We used a headstart paradigm to examine the preparation readers could gain from pre-exposing a part of a written target stimulus. When native Taiwan Mandarin Chinese readers saw the radical 100 ms before the whole character, they responded faster in a lexical decision task. In addition, we found an interaction effect between character structures and types of headstart which indicated that the headstart effect was not only due to visual repetition. We further investigated the neuronal substrates of processing visual Chinese character using magnetoencephalography (MEG) which provides a good temporal resolution for investigating the neuronal processes. MEG also has a better spatial resolution than electroencephalography which allows us to have a better estimation on the brain regions involved in the processes. Our results indicated that the headstart effect was reflected in induced gamma band activity at around 70~100 Hz over posterior occipital areas. When the readers saw the headstart, the induced gamma synchronization was weaker in comparison to when they did not see the headstart. We replicated the interaction effect between character structures and types of headstart behaviorally, but the induced gamma power did not reflect it. Given that seeing a headstart is a special situation which allows the beginning of processing the target 100 ms ahead, we speculate that the induced gamma responses are not only due to the visual repetition, but also due to dynamics within the linguistic-perceptual network. Further study is needed for clarifying the functional role of induced gamma oscillatory activity at the posterior area.

## **Similar Anticipatory Eye Movements Elicited by Visually and Linguistically Presented Action Sequences**

Kristoffer Dahlslätt, Edita Poljac, Harold Bekkering

Predictions are important not only in motor control, but are also increasingly recognized as a necessity for optimal interaction with others and the environment. When observing and listening to others, we tend to predict the upcoming content of actions and speech. In the present study, we addressed the question whether predictions in action observation and language comprehension both rely on a similar (neuro)cognitive mechanism. Participants' eye-movements were recorded while they observed videos of action sequences or listened to sentences describing the same action sequences. Similar patterns of anticipatory eye-movements to upcoming action targets were found in both settings. Moreover, in accordance with a computational model of action observation, we found more anticipation towards the final goal of the action relative to preceding action steps in the action sequence. Altogether the present results suggest a possible role for simulation underlying predictions both during observation of actions and comprehension of linguistically described actions.

## **Semantic Context Effects of Picture and Word Distractors in Overt Translation: RT and EEG Data**

Svetlana Gerakaki, Ardi Roelofs, Ton Dijkstra, Vitória Piai

Two studies involving Dutch-English bilinguals explored the impact of word and picture distractors on overt backward (English to Dutch) translation of single words, with the aim to contribute to the discrete-cascade debate in language production. First, two behavioral reaction time (RT) experiments attempted to replicate the findings of Experiment 1 by Bloem and La Heij (2003). They manipulated semantic relatedness for target-distractor pairs to demonstrate a complete reversal of context effects in the overt backward translation task dependent on distractor modality. In line with these authors, we demonstrated facilitatory effects of related distractor pictures, but, contrary to them, we did not find any evidence of interference by related distractor words. We argue that picture distractors have a robust (facilitatory) impact on language production during overt backward translation, whereas word distractors have a much less stable effect by inducing effects going from no interference at all to even small but significant facilitation. Second, in an electrophysiological (EEG) experiment, we considered semantic context effects of picture distractors rather than word distractors in overt translation. An N450 component showed a larger negative deflection in the semantically unrelated than in the related condition. This finding is indicative of a response level facilitation effect. It thereby supports a cascade view on language production and positions the locus of the semantic facilitation effect at the lexical level.

## **The Representation and Processing of Identical Cognates by Late Bilinguals: RT and N400 Effects**

David Peeters, Ton Dijkstra, Jonathan Grainger

Across the languages of a bilingual, words can have the same orthographic form and a similar meaning. How such words, called identical cognates, are processed and represented in the bilingual brain is not well understood. We collected reaction time data and event-related potentials in response to identical cognates and control words while late French-English bilinguals performed a lexical decision task in their L2, English. The behavioral data showed facilitatory effects of cognate status and English frequency. Further analysis on the identical cognates revealed effects of both English and French frequency. Cognates with a low English frequency showed a larger facilitation effect than cognates with a high English frequency. The electrophysiological data showed N400 effects of cognate status and both English and French frequency of the identical cognates. All results are discussed in terms of the processing of identical cognates and the way they are represented in the bilingual brain.

## Institutes associated with the Master's Programme in Cognitive Neuroscience



Donders Institute for Brain, Cognition  
and Behaviour:

Centre for Cognitive Neuroimaging  
Kapittelweg 29  
6525 EN Nijmegen

P.O. Box 9101  
6500 HB Nijmegen  
[www.ru.nl/neuroimaging/](http://www.ru.nl/neuroimaging/)

Donders Institute for Brain, Cognition  
and Behaviour:  
Centre for Neuroscience  
Geert Grooteplein Noord 21, hp 126  
6525 EZ Nijmegen

P.O. Box 9101  
6500 HE Nijmegen  
[www.ru.nl/neuroscience](http://www.ru.nl/neuroscience)

Donders Institute for Brain, Cognition  
and Behaviour:  
Centre for Cognition  
Montessorilaan 3  
6525 HR Nijmegen

P.O. Box 9104  
6500 HB Nijmegen  
[www.ru.nl/cognition/](http://www.ru.nl/cognition/)



MAX-PLANCK-GESELLSCHAFT

Max Planck Institute for Psycholinguistics  
Wundtlaan 1  
6525 XD Nijmegen

P.O. Box 310  
6500 AH Nijmegen  
<http://www.mpi.nl>



Universitair Medisch Centrum St Radboud  
Geert Grooteplein-Zuid 10  
6525 GA Nijmegen

P.O. Box 9101  
6500 HB Nijmegen  
<http://www.umcn.nl/>

Nijmegen Centre for Molecular Life Sciences  
Geert Grooteplein 28  
6525 GA Nijmegen

P.O. Box 9101  
6500 HB Nijmegen  
<http://www.ncmls.nl>

Baby Research Center  
Montessorilaan 10  
6525 HD Nijmegen

P.O. Box 9101  
6500 HB Nijmegen  
<http://babystudycenter.nl>

